Department of Pharmacology and Toxicology

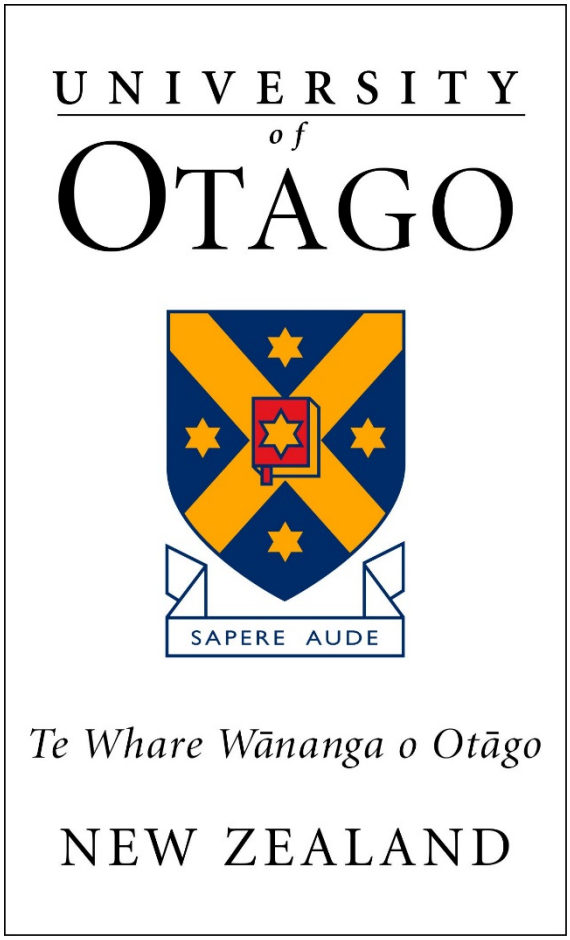

Development of a viral chemokine binding protein as a diagnostic tool for chemokine detection.

Rory Burgess (BSc, PGDipSci)

A thesis submitted for the degree of Master of Science in Pharmacology.

February 2019

Abstract

Chemokines serve an integral role in the inflammatory response, specifically through the development of a chemotactic gradient which directs the trafficking of inflammatory leukocytes to the site of tissue damage or infection. Chemokines exert their effects through interactions with both chemokine receptors and glycosaminoglycans (GAGs).

Targeting chemokines for therapeutic benefit has yielded limited success, likely due to the promiscuity of the system, where blocking individual chemokines does not necessarily inhibit chemotaxis. Alternately, the use of chemokines as diagnostics/prognostics for cancer, inflammatory disease, and autoimmune disease is a more promising area of research. The utilisation of chemokine targeting for both diagnostics and therapeutics has classically been undertaken utilising antibodies which are monospecific, hence issues may arise with regards to chemokine promiscuity.

Viruses have developed numerous techniques to subvert the host inflammatory response, including the secretion of viral chemokine binding proteins (vCBPs). These proteins can exhibit binding specificity for multiple classes of chemokines, therefore offering a unique potential for use in clinical diagnostics.

This study investigated the use of a vCBP derived from Orf virus stain NZ2, which binds across three classes of chemokines, as a diagnostic tool. The utility of CBP was investigated in assays for which antibodies are currently utilised, namely immunofluorescent cytology, western blotting, and enzyme-linked immunosorbent assays (ELISA).

For use in immunofluorescent cytology, a protocol was developed to enable different levels of fluorophore conjugation to CBP. The fluorophore utilised was DyLight®594. Fluorophore conjugation to CBP was then assessed, indicating the extent of fluorophore conjugation did not

impact binding to chemokines across different classes or species, including mouse CCL2 and CXCL2, and human CCL2 and CCL5. The ability of fluorophore-conjugated CBP to detect chemokines was then assessed in a cell-based inflammatory assay utilising the human monocyte cell line THP-1, expressing CCL2 and CCL5 in response to treatment with lipopolysaccharide (LPS). The ability of the fluorophore-conjugated CBP to detect chemokines in these cells was directly compared with a fluorophore-conjugated anti-CCL2 antibody using immuno-fluorescent microscopy. Whilst the antibody successfully detected CCL2 in activated THP-1 cells, the CBP exhibited reduced sensitivity and showed equivalent levels of detection irrespective of LPS stimulation. The specificity of chemokine binding exhibited by CBP and anti-CCL2 antibody was then assessed via pre-binding with soluble CCL2 and competitive inhibition with unlabelled CBP or antibody. Whilst chemokine binding by the fluorophore-conjugated antibody was affected following pre-binding and competition, neither had a substantial impact on CBP binding. The potential of a GAG-CBP interaction was then assessed through pre-binding with soluble heparin. The findings indicated that the observed THP-1/CBP interaction is mediated, at least in part, through cell-surface GAGs.

Preliminary investigations into the use of fluorophore conjugated CBP in western blotting indicated that CBP is unable to detect denatured CCL2. The use of native CBP was also trialled within ELISA protocols, where CBP was shown to both detect capture-antibody bound CCL2, and when immobilised successfully captured CCL2 for antibody detection.

This study suggests that fluorescent conjugation of CBP is easily achievable and does not impact protein function. Although CBP may not detect cellular chemokine expression, the findings here are the first to indicate that this specific CBP can bind heparin, and as such may have potential as a GAG targeting diagnostic. The use of the native CBP in ELISA protocols was also well supported, but its utility across a range of chemokine ELISA platforms needs to be further evaluated.

Acknowledgements

To Lyn,

Thank-you for allowing me to return and for your guidance through this process. I know at times it's been difficult, but the effort you put into me and all your students is admirable, and I thank you for that.

To Gabs, Ellie, and Nicky,

Thank you so much for all the help over my time here and for teaching me all the lab work I would ever need to know. And more importantly thanks for making the lab a fun place to be.

To Abby, Steph, Sergio, Adam, Katie, and the other post-graduate students,

Thanks for making studying enjoyable and the department a great place to be…along with all the help with getting through my research (obviously).

To my parents and sister,

Thanks for helping me through the stress and the difficulties. Your never-ending support does tend to come in handy.

Lastly, to Max, Teresa, David, Chris, and all my other friends,

Thanks for providing a great balance against study and for making my last years in Dunedin great. It would have been a miserable time without you.

Table of Contents

List of Abbreviations

2-ME	β-mercaptoethanol
ANOVA	Analysis of variance
BPSV	Bovine popular stomatitis virus
BSA	Bovine serum albumin
CCL	CC chemokine ligand
CCR	CC-chemokine receptor
CD	Crohn's Disease
CX3C	CX3C chemokine ligand
CXCL	CXC-chemokine ligand
CXCR	CXC-chemokine receptor
DCs	Dendritic cells
ELISA	Enzyme-linked immunosorbent assay
GAGs	Glycosaminoglycans
GDP	Guanosine diphosphate
GIF	Granulocyte-macrophage colony-stimulating factor/IL2 inhibitory factor
GM-CSF	Granulocyte-macrophage colony-stimulating factor
GPCR	G-protein coupled receptor
GTP	Guanosine triphosphate
HIV	Human immunomodulatory virus
HEK 293 cells	Human embryonic kidney cells
HRP	Horseradish peroxidase
HS	Heparin Sulfate
IBD	Inflammatory bowel disease
IL	Interleukin
LPS	Lipopolysaccharide

MHV-68	Murine gammaherpesvirus-68
MS	Multiple Sclerosis
NIR	Near infra-red
NK cells	Natural killer cells
NSAIDs	Nonsteroidal anti-inflammatory drugs
NSCLC	Non-small cell lung carcinoma
ORFV	Orf virus
PMA	Phorbol myristate acetate
PSA	Prostate specific antigen
RA	Rheumatoid Arthritis
RSV	Respiratory syncytial virus
SEM	Standard error of the mean
SIV	Simian immunomodulatory virus
SPR	Surface plasmon resonance
TNF-α	Tumour necrosis factor-α
vCBPs	Viral chemokine binding proteins
VEGF	Vascular endothelial growth factor
XCL	C-chemokine ligand

1 Introduction

1.1 Inflammation

Inflammation (or the inflammatory response) is a complex defence mechanism designed to protect the body against harmful stimuli, including pathogens, damaged cells, and toxins (Punchard *et al*., 2004). The inflammatory response is the initial action of the immune system against infection and injury, acting to remove any potentially harmful stimuli and allowing for the commencement of the healing process (Kohn *et al*., 2013). Inflammation is symptomatically characterised by redness, swelling, heat, and pain, mainly due to complex microcirculatory events which enhance blood flow towards the afflicted area (Punchard *et al*., 2004). By increasing vascular permeability at the site of damage or infection, the infiltration of essential inflammatory mediators is permitted for the required response (Punchard *et al*., 2004). The later mitigation of this response allows for the commencement of healing processes, without any impediment caused by pathogens or dead tissue (Punchard *et al*., 2004).

The initiation of the inflammatory response can be simplified to key events, commencing with the detection of harmful or foreign stimuli, such as a viral pathogen (Kara *et al*., 2014). Upon detection, inflammatory mediators are activated which promote the recruitment of inflammatory cells (Kara *et al*., 2014). The recruitment of inflammatory cells to the site of infection leads to the destruction of harmful stimuli (Kara *et al*., 2014). Realistically, the inflammatory response is a hugely intricate cascade of interactive events, characterised by the recruitment of varying subsets of inflammatory mediators and cells specifically tailored to ensure the destruction of a particular stimuli (Kara *et al*., 2014).

The inflammatory response is critical for both homeostatic function and defence of the host, however disease can result with disruption or dysregulation. Gathering evidence indicates the

involvement of inflammation within the pathologies of almost all disease states (Raman *et al*., 2011). Diseases which are primarily driven by excessive inflammation include autoimmune diseases and inflammatory diseases, in which inflammation causes damage to the host (Haringman *et al*., 2003). Alternately, there are several diseases of which inflammation plays more subdued roles, such as cancers, where the inflammatory response can help potentiate cancer growth and development (Keeley *et al*., 2010). Specifically, the dysregulation of the inflammatory response has impacts upon several biological functions within disease pathogenesis including; excessive tissue destruction, remodelling, and growth; impeded immunity against pathogens; impeded wound healing (Loberg *et al*., 2007; Rees *et al*., 2015).

When the inflammatory response becomes detrimental to health, a multitude of therapeutics can be utilised which act to dampen the response and protect against detrimental effects caused by excessive inflammation. Common therapeutics include; nonsteroidal anti-inflammatory drugs (NSAIDS) such as acetaminophen (paracetamol); and steroid based anti-inflammatory drugs, such as corticosteroids (e.g. prednisone) (Jin, 2015; Barnes, 2006). Both NSAIDs and corticosteroids work to systemically dampen the inflammatory response in order to mitigate disease-induced damage. However, the use of systemic anti-inflammatory drugs can swing the homeostatic balance of inflammation from over-activation to suppression, which impedes upon crucial biological functions such as wound healing, and fighting infection (Hsu and Katelaris, 2009). Considering the development of anti-inflammatory therapeutics, the fundamental failure is a lack of specificity for the pathological inflammation, as opposed to inflammation for homeostatic function. Proposedly, a therapeutic possessing the ability to ameliorate excessive inflammation, without disrupting the homeostatic role of the inflammatory response in unafflicted areas would provide a most effective treatment (Hsu and Katelaris, 2009).

With the inflammatory response being a complex and multifactorial process, targeting specific factions of the inflammatory cascade could lead to both inhibition of the pathological

inflammatory response and the maintenance of the homeostatic role of inflammation. Targeting a family of chemoattractant cytokines (chemokines) involved in the recruitment of inflammatory cells theoretically may provide a therapeutic which could achieve this currently unachievable goal.

1.2 Chemokines

Chemokines are a family of chemoattractant cytokines with the primary responsibility of recruiting immune and inflammatory cells to the site of infection or damage through chemotaxis (Keeley *et al*., 2010). Chemokines are produced as a response to the detection of invading pathogens, such as viral particles, bacteria, and in response to tissue damage. Several cell types are capable of producing chemokines including both structural and immune cells (Raman *et al*, 2011; Table 1). Chemokines are not only present during tissue damage, as there is some constitutive expression of homeostatic chemokines such as CXCL12 which circulates the body, possessing varying roles such as homing of leukocytes to lymphatic tissues (Sanchez-Martin *et al*., 2011).

1.2.i Chemokine structure and function

Chemokines are small proteins, typically sized between 7 and 10 kDa (Luster, 1998). Chemokines have four major classes separated by slight structural differences (Mellado *et al*., 2001). Chemokines are categorised based on the precise expression of conserved cysteine residue located near the N-terminus of the protein (Mellado *et al*., 2001). C chemokines are characterised by a singular conserved cysteine residue; CC chemokines have two adjacent cysteine residues, CXC chemokines have two cysteine residues adjacent to each other with a singular, random amino acid in between; and CX3C chemokines have two conserved cysteine residues, with three random amino acids between them. The tertiary structure of all chemokines is substantially homologous, constituting of a disordered N-terminus, a three-stranded β-sheet,

and a C-helix towards the bottom of the proteins (Kufareva *et al*., 2015). A notable difference between chemokine classes is found within dimer formation of these proteins (Kufareva *et al*., 2015). Generally, CXC chemokines form dimers via direct interaction of the first β-sheet of both proteins, such as CXCL8. Alternately, CC chemokines form dimers through adjacent interactions towards the N-terminus of the proteins, which directly involves the conserved cysteine residues referred in the chemokine class nomenclature (Kufareva *et al*., 2015). Lastly, the C class chemokine, XCL1, possesses the most divergent 3D structure compared to normal, having a four-stranded β-sheet tertiary structure which dimerises through extensive β-sheet interactions, with a "head-to-tail" dimer structure (Kufareva *et al*., 2015.

Table 1. *Characterising expression, interaction, and biological role of several chemokines.*

Chemokine	Produced by	Receptor	Cells Attracted	Overexpression in disease	References
C Class					
XCL1	CD8, CD4 T cells	XCR1	Dendritic cells NK cells	RA	(Lei and Takahama, 2012)
CC Class					
CCL2	Monocytes Macrophages Fibroblasts Keratinocytes	CCR2, CCR4	Monocytes NK cells T cells Basophils Dendritic cells	MS, CD, Pancreatic cancer progression	(Deshmane *et al*., 2009)
CCL5	T-lymphocytes Macrophages Platelets Synovial fibroblasts epithelium	CCR1 CCR3 CCR5	Monocytes NK cells T cells Dendritic cells Eosinophils	RSV, RA, MS, Promoting cancer invasion	(Aldinucci and Colombatti, 2014)
CXC Class					
CXCL2	Monocytes Macrophages Neutrophils	CXCR2	Neutrophils T cells Fibroblasts	Cancer Angiogenesis	(Iida and Grotendorst, 1990)
CXCL4	Platelets	CXCR1	Neutrophils Fibroblasts Monocytes	RA, Lung Cancer	(Lasagni *et al*., 2003)
CXCL8	Monocytes Macrophage Fibroblasts Keratinocytes Endothelium	CXCR1, CXCR2	Neutrophils T cells	CD & IBD, NSCLC, RA	(Kohidai and Csaba, 1998)
CXCL12	Stromal cells (across a majority of organs)	CXCR4 CXCR7	Mesenchymal cells Endothelial cells	Leukocyte homing, cancer invasion, RA	(Sanchez-Martin *et al*., 2011)
CX3C Class					
CX3CL1	Endothelial cells	CX3CR1	T cells Monocytes	RA	(Bazan *et al*., 1996)

Modified from Griffith et al. (2014). Multiple Sclerosis (MS), Crohn's disease (CD), Respiratory syncytial virus (RSV), Rheumatoid arthritis (RA), Inflammatory bowel disease (IBD), Non-small cell lung carcinoma (NSCLC), Natural killer (NK) cells.

Variations in chemokine structures lead to a plethora of chemokine-receptor interactions, (Mellado *et* al., 2001; Table 1). To date, there are over 50 identified chemokines, with approximately 20 different chemokine receptors. The miss-match in the number of chemokines to receptors leads to the overlapping of ligand-receptor interactions; combined with the capacity of chemokines to bind several receptors, results in the understood promiscuity of the inflammatory system (Pease and Horuk, 2010; Table 1). This promiscuity leads to the numerous variations of chemokine induced inflammatory cell chemotaxis.

When tissue is damaged chemokines are produced and secreted, resulting in a local increase in chemokine concentration, forming what is known as a chemotactic gradient (Proudfoot *et al*., 2003) (Figure 1). The formation of this gradient creates a chemical signalling process which drives the attraction of other inflammatory cells/leukocytes to the site of damage or infection to exert the desired effect via extravasation through endothelium (Figure 1) (Proudfoot *et al*., 2003).

The process is commenced upon a local release of chemokines in response to damage or infection (Figure 1) (Luster, 1998). In situations where the skin barrier is damaged, dermal cells release chemokines, whereas in response to infection or allergen exposure, infected cells, or the immune cells that identify the allergen, mediate chemokine release (Oskeritzian, 2012).

Upon chemokine release, the chemokines associate with long polysaccharide chains known as GAGs found on the cell membrane of most cells (Figure 1) (Garcia *et al*., 2016). GAG interactions are fundamental for the formation of the chemotactic gradient as they stabilise chemokine binding to their receptors (Thompson *et al*., 2017). Heparin sulphate (HS) is the most abundant GAG found on the surface of endothelial cells (Farrugia *et al*., 2018). Studies have indicated that inhibition of HS synthesis significantly decreases the amount of neutrophil extravasation through the endothelial wall (Farrugia *et al*., 2018).

The association of chemokines to these GAGs promotes the expression of selectins, which are weakly adherent glycoproteins (Barthel *et al*., 2007). The increased expression of selectins leads to the adhesion of circulating (rolling) lymphocytes to the cell surface, which also express selectins. GAG-immobilised chemokines presented to chemokine receptors on the surface of the leukocyte leads to the cell-surface expression of integrins which facilitate adhesion to the endothelium (Figure 1) (Barthel *et al*., 2007). Chemokine receptors are comprised of 7-transmembrane spanning domains, coupled with a G-protein unit for intracellular signal transduction (Kufareva *et al*., 2015). Upon chemokine binding, receptor activation triggers an increased flux of intracellular calcium ions (Ca^{2+}), which leads to the exchange of a phosphate onto the inactive GDP, to form GTP, cleaving the G-protein subunits, allowing for second messenger molecules, such as PIP2, IP3, and DAG to be released and mediate several cellular pathways (Lodowski and Palczewski, 2009). These second messengers stimulate both cell polarisation, and selectin or integrin expression. Leukocyte polarisation leads to migration towards the area of high chemokine concentration, thereby the extravasation of the cell through the endothelium towards the area of damage or infection. Once released from the endothelium, the cell can act to protect the body. Following their activation, the chemokine receptors are often internalised in response to elevated chemokine concentration (Neel *et al*., 2005). Receptor internalisation is a part of the homeostatic control of the inflammatory response. A decreased degree of receptor activation due to the reduction of receptor presence, will result in a diminishing expression of the chemotactic gradient, leading to the eventual abolishment of inflammation at the site of damage, allowing for the commencement of healing processes.

1.2.ii Chemokines in health and disease

Chemokines are involved in the recruitment of inflammatory cells and are a critical part of physiological function. Chemokines possess a plethora of roles within the body, outside of the more obvious inflammation mediatory role (Raman *et al*., 2011).

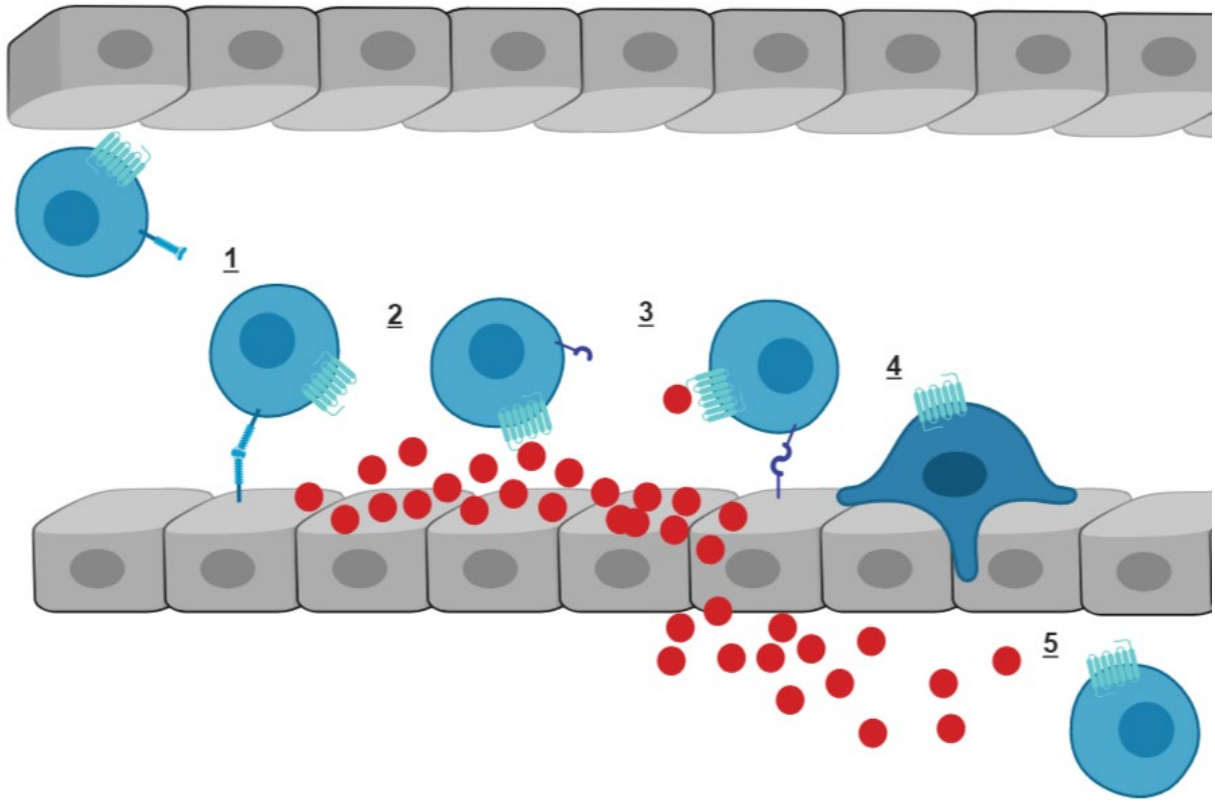

Figure 1. The role of chemokines in leukocyte extravasation. (1) circulating leukocytes interact with chemokine induced selectin expressed on the cell surface. (2) selectin interaction allows for GAG associated chemokine-receptor binding on the leukocyte. (3) Chemokine (red) activation of receptors allows for the expression of integrins to promote leukocyte adhesion. (4) Leukocyte undergoes extravasation through the endothelium, towards high concentrations of chemokines. (5) Leukocyte has successfully migrated across the endothelium.

During infection chemokines exhibit the role of chemoattractant proteins for varying inflammatory cells such as T cells and monocytes (Haringman *et al*., 2003). The chemoattraction of these cells leads to the promotion of pathogen clearance, where these cells can actively destroy the source of infection and develop immunity against them, thus protecting the host from disease. However, several diseases are linked with the disruption of chemokines in this role.

Inflammatory disease and autoimmune disease are prime examples as they are governed by an excessive inflammatory response to stimuli. Pathogenesis arises from inflammation-based damage and cellular destruction. In several inflammatory diseases including Crohn's disease (CD) and ulcerative colitis (UC), being two forms of inflammatory bowel disease (IBD), the activity of several inflammatory cells such as T cells are linked with tissue damage via the

potentiation of the inflammatory response (Pallone and Monteleone, 2001). Several chemokines have been identified as being involved in excessive chemotaxis of inflammatory cells resulting in tissue damage. CXCL8 has been shown to exhibit upregulation within IBD, with a positive correlation to the severity of disease (Keshavarzian *et al*., 1999). Similarly, CCL25 has been shown to promote colonic remodelling in a mouse model, the pathology of which was substantially attenuated via chemokine inhibition (Bekker *et al*., 2015).

Chemokines are also involved in the angiogenic process, exemplified during the wound healing process. Damaged tissue upon remodelling, needs to become re-vascularised as to promote growth and survival of the tissue. Several chemokines have been identified for involvement within this response, including CCL2 and CCL5 (Stamatovic *et al*., 2006). Regrettably, cancers have developed the ability to modulate the chemokine system as to promote angiogenesis for tumour growth, thereby enhancing disease progression. As a cancerous tumour progresses it requires an immense blood supply to provide nutrients necessary for growth. The upregulated production of chemokines in order to promote angiogenic pathways has been observed across several cancers (Sarvaiya *et al*., 2013). The presence of several chemokines including CXCL2, are noted to be potent promoters of tumour-associated angiogenesis, associated with poor prognostic outcomes in several cancers including prostate (Keeley *et al*., 2010). The inhibition of CXCR2, therefore a decrease in chemokine-mediated activation was directly shown to inhibit tumour-associated angiogenesis in pancreatic cancer (Wente *et al*., 2006). Similarly, in human prostate cancer, a reduction in the production of CXCL8 at the tumour site leads to significantly lowered vascularisation and a lowered tumour growth (Sun *et al*., 2001).

The chemotactic effects of chemokines are not always specifically pro-inflammatory. During the wound healing process, along with the promotion of angiogenesis, chemokines also direct the trafficking of structural cells for the remodelling and proliferative stages of wound healing (Yates *et al*., 2009). Therefore, the disruption of chemokine involvement within this process

can lead to poor wound healing. CXCR2 has been noted for particular importance, as deletion of this receptor, thereby chemokine disruption leads to poor healing including a notable reduction in keratinocyte migration for epithelialisation. Similarly, in CXCR3 knockout mice, re-epithelialisation and basement membrane remodelling is delayed (Yates *et al*., 2009).

Cancers also manipulate the chemokine system in ways that promote its own proliferation and invasion. Both melanomas and breast cancers have been identified to overexpress the CXCR4 receptor and are observed to frequently metastasise and invade utilising the lymphatic system. CXCL12 is a chemokine present in abundance in the lymph nodes, which allows the cancer to traffic into the system, often leading to cancer progression and death (Itatani *et al*., 2016). Numerous cancers have been indicated to exploit CXCL12/CXCR4 mediated migration, including breast, lung, melanoma, ovarian, prostate, and pancreatic (Raman *et al*., 2011).

Although certain chemokines are identified as important across several diseases, often the true extent of chemokine involvement is extreme, as exemplified by rheumatoid arthritis (RA). RA is an autoimmune disease, characterised by excessive transient inflammation against the synovium of joints (van de Sande *et al*., 2011). RA is noted to have progressive phases of disease, characterised by inflammation, joint destruction, and invasion of fibrous tissues resulting in joint immobility (van de Sande *et al*., 2011). As reviewed by Szekanecz *et al*. (2010), numerous chemokines have been identified, exhibiting various effects across differing stages of disease. CXC-chemokines CXCL1, CXCL4, CXCL5, CXCL6, CXCL7, CXCL8, CXCL9, CXCL10, CXCL12, CXCL13, and CXCL16 have been detected in sera, synovial fluids, and synovial tissues of patients with RA produced by synovial macrophages. Similarly, CC chemokines that have been identified in serum and synovia include CCL2, CCL3, CCL5, CCL7, CCL8, CCL13, CCL14, CCL15, CCL16, CCL17, CCL18, CCL19, CCL20, CCL21, and CCL28. XCL1 has also been implicated in the accumulation of T cells in subchondral mesenchymal cells of afflicted joints.

With clearly extensive involvement of chemokines within the pathogenesis of disease, the movement towards targeting chemokines for therapeutic development was a natural progression.

1.3.iii Chemokines as therapeutic targets

The specific targeting of chemokines is primarily achieved by antibody-based therapeutics, whereas non-biological inhibitors are typically used to target chemokine G-protein coupled receptors (GPCR) (Lodowski and Palczewski, 2009). This review will concentrate on specific targeting of chemokines by antibodies. Antibodies are proteins produced by the immune system that specifically recognise, bind, and disable or destroy the target protein (antigen) (Suzuki *et al*., 2015). Antibodies possess a variable 'Fab' region which binds to a singular epitope, being a small and specific sequence of amino acids (Sela-Culang *et al*., 2013). Antibodies can block the target cell or protein by occluding a substantial portion of the protein surface required for function. Binding can result in the agglutination of the antigen or stimulation of a complement attack system via the 'Fc' region of the antibody, resulting in direct phagocytosis of the bound proteins (Sela-Culang *et al*., 2013).

The use of antibody-based therapeutics in targeting the inflammatory response has yielded successful indications within autoimmune disease. RA is one particular disease in which the use of therapeutic antibodies has been investigated, suggesting some degree of success, for example the approved TNFα inhibitor Infliximab (Perdiger, 2009). The use of therapeutic antibodies against chemokines however has not yielded such advancement, although animal models suggest otherwise.

An antibody against CCL5 was investigated for the treatment of an induced arthritis model in rats (Barnes *et al*., 1998). The antibody indicated both substantial reductions in serum CCL5 levels, supported by an improved radiological score which considers cartilage loss, joint

erosion, and bone ossification. These findings were matched with the use of a systemic anti-inflammatory as a positive control. Similarly, in another arthritis model in mice, daily injection of an anti-CCL2 antibody prevented the onset of arthritis, also exhibiting improvements in joint quality when administered during later disease progression (Gong *et al*., 2007). The prevention of macrophage invasion in rat joints in an arthritis model was also observed with administration of a CCL2 neutralising antibody, giving a basis for the mechanism of chemokine inhibition for disease amelioration (Ogata *et al*., 1997).

Based upon animal findings, the use of anti-CCL2 antibodies were assessed for the use in patients with RA. A randomised control trial was conducted where anti-CCL2 antibody ABN912 was administered via IV on days 1 and 15, of the entire 120-day trial (Haringman *et al*., 2006). Of all the parameters assessed there was no indicated improvement of clinical symptoms, nor an indication of a reduced disease activity (indicated by biomarkers).

Alongside failings in translatability of chemokine-targeting antibody efficacy from animal to human models of arthritis, similar discrepancies are found within the use of chemokine targeting antibodies in cancers. Loberg *et al*. (2007) investigated the potential use of antibody targeting of CCL2 in a mouse model for treatment against the progression of prostate cancer tumours. With systemic administration of anti-CCL2 antibody CNTO888, an average of 42% reduction in tumour volume was observed compared to antibody control. The human antibody CNTO888 also reduced the average number of vascular sprouts from tumour sections, from 27 to 1, compared to the antibody control. In a phase II clinical trial conducted by Pienta *et al*. (2013) the potential use of an anti-CCL2 antibody was investigated in metastatic castration-resistant prostate cancer patients. Regrettably, in this study there was no notable reduction observed regarding the metastasis and invasion of the tumour, including no observed increase in progression free survival. From analysis of serum samples, a significant reduction in serum CCL2 was observed immediately post-dosage, however this reduction was not maintained.

As reviewed by Szekanecz and Koch, (2015), antibody-based human trials have had limited success, with less than 15% of human trials showing any treatment efficacy, irrespective of the significant efficacy observed in animal models. It was suggested a high receptor occupancy is required to successfully inhibit the extravasation of inflammatory cells to the joint mediated by chemokines. However, with systemic expression of these receptors, reaching a substantial amount of chemokine inhibition is unlikely. As there is significant promiscuity in the chemokine network, with vast numbers of chemokines performing redundant roles, studies have also investigated targeting chemokine receptors to increase the inhibitory potential of the therapeutic. However, researchers have struggled to generate antibodies translatable to human populations, as may antibodies found to bind chemokine receptor produce no neutralisation effect (Dorgham *et al*., 2016). To date, only one antibody targeting a chemokine receptor (CCR4) has been approved for use (Vela *et al*., 2015). Alternately, small molecule drugs have been developed that successfully target and inhibit specific chemokine receptors. However, none have shown clinical success for treating inflammation (Pease and Horuk, 2010).

Although there has been limited success with the development of efficacious therapeutics against chemokines, utilising antibodies against chemokines as diagnostic tools may still lead to valuable insights within the realm of inflammatory disease.

1.3.iv Chemokines as diagnostics

Chemokines have important roles as markers for inflammation, indicators of general inflammatory levels, along with providing essential information toward the characterisation of migrating inflammatory cells. Chemokine involvement in disease is often determined through quantification within sera or biological samples. The development of chemokine-based diagnostic markers is ongoing, with several being indicated for dynamic detection and characterisation of disease, including within cancers and autoimmune disease.

Cancers are known to both overexpress chemokines and chemokine receptors. For prostate cancer, the use of prostate specific antigen (PSA) as a biomarker is limited, as the prognostic abilities are questionable. Alternately, CCL2 has been identified as a prognostic, potentially being more effective towards identifying disease severity in low level PSA patients (Macoska *et al*., 1997; Tsaur *et al*., 2014). Similarly, the limited sensitivity of viral strain detectors for predicting the correlation of human papilloma virus (HPV) infection with cervical lesions and cancer development prompted the investigation of chemokines, specifically CCL2, as prognostic indicators (Bhatia *et al*., 2018). In blood samples from lung cancers patients, several CXC chemokines were investigated, indicating a correlation between the presence of CXCL4 and CXCL5 and a greater likelihood of relapse post-surgical intervention (Spaks *et al*., 2017).

The use of chemokines as diagnostics is being investigated for diseases such as RA and other forms of arthritis. Soluble chemokine concentrations were determined within bone marrow samples of RA and osteoarthritis patients in relation to T cell accumulation (Dominguez-Villar M and Hafler, 2018). CX3CL1 and CCL5 were identified to be overexpressed, likely contributing to T cell accumulation, whereas CCL2, CXCL12, and CXCL1 were not (Warnawin *et al*., 2016). In another study examining the serum samples of RA patients, CXCL13 was identified as a positive serum diagnostic for RA compared to healthy controls (Allam *et al*., 2018). Interestingly, there was a higher correlation of expression with patients with recently identified RA (< 12 months) compared to patients with established RA. As early diagnosis is mandatory for successful intervention, a marker which indicates the establishment of disease could be critical for treatment.

Arguably the most interesting use for the manipulation of chemokines for diagnostic purposes, would be the use of *in vivo* methods of imaging. By utilising the biological role of chemokines, the ability to target chemokine receptor expression has been developed. In a study conducted by Meincke *et al*. (2011), conjugates of CXCL12 and a near infra-red (NIR) fluorophore were

created and screened for use for CXCR4-expressing MCF-7 breast cancer tumours in mice. Optical imaging offered a successful, non-invasive, and sensitive tumour detection method. Similarly, CXCR7 is often overexpressed in the tumour microenvironment. The use of a radiolabelled antibody against this receptor allowed for the enhanced detection of high CXCR7-expressing breast, lung, and oesophageal cancer xenografts utilising SPECT imaging techniques, suggesting the utility of radiolabelled identification of the chemokine network (Behman *et al*., 2016). However, Nishizawa *et al*. (2010) found that upon investigation for a fluorescently labelled antibody, the antagonist identified both CXCR4 receptors expressed on urothelial cancer cells and leukocytes. This suggests a fundamental failure for cancer targeting, where there is a loss of specificity due to background detection.

Although certain chemokines do indicate positive diagnostic ability, targeting singular chemokines may limit the discovery of the true extent of chemokine involvement. In situations where several chemokines, or a class of chemokines needs be identified, several antibodies must be employed. Here, issues can arise when it comes to experimental procedure, often requiring entirely separate sample testing for each singular chemokine. A solution for this may come from a viral source, specifically, secreted proteins from viruses that bind multiple chemokines as a means of defending themselves against the host immune response.

1.3 Viral Immune Evasion

Viruses are infectious agents which reproduce within another 'host' organism. They infect the host, then integrate themselves into biological processes such as gene transcription, producing proteins required for viral replication (Walsh *et al*., 2013). Many organisms have complex defence mechanisms against viral infection, such as an adaptive immune system. The immune system is able to recognise the invading viral pathogen and destroy it, eliminating the ability for the virus to successfully replicate (Walsh *et al*., 2013). The complexity and intricacy of virus propagation in host organisms has stemmed from the co-evolution of viruses alongside their

hosts (Sharp and Simmonds, 2011). Where a host evolves new mechanisms to protect against viral infection, the virus develops new methods of evasion. There are a range of immune evasion strategies viruses employ, with different families of viruses often utilising distinct evasion techniques, including antigenic drift, latency, and immune modulation.

Antigenic drift is a method of immune evasion, famously employed by viruses such as Influenza virus (Boni *et al*., 2009). Antigenic drift is the creation of "immune-escape variants" of the virus strain via deliberate mutation of proteins on the virion surface that are recognised and targeted by host antibodies. Through regular mutations in these proteins, the host immune system may not recognise the "newer" viral strain thereby resulting in the ability of a virus to re-infect the host.

Latency is a method in which a virus successfully replicates within the host and becomes permanently integrated within host cells (Nicoll *et* al., 2012; Mbonye and Karn, 2017). After initial infection, the viral genome can become integrated within host cells, being in a reversibly inactive state of infection. This allows the virus to persist in the host long after the initial "active" infection is cleared. Human immunodeficiency virus (HIV) is the most infamous of viruses to employ this tactic for survival, developing genomic reservoirs within individual T cells, and constantly producing low levels of infectious virus. Herpes simplex virus-1 employs a similar strategy in which the viral genome is maintained in a seemingly inactive state within neurons, only emerging when the host is stressed, and the immune system is likely weakened.

Immune modulation is a method by which a virus can avoid elimination (Engel and Angulo, 2012; Alcami, 2003). Immune modulation often involves the direct modulation of the host immune system, including direct interactions with host cytokines and chemokines. The interactions with these host proteins is undertaken by secreted virulence factors. Virulence factors are proteins secreted via host cells, after viral integration into host DNA during infection. These proteins then subvert the immune response of the host via the direct modulation

of the immune response against infection (Engel and Angulo, 2012). These virulence factors often mimic, either structurally and/or functionally, host proteins involved in typical immune regulation. This secretion of homologous proteins observed by viruses is a result from the virus previously capturing host genes, or even evolving its own (Felix and Savvides, 2017).

There are numerous forms of these virulence factors employed, targeting varying areas of the inflammatory cascade in order to subvert and evade host immunity. Known virulence factors include; homologues of host cytokines and chemokines, homologues of their receptors, and inhibitory binding proteins of which are unrelated structurally to host proteins (Alcami, 2003; Felix and Savvides, 2017). Large DNA viruses, including poxvirus and herpesvirus families, are almost exclusively the only viral family to produce protein homologues for the purpose of immune evasion. These viral homologues are mimics of host proteins, which are utilised to block different aspects of the immune response to which the virus is exposed (Alcami, 2003). Protein homologues found within these families of viruses include growth factors, cytokines, and chemokines. Another class of virulence factors are cytokine and chemokine binding proteins (Gonzalez-Motos *et al*., 2016). These virulence factors can be homologous to known host receptors or share no homology to any known host protein (Gonzalez-Motos *et al*., 2016).

1.3.i Viral chemokine binding proteins

Viral chemokine binding proteins (vCBPs) function to act as soluble inhibitory proteins, engaging in extensive interactions across several host chemokines, inhibiting the chemokines typical biological function. These vCBPs have been identified across a range of viruses, including strains of Herpesvirus and several in the family of Poxviruses (Table 2).

Table 2. *Secreted viral chemokine binding proteins.*

Virus Family	vCBP	Virus Species	Binding Site	Target(s)	Potential therapeutic role
Poxvirus	35-kDa	Ectromelia, Cowpox, Vaccinia	GCPR binding domain	CC chemokines	Asthma Wound healing Inflammatory skin
	M-T1	Myxoma	GPCR binding domain	CC chemokines Direct interaction with GAGs	Transplant vasculopathy
	CBP (orf) BPSV CBP (BPSV)	Orf virus BPSV	GPCR binding domain GAG binding domain (?)	C, CC, and CXC chemokines Direct interaction with GAGs	Stroke Inflammatory skin
	M-T7	Myxoma	GAG binding domain	C, CC, and CXC chemokines	Transplant vasculopathy
	A41L	Varicellovirus, Ectromelia virus	GAG binding domain	CC chemokines Direct interaction with GAGs	
Herpesvirus	M3	MHV-68	GPCR and GAG binding domains	C, CC, CXC, CX3C chemokines	Pancreatitis Intimal hyperplasia Inhibition of B cell chemotaxis

Adapted from Lucas and McFadden, (2004); Heidarieh et al. (2015); Gonzalez-Motos et al. (2016). Bovine popular Stomatitis virus (BPSV).

The inhibitory action of the proteins can vary, where vCBPs can mask different parts of the chemokine, thereby inhibiting varying protein interactions. Classical inhibition would be considered the blocking of the receptor binding site which engages the chemokine receptors, thereby blocking the GPCR signalling cascade, and subsequently inhibiting the formation of the chemotactic gradient. Alongside this form of inhibition, several of the vCBPs bind to the GAG binding domain of the chemokine inhibiting the adhesion and stabilisation of the circulating chemokine. Lastly, vCBPs can interact directly with GAGs, thus inhibiting the arrest of circulating chemokines through a competitive interaction.

One of the vCBPs that is conserved amongst *Orthopoxviruses* is classed as secreted CC chemokine binding proteins, called 35 kDa (Lalani *et al*., 1998). These proteins function to competitively inhibit CC binding to cellular receptors, binding the chemokine with high affinity. Binding of the chemokine inhibits the cellular chemokine receptor activation, thus inhibiting the increase in calcium concentration required to migration of cells along the chemotactic gradient. There are two other 35 kDa-like CBPs that have been discovered, M-T1 and CBP, which are distinguishable as possessing more extensive roles. M-T1, from *Myxoma*

virus, a *Leporipoxvirus,* also possesses the unique ability to interact with GAGs, having a conserved GAG binding domain (Seet *et al*., 2001). This interaction could allow for the secreted protein to persist in the inflamed area, thus enhancing its inhibitory effect. The vCBP derived from *Orf virus* (ORFV), a *Parapoxvirus*, known as CBP, has extensive chemokine interactions across multiple classes of chemokines (Counago *et al*., 2015). It has been identified that CBP has the ability to bind with high affinity across C, CC, and CXC classes, inhibiting receptor activation. There has also been a proposed GAG interaction discovered, however complete characterisation is yet to occur. M-T7 from myxoma virus is also a broad range chemokine inhibitor of C, CC, and CXC chemokines, however, binding occludes the GAG binding domain of the chemokine (Lalani *et al*., 1997). The A41 vCBP exhibits similarities to the 35 kDa vCBPs, being able bind to CC chemokines, but is unable to do this in the presence of GAGs (Bahar *et al*., 2008). This suggests that the protein both impedes the binding of GAGs to chemokine, and also exhibits interactions with GAGs itself. The M3 vCBP from *Gammaherpesvirus 68* is a unique protein, exhibiting the ability to bind chemokines across all chemokine classes (Alexander-Brett and Fremont, 2007). The M3 protein binds with high affinity to prevent both the chemokine-chemokine receptor interaction, and the chemokine-GAG interaction.

Interestingly, as vCBPs bind specific chemokines across varying classes, the novelty of achieving multiple chemokine inhibition may be achievable. Where antibodies target and inhibit singular proteins, vCBPs indicate the ability to bind and inhibit several.

1.3.ii Viral chemokine binding proteins as therapeutics

Chemokine targeting is a somewhat novel approach for subverting the inflammatory response, having led to the development of a large field of therapeutic investigation. For diseases which are intrinsically involved with the overexpression of chemokines, the application of vCBPs provides a new scope for therapeutics. The ability to bind several chemokines may provide

novel insights to therapeutic development, as the failings of current anti-chemokine therapeutics are often based upon the theory of chemokine and receptor redundancy (Szekanecz and Koch, (2015).

One of the most investigated vCBPs for therapeutic development is a 35 kDa vCBP from the orthopoxvirus *Vaccinia virus*; vCCI. This vCBP has been shown to inhibit chemokine-induced eosinophil migration *in vivo* guinea pig skin wound model (Reading *et al*., 2003). Similarly, vCCI has exhibited anti-eosinophil migration in mouse lungs (Reading *et al*., 2003). These led to the intranasal administration of vCCI in an allergic-asthma mouse model. Treatment drastically improved pulmonary and physiological function of the airways, decreasing localised inflammation, with no observation of systemic immune-suppression (Dabbagh *et al*., 2000).

Several vCBPs have been reported to inhibit the migration of numerous cell types during the wound healing and skin inflammation processes. The administration of a vCBP from the parapoxvirus *Bovine popular stomatitis virus* (BPSV), to murine skin stimulated with bacterial lipopolysaccharide (LPS) for the initiation of an inflammatory response, indicated a substantial reduction in the infiltration of neutrophils and macrophages to the skin. Similarly, in a dermal punch model, this vCBP was identified to inhibit wound inflammation in mice in ways which mimic the pathogenesis of viral lesions produced during BPSV infection. The genetically related CBP indicated a similar effect, where in both an *in vitro* chemotaxis assay and LPS-stimulated skin model, a substantial reduction in monocyte recruitment was observed (Lateef *et al*., 2009). In a similar study, the administration of CBP inhibited the chemotaxis of dendritic cells (DCs) to inflamed skin, and also from the skin to the draining lymph nodes, thereby preventing T cell activation (Lateef *et al*., 2010). Topical administration of vCCI to skin wounds was also shown to inhibit CCL2, CCL5 and NF-kB p65 subunit expression, enhancing neovascularisation and wound closure in mice (Ridiandries *et al*., 2017).

In a murine stroke model, Lee *et al*. (2015) found that a single administration of the BPSV CBP significantly reduced the plasma levels of CCL2 and CXCL2, exhibiting a protective, albeit temporary effect against leukocyte infiltration into the brain. Infarct development was delayed following treatment, suggesting the use of a vCBP could provide a window of opportunity for other therapeutic interventions.

The herpesvirus M3 vCBP has been shown to inhibit B cell chemotaxis via the inhibition of CCL19 and CCL21 (Jensen *et al*., 2003). This vCBP has also shown efficacy across transgenic mice studies for both intimal hyperplasia and pancreas-specific leukocyte infiltration, coincidentally being where the virus typically develops latency (Pyo *et al*., 2004; Jensen *et al*., 2003).

During organ transplantation there is a high incidence of inflammatory responses against the grafted tissue, which is responsible for the majority of cardiac graft losses (Miller *et al*., 2000). Both myxoma virus vCBPs, M-T1 and M-T7, have been successfully indicated in animal models to attenuate CCL2 based promotion of fibrosis within newly grafted tissue (Liu *et al*., 2004; Belperio and Ardehali, 2008).

Research directed towards the development of therapeutics for inflammatory diseases, utilising these viral proteins, highlights key features of the vCBPs which are beneficial and could improve upon previous failings. Key features which suggest vCBPs could be successful therapeutically include their high affinity, small size, and broad spectrum of inhibition (Counago *et al*., 2015; Lalani *et al*., 1998; Alexander-Brett and Fremont, 2007; Bahar *et al*., 2008). Similarly, with many anti-inflammatory therapeutics, studies utilising vCBPs have highlighted common issues with the therapeutic targeting of inflammation. A study conducted by Lee *et* al. (2015) indicated that the BPSV CBP which initially dampened the inflammatory response in a stroke model, later potentiated the inflammatory response and increasing infarct damage, in a manner similar to reperfusion injury. Similarly, Culley *et al*. (2006) demonstrated

the inhibition of chemokine mediated inflammatory response via inhibition of CCL5 in an RSV model utilising an antibody. However, upon progressing infection a characterised "second wave" of CCL5 production was observed, even greater in mice previously treated with the antibody against CCL5. These findings further illustrate the complexity of targeting the chemokine network, as had previously been demonstrated with failings of human anti-chemokine therapies. Another potentially serious limitation with therapeutic application of CBPs are immunogenic reactions which may limit the time period for which CBPs may be utilised, and could further exasperate disease (Baker *et al*., 2010).

As the risks associated with CBP use as therapeutics could out-weigh their potential benefits, it may therefore be more appropriate to explore their utility in a diagnostic setting. As chemokines are being explored as biomarkers for autoimmune diseases and cancer, the use of a high affinity broad spectrum viral CBP may have utility in these clinical scenarios fulfilling the role the currently played by antibodies.

1.3.iii Viral chemokine binding proteins as diagnostics

Viral CBPs have shown utility as chemokine inhibitors, but like antibodies may have their issues as therapeutics. Detection of chemokines may be beneficial to diagnose inflammation, through the detection of inflammatory chemokines in the blood or tissues, previously via the use of antibodies. The use of vCBPs may even offer greater sensitivity than antibodies as diagnostics due to their broader chemokine selectivity and high affinity. But no-one to date has looked at the use of vCBPs as diagnostics.

1.4 Project Objective

The intention of this study is to investigate the potential utility of a vCBP as a tool for detecting inflammatory chemokines in a range of diagnostic platforms. The vCBP chosen for this study is derived from the poxvirus, ORFV. This virus causes contagious pustular dermatitis in its host (sheep and goats) and also commonly known as orf (disease) when it is transmitted to humans (Fleming *et al*., 2015). Active infection replicates within regenerating epidermal skin cells. Infection causes a robust anti-viral immune response characterised by early neutrophil invasion, followed by a later influx in a plethora of other leukocytes including T cells and B cells. The primary infection typically persists for 4-6 weeks, with the ability to re-infect its host. These characteristics of infection have largely been attributed to production of virulence factors by the virus, including vascular endothelial growth factor (VEGF) and interleukin (IL)-10 homologues, a granulocyte-macrophage colony-stimulating factor (GM-CSF) and IL-2 inhibitory factor designated GIF, and CBP. The CBP protein successfully binds and inhibits the activity of chemokines across C, CC, and CXC chemokines with high affinity (Seet *et al*., 2003; Lateef *et al*., 2009; Lateef *et al*., 2010; Counago *et al*., 2015). This vCBP has a critical role in virus virulence and pathogenesis, as deletion of the CBP encoding gene leads to a substantially diminished disease state (Fleming *et al*., 2017). The vCBP CBP, could offer potential as a broad-spectrum chemokine detector to be used in clinical diagnostics based on these characteristics.

1.4.i Hypothesis

The use of CBP will provide a dynamic tool for the detection of chemokines, with a greater sensitivity than antibodies which are specific for singular chemokines. The CBP will be able to be employed across both immuno-fluorescent cytology and enzyme-linked immunosorbent assay (ELISA) techniques for the detection of chemokines in their native state. The use of CBP will not prove functional in western blotting techniques as the chemokine is in a denatured state.

1.4.i Aims

Aim 1: To develop a fluorescently labelled CBP and assess the resulting impact on protein functionality.

- *Develop a protocol for conjugation of a fluorescent label to CBP.*
- *To assess the impact fluorescent conjugation to CBP in chemokine binding assays.*

Aim 2: To assess the efficacy of fluorescently labelled CBP in immuno-fluorescent cytology protocols.

- *Develop a protocol for an inflammatory assay characterised by inflammatory chemokine production.*
- *Compare the abilities of fluorescently labelled CBP with a fluorescently labelled chemokine-specific antibody to detect inflammatory chemokines in this assay.*

Aim 3: To assess the efficacy of CBP in Western blotting protocols.

- *Compare the abilities of fluorescently labelled CBP with a fluorescently labelled chemokine-specific antibody to detect an inflammatory chemokine by western blotting.*

Aim 4: To assess the efficacy of CBP in ELISA protocols.

- *Incorporate CBP into a capture ELISA protocol as a substitute for the capture antibody and assess its efficacy.*
- *Incorporate CBP into a capture ELISA protocol as a substitute for the detection antibody and assess its efficacy.*

2 Methods

2.1 Protein Production

2.1.i General reagents

Dulbecco's Modified Eagle Medium (DMEM) (pH 7.4) – 1 packet DMEM powder (Gibco #12800-017), 3.7g $NaHCO_3$, 4.77g Hepes, 1.5µL β-mercaptoethanol, 1L milliQ H_2O filter sterilised (0.25µm).

Dulbecco's Phosphate Buffered Saline (DPBS) – Dulbecco A PBS tablet (Oxoid Ltd) in 100mL milliQ H_2O filter sterilised (0.2µm).

293T Medium – 200mL DMEM containing 20mL foetal calf serum (FCS) (ThermoFisher) (heat inactivated at 56ºC for 30 minutes), 2mL PSK (100µg/mL penicillin, 100µg/mL streptomycin sulphate, 120µg/mL kanamycin sulphate), 400µL hygromycin B 50mg/mL).

293T Serum Free Medium – 200mL DMEM containing 200mg bovine serum albumin (BSA) (Sigma) 2mL PSK.

Freezing Solution – 90% FCS (heat inactivated), 10% Dimethyl sulfoxide (DMSO) (Invitrogen), filter sterilised.

2.1.ii Cell line

Human embryonic kidney (HEK)-293T - Transformed HEK-293 cell line stably expressing FLAG-tagged ORFV NZ2 CBP from the pAPEX ORFV 112 CBP plasmid (Seet *et al*., 2003).

The cell line was stored in liquid nitrogen, then revived through thawing in a 37ºC water bath. Cells were then transferred into 10mL of 293T media, centrifuged at 300g for 5 minutes, and

media was removed leaving pelleted cells. Cells were then re-suspended in 12mL of media and transferred into T75cm^2 tissue culture flasks for bulking.

All cells were maintained in T175cm^2 tissue culture flasks in applicable medium at 37ºC with 5% CO_2.

For freezing, cells were centrifuged at 300g for 5 minutes, followed by resuspension in freezing solution, at a concentration of 1x10^7 cells per mL. Cells were then aliquoted into 1mL freezing tubes and stored in liquid nitrogen.

2.1.iii Production of CBP

For protein production, CBP expressing HEK-293T cells were grown until reaching 80% confluency, in T175cm^2 flasks. Upon desired level of confluency, cells were gently washed with warmed DPBS. Fresh, warmed serum free medium was then added, to allow for the protein to be produced in the absence of chemokines found within the FCS. Cells were incubated for 3 days before supernatant was collected and stored at -80ºC for later protein purification.

2.2 Protein Purification and Concentration

2.2.i General reagents

Tris-buffered Saline (TBS) (pH 7.4) – 8g NaCl, 0.2g KCl, 3g Tris-base, in 1L milliQ. Adjust to pH 7.4 using HCl.

TBS/T – TBS containing 0.02% Tween 20.

TBS-G-A – TBS containing 50% glycerol and 0.02% sodium azide.

5M NaCl – 146.1g NaCl, in 500mL milliQ.

10X PBS – 80g NaCl, 2g KCl, 11.35g $Na_2H_2PO_4$, 2g KH_2PO_4, in 1L milliQ.

1X PBS – 100mL 10X PBS, in 900mL milliQ.

Glycine (pH 3.5) – 3.75g glycine, in 500mL milliQ.

2.2.ii Anti-FLAG immunoprecipitation

Cell supernatant containing the FLAG-tagged CBP (200mL) was adjusted for optimal purification by the addition of 6mL 5M NaCl, and adjustment of pH to 7.0 using 1M HCl. Supernatant was then decanted into four 50mL samples. Gravity flow columns (Biorad) were rinsed with 1mL TBS twice followed by the addition of 200µL of Anti-FLAG® M2 affinity gel (Sigma), and another TBS wash. Beads were then washed with glycine (room temperature) thrice, ensuring glycine is not exposed to beads longer than 20 minutes, followed by five cold 4ºC TBS washes, leaving 1 mL. Remaining beads suspended in TBS were mixed, and 50µL was added to each 50mL supernatant sample. Supernatant was rotated with the M2 beads for 2 hours at room temperature. Supernatant was then centrifuged at 300g or 5 minutes at 4ºC, with the top 45mL of supernatant removed, and stored at -80ºC for later re-immunoprecipitation. Remaining supernatant was run through the affinity column, followed by three 1mL TBS/T washes, leaving the final TBS-T in the column, which was sealed then rotated for 10 minutes. For protein elution, 25µL of FLAG-peptide (Sigma; 5mg/mL) was added with 1mL of TBS/T to affinity column, then rotated for 10 minutes. Protein was then eluted for collection, and concentration. Each supernatant sample was immunoprecipitated 4X, for protein collection.

2.2.iii Protein concentration

Vivaspin (500µL; 10kDa molecular weight cut off) centrifugal concentrators (Sartorius) were prepared for the concentration of purified CBP. The concentrators were first dialysed with milliQ, then blocked with 500µL 1% BSA in DPBS at room temperature, for 1 hour. Concentrators were then washed with 200µL DPBS 3X. Purified protein in TBS/T was then added, and centrifuged at 10,000g at 4ºC until remaining volume was under 30µL. The protein

eluate was then buffer-exchanged, by adding 100µL DPBS to concentrator, and centrifuged until the remaining volume was under 30µL twice. Concentrated protein was stored at -80ºC for later quantification.

2.3 Conjugation of Fluorophore

DyLight®594 NHS Ester fluorophore (ThermoFisher) was added to DPBS. Desired amounts of both fluorophore and protein were then combined (total 100µL), vortexed for 5 seconds, and incubated for 1 hour (in dark), at room temperature. Fluorophore-labelled protein was added to dialysed and pre-blocked concentrators (refer to 2.2.iii) then centrifuged at 10,000g until 50µL remained. DPBS was then added to increase the volume to 100µL, which was then spun down to 50µL. Remaining protein in DPBS was then carefully removed, and aliquoted for storage at -80ºC.

For this research, varying degrees of fluorophore present on CBP was required, utilising varying amounts of fluorophore. For each reaction, 30µL of 0.3mg/mL of CBP was utilised. For antibody conjugation, protocol 1 was followed.

Protocol 1 utilised the highest amount of fluorophore preparation. A needle was added to the fluorophore vial, ensuring approximately 3mm coverage. The dye on the needle was then added to 80µL of DPBS, with 70µL added to the CBP.

Protocol 2 utilised an intermediate amount of fluorophore. A 1 in 10 dilution was prepared from the fluorophore mix in protocol 1, of which 70µL was added to the CBP.

Protocol 3 utilised the lowest amount of fluorophore. The fluorophore mix from protocol 1 was diluted to 1 in 100 in DPBS, with 70µL added to the CBP.

Degree of fluorophore conjugation was then determined using the DeNovix DS-11 FX^{+} spectrophotometer and fluorometer. After inputting the extinction coefficient of the protein

(obtained via imputing protein amino-acid sequence in ProtParam, via ExPASy), 2µL of conjugated protein was placed in the fluorometer. Absorbance was then read at 280nm (for protein concentration) and a pre-set 594nm fluorophore absorbance, for quantitation of fluorescent conjugation.

2.4 Protein Analysis

2.4.i General reagents

Resolving Buffer (pH 8.8) – 27.23g Tris base, in 150mL milliQ (pH achieved using HCl).

Stacking Buffer (pH 6.8) – 6g Tris base, in 100mL milliQ (pH achieved using HCl).

Sample Buffer – 8.4mL 0.05% bromophenol blue, 2mL 0.5M Tris-HCl, pH 6.8, 1.6mL glycerol, 3.2mL 10% SDS.

Reducing Sample Buffer – 1mL sample buffer, 50µL β-mercaptoethanol (2-ME).

10X Running Buffer – 30g Tris, 144g glycine, 10g SDS, make up to 1L with milliQ.

10X Transfer Buffer – 25mM Tris, 192M glycine, 20% methanol, make up to 1L with milliQ.

Wash Buffer – 1L 1X TBS, 2mL 10% Tween 20.

Blocking Buffer – 20mL wash buffer, 1g skimmed milk powder (Pams).

Coomassie blue stock – 4mL ortho-phosphoric acid, 20g $(NH_4)_2SO_4$, 4mL CB-G250 dye (Sigma), 192mL milliQ.

Coomassie blue – 20mL Coomassie blue stock, 5mL methanol.

Ponceau S – 1g Ponceau S (Sigma), 50mL acetic acid, in 1L milliQ.

2.4.ii SDS-PAGE

Gels were made and run using a Mini-Protean Tetra system from Bio-Rad. SDS-PAGE gels were prepared, using the gel mixture outlined in Table 3. Gels were layered, with equal sized 15% and 10% sections, with 3% utilised for the stacking portion. Protein samples were diluted 1 in 2 by adding reducing sample buffer, followed by boiling for 15 minutes. Samples were loaded with 3µL full-range rainbow marker (Amersham, RPN800E) loaded into the far left well. The gels were run at 100V for 2 hours in 1X running buffer.

Table 3. *SDS-PAGE acrylamide gel mixtures.*

	Upper Stacking Gel	**Lower Resolving Gel**	
	3%	10%	15%
Distilled Water	3.25mL	3.47mL	1.8mL
10% SDS	50µL	100µL	100µL
50% Glycerol	-	200µL	200µL
Resolving Buffer	-	2.5mL	2.5mL
Stacking Buffer	1.25mL	-	-
30% Acrylamide/Bis Solution (BioRad)	0.5mL	3.33mL	5mL
10% Ammonium Persulphate	30µL	60µL	60µL
TEMED	15µL	30µL	30µL

For protein quantification, both purified protein and a known concentration of carbonic anhydrase (CA) were diluted 1 in 2, in sample buffer, boiled for 15 minutes, and loaded onto the gel. Varying volumes of samples were added to SDS-PAGE gels (20, 8, and 3 µL), and resolved on the gel.

2.4.iii Coomassie blue staining

Proteins resolved by SDS-PAGE gels were stained using Coomassie blue overnight shaking, at room temperature. Coomassie blue was then removed, and gels were washed 5X in milliQ, with the final wash lasting at least 30 minutes. Gels were then imaged using the BioRad GS-710 calibrated imaging densitometer.

Coomassie blue stain allowed for the assessment of the protein density of samples. Image J was used to find the integrated density of the protein bands, utilising gel background as control. A standard curve was obtained using the known concentration and optical density of CA. The associated density of the unknown samples was extrapolated against the standard curve, allowing for the quantification of the protein density, therefore, the concentration.

2.4.iv Western blotting

Sponge pads, blotting papers, nitrocellulose membrane (0.45µm) (Hybond-C Extra; GE Healthcare Life Sciences), and (unstained) SDS-Page gel were soaked in cold 1X transfer buffer for 15 minutes. After assembly of western transfer apparatus (Bio-Rad), the transfer was run at 100V for 1 hour in cold 1X transfer buffer.

For Ponceau S staining, 10mL of Ponceau S was added, and incubated for 5 minutes, at room temperature. Membranes were then lightly rinsed with 10mL milliQ 3X, before imaging using the BioRad Versadoc MP imager. For fluorescent protein analysis, blots were imaged immediately after transfer process had ended.

For anti-FLAG western blotting nitrocellulose membranes were incubated in blocking buffer, overnight, at 4°C. After incubation, nitrocellulose membranes were washed in 10mL wash buffer, 3X, for 5 minutes, followed by the addition of anti-FLAG antibody (Table 4) diluted in wash buffer. Membranes were then incubated for 2 hours, shaking (in dark), at room temperature. After incubation, membranes were washed 3X with 10mL wash buffer, for 5 minutes. Membranes were then developed using Pierce SuperSignal Chemiluminescent substrate for 5 minutes immediately prior to imaging. Developed membranes were imaged using the BioRad Versadoc MP imager.

For western blotting with the labelled CBP and anti-CCL2 antibody (Table 4), nitrocellulose membranes containing *E. coli* expressed recombinant human CCL2 (R&D) were incubated in

blocking buffer, overnight, at 4°C. After incubation, nitrocellulose membranes were washed in 10mL wash buffer, 3X, for 5 minutes, followed by the addition of CBP or antibody diluted in wash buffer. Membranes were imaged using the BioRad Versadoc MP imager.

Table 4. *List of the antibodies and proteins utilised across several forms of western blotting protocols.*

Name	Host	Target	Conjugate and substrate	Dilution	Imaging
Anti-FLAG M2-Peroxidase (HRP) (Sigma)	Mouse M2	FLAG-Tag	HRP and Pierce chemiluminescent substrate.	1:2000	Colourmetric
Anti-CCL2 antibody (ThermoFisher)	Mouse (2H5)	Mouse CCL2	DyLight®594 (Saturated)	275nM - 69nM.	Fluorescent
CBP (Custom)	Orf virus strain NZ2	Mouse CCL2	DyLight®594 (Saturated)	275nM - 69nM.	Fluorescent

2.5 Enzyme-Linked Immunosorbent Assays (ELISAs)

2.5.i General reagents

Coating buffer (pH 6.5) – 1.249g Na_2HPO_4, 1.547g NaH_2PO_4, made up to 100mL milliQ, stored at 4ºC.

Coating buffer (pH 9.6) – 1.59g Na_2CO_3, 2.43g $NaHCO_3$, made up to 100mL milliQ, stored at 4ºC.

Blocking buffer – 100mL 1XPBS, 1g BSA.

PBS/T – 1L 1X PBS, 5mL 10% Tween 20.

Stopping solution – 0.16M H_2SO_4.

2.5.ii Direct binding ELISA for determining chemokine/cytokine concentration in samples

A direct binding ELISA technique was used to examine the presence of chemokine or cytokine within a sample.

The ELISA protocol was adapted utilising the BD commercial method for ELISA (BD Biosciences, 2019). Maxisorp 96-well flat-bottomed ELISA plates (ThermoFisher) were incubated with chemokine or cytokine capture antibody in relevant coating buffer, overnight, at 4ºC (Table 5). Plates were washed with PBS/T between each step/incubation. Plates were then blocked using 100µL of blocking buffer for 1 hour at room temperature.

Table 5. *Cytokine and chemokines used in ELISA protocols, including dilution factor.*

		ELISA Kits				
Chemokine/Cytokine	Species	ELISA Kit Number	Standard Working Concentration	Coating Buffer	Capture Antibody Dilution	Detection Antibody Dilution
CCL2/MCP-1	Mouse	BD #555260	2,000pg/mL	pH 6.5	1:100	1:100
CCL2/MCP-1	Human	BD #555179	2,000pg/mL	pH 9.6	1:200	1:200
CCL5/RANTES	Human	R&D DY478	4,000pg/mL	PBS (pH 7.4)	1:200	1:200
CXCL8/IL-8	Human	BD #555244	4,000pg/mL	pH 9.6	1:100	1:100
CXCL2/MIP-2	Mouse	R&D DY452	4,000pg/mL	PBS (pH 7.4)	1:50	1:25
CXCL4/PF4	Human	Individually sourced (R&D)	4,000pg/mL	PBS (pH 7.4)	1:100	1:100
CXL1/Lymphotactin	Human	Individually sourced (R&D)	32,000pg/mL	PBS (pH 7.4)	1:50	1:25
TNFα	Human	BD #555212	1,000pg/mL	PBS (pH 7.4)	1:500	1:250

Supernatant samples were then added to the coated plate, incubated for 15 minutes, shaking, at 37ºC. After incubation, supernatant was removed, and premixed detection antibody and 1 in 40 dilution of SA-HRP was added to each well, and incubated for 1 hour, at room temperature (in dark). Later, TMB substrate was added, followed by incubation in the dark until the colour develops. Reaction is stopped using stopping solution. Absorbance of the plate is then read at 450nm to determine captured chemokine or cytokine concentration.

For analysis, a standard curve was created based upon known chemokine concentration. Utilising the standard curve, the concentration of chemokine remaining in the samples was determined. Data was then presented as chemokine concentration.

2.5.iii Indirect chemokine binding ELISA as a measure of CBP activity

An indirect binding ELISA was utilised to examine the binding profile of CBP, specifically the ability of CBP to bind soluble chemokine.

All ELISAs utilised, were based on the R&D commercial method (R&D Systems, 2019). Maxisorp 96-well flat-bottomed ELISA pates were incubated with capture antibody, in relevant coating buffer, overnight, at 4ºC (Table 5). Plates were washed with PBS/T between each step/incubation. Plates were then blocked using 100µL of blocking buffer, for 1 hour, at room temperature.

A serial dilution was prepared for the CBP, which was then incubated with relevant chemokine standard at the working concentration (Table 5), in a non-absorbent 96-well plate for 45 minutes, at 37ºC, shaking. The CBP-chemokine mix, and a doubling dilution of the chemokine standard were then transferred to the coated ELISA plate, and incubated for 15 minutes, shaking, at 37ºC. Captured chemokine was detected via addition of relevant detection antibody conjugated with horseradish peroxidase and incubated for 2 hours, at room temperature (Table 5). TMB substrate was then added, followed by incubation in the dark for up to 30 minutes, or until colour developed. Reaction was stopped using stopping solution. Absorbance of the plate is then read at 450nm to determine captured chemokine concentration.

For analysis, a standard curve was created based upon known chemokine concentration. Utilising the standard curve, the concentration of chemokine remaining in the samples was determined. Data was then presented as a percentage of unbound chemokine.

2.5.iv Indirect binding ELISA, with CBP substituted for the detection antibody

A modified version of an indirect binding ELISA was designed to examine the potential ability of CBP to bind chemokine captured by the pre-coated, capture antibody. In this case, after coating and overnight incubation, the standard dilution series and working concentration of chemokine was added and incubated for 15 minutes, shaking, at 37ºC. A serial dilution series of CBP was then added to wells, followed by another 15-minute incubation, shaking, at 37ºC. ELISA was then continued following the indirect binding ELISA protocol.

For analysis, a standard curve was created based upon known chemokine concentration. Utilising the standard curve, the concentration of chemokine remaining in the samples was determined. Data was then presented as a percentage of unbound chemokine.

2.5.v Direct binding ELISA, with CBP substituted for the capture antibody

A modified version of a direct binding ELISA was designed to examine the potential ability of CBP to be utilised as a substitution for the capture antibody. In this case, wells were coated with 1µg/mL of CBP in PBS and incubated overnight, at 4ºC. Selected dilution series of chemokine standard were added to plates. Protocol after addition of standard is identical with the previously described direct binding ELISA protocol.

For analysis, a standard curve was created based upon known chemokine concentration. Utilising the standard curve, the concentration of chemokine remaining in the samples was determined. Data was then presented as a percentage of unbound chemokine.

2.6 Immunofluorescence

2.6.i General reagents

Roswell Park Memorial Institute Medium (RPMI) (pH 7.4) – 1 packet RPMI powder (Gibco #31800-022) 2.0g $NaHCO_3$, 4.77g Hepes, 1.5µL β-mercaptoethanol, 1L milliQ H_2O filter sterilised (0.25µm).

THP-1 Medium – 200mL RPMI containing 20mL FCS (heat inactivated at 56ºC for 30 minutes), 2mL PSK, 2mL 100mM Sodium Pyruvate.

TBS (pH 7.6) - Tris-buffered Saline (TBS) (pH 7.4) – 8g NaCl, 0.2g KCl, 3g Tris-base, in 1L milliQ. Adjust to pH 7.6 using HCl.

Lipopolysaccharide (LPS) (Escherichia coli 055:B5, Sigma) – LPS diluted in DPBS.

Phorbol 12-myristate 13-acetate (PMA) (Sigma) – Diluted in DPBS.

Methanol – 100% methanol, used at -20ºC.

10% Triton X - Triton™ X-100 (Sigma), diluted 1 in 10 in milliQ.

4',6-diamidino-2- phenylindole (DAPI) (D3571, Intrivtrogen) - 75 nM, diluted in diluent.

Diluent – TBS, 1% BSA, 0.5% 10% Triton X.

2.6.ii Cell line

THP-1 – Human monocytic cell line derived from an acute monocytic leukaemia patient (Bosshart and Heinzelmann, 2016).

The cell line was stored in liquid nitrogen, then revived through thawing in a 37ºC water bath. Cells were then transferred into 10mL of THP-1 medium, centrifuged at 300g for 5 minutes,

and media was removed leaving pelleted cells. Cells were then re-suspended in 12mL of media, and transferred into T75cm^2 tissue culture flasks for bulking.

THP-1 cells were grown in T75cm^2 flasks. Upon desired cell concentration, cells were centrifuged at 300g for 5 minutes, followed by removal of supernatant. Pelleted cells were then re-suspended in fresh media for assay use.

For freezing, cells were centrifuged at 300g for 5 minutes, followed by resuspension in freezing solution, at a concentration of 1x10^7 cells per mL. Cells were then aliquoted into 1mL freezing tubes and stored in liquid nitrogen.

2.6.iii Cell stimulation

Human THP-1 cells, a monocyte cell line, were used for immunofluorescent analysis. Cells were seeded at 1x10^5/mL media cells per well, containing sterile coverslips. Cells were then treated with PMA (5ng/ml), or no PMA. After 24 hours, 500µL of media was removed, and replaced with either 500µL of media containing 100ng/mL of LPS, or plain media. Cell supernatant was collected at 3, 6, and 24 hours post-LPS treatment. Supernatant was centrifuged at 300g for 5 minutes to remove cellular debris, and supernatant was stored at -80^{o}C for later analysis. Immediately post-supernatant collection, cells were washed with warmed, sterile PBS.

2.6.iv Cell fixation and permeabilisation

Cells were then fixed in ice cold, 100% methanol for 10 minutes. Methanol was then removed, and remainder allowed to evaporate. PBS was removed and then cells were permeabilised using 0.1% Triton in PBS, for 10 minutes. After permeabilisation, cells were gently washed with 1mL PBS, 3X. Fixed cells were then stored at 4^{o}C until further use.

2.6.v Incubation with fluorophore-conjugated anti-CCL2 antibody or CBP

For staining, 200µL of diluent-diluted antibody or CBP was added to each well, and incubated for 2 hours, at room temperature, followed with incubation overnight (in dark), at 4ºC.

After incubation, 100µL of DAPI diluted in diluent was added, and incubated for 30 minutes, at room temperature in the dark. After incubation, cells were washed 3X with TBS.

After staining, coverslips were placed on a 5µL of SlowFade™ Gold Antifade Mountant (ThermoFisher), face down, on glass slides. Slides were then stored at 4ºC in the dark, for up to 3 days. Coverslips were then imaged using 20X magnification on an Eclipse Ni-E upright fluorescence microscope and NIS-Elements D Software (Nikon, Tokyo, Japan).

2.6.vi Competition with fluorophore-conjugated antibody or CBP

To prevent binding of the labelled antibody or CBP to chemokines within cells, two approaches were taken.

Firstly, cells were pre-incubated with unlabelled antibody or CBP (2µM) 2 hours, at room temperature, followed with incubation overnight (in dark), at 4ºC. After incubation, liquid was removed, and protocol was continued following the previously outlined method (2.6.v). Following washing steps, the labelled antibodies and CBP were added and detected as described above.

Alternatively, the labelled antibody or CBP were pre-incubated with 4-fold molar excess of *E. coli* expressed recombinant human CCL2 (R&D) or heparin sodium salt sourced from porcine intestinal mucosa (BioReagent) (heparin) for 5 minutes, shaking at 37ºC, in the dark. The solution was then added to cells, incubated and detected following the previously outlined method (2.6.v).

2.6.vii Quantitation of immunofluorescence

Replicates of 5 merged images were taken at random per coverslip (1 red (A) + 1 blue (B) per technical replicate) (Figure 2). Images were analysed using Fiji, utilising threshold measurement, determining the area of staining. Stacked images were analysed separately, where the threshold was set, based upon visible comparison between coloured particles. After data collation, the area value of fluorescence (red) was divided by the area value of DAPI staining (blue). This value was recorded as the relative fluorescence. Replicates of 5 values were averaged per coverslip, providing one biological replicate. Three replicates were obtained per treatment and presented as a mean relative fluorescence value. Images were presented as a layered image (C) of both (A) and (B).

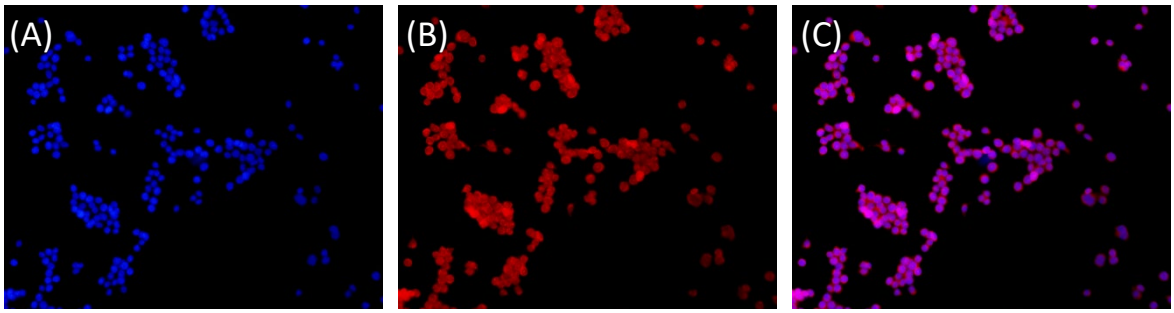

Figure 2. Immunofluorescent images utilised for Fiji analysis. (A) image representing DAPI stain, imaged at 400nm. (B) representing Dylight®594 fluorescence, imaged at 595nm. (C) represents a merged image of both (A) and (B).

2.7 Statistical Analysis

All data within this study was analysed using GraphPad Prism 6. Data was presented as mean ± SEM. Based upon the comparison, either T-test, 1-way ANOVA, or a 2-way ANOVA was utilised (appropriate test reported in figure legend). If appropriate, and significance was achieved, a Bonferonni post-hoc test for multiple comparisons was used. Significance was reported at $p < 0.05$.

3 Results

Chemokines are expressed during inflammation, and their detection can be useful diagnostically. Viral CBPs exhibit broad chemokine selectivity and high affinity, so may be able to detect chemokines in inflamed blood or tissues in a manner similar to diagnostic antibodies. The aim of this thesis was to develop a vCBP as a diagnostic tool and test it in situations in which antibodies have shown to be effective. The vCBP chosen for this work was from ORFV strain NZ2, as it is capable of binding across three classes of chemokine with high affinity (Counago *et al*., 2015: Lateef *et al*., 2009; Lateef *et al*., 2010). First, CBP was conjugated to a fluorescent dye and assessed for potential impact upon CBP function. Secondly, labelled CBP was evaluated for its use in direct immuno-fluorescent cytology. Next, labelled CBP was evaluated for its use in western blotting protocols. Finally, the native CBP was evaluated for its use in ELISAs.

3.1 CBP in Immunofluorescent Cytology

For use in cytology CBP needs to be detectable in a system, of which can be achieved through conjugation of a fluorescent protein. In this research, the logistics of fluorescent conjugation were assessed, specifically its impact on protein functionality. Next, an inflammatory immunological assay was developed to directly compare between a labelled antibody and the labelled CBP for detection. Several factors were assessed, including the specificity of binding to inflamed cells by the antibody and the CBP.

3.1.i Conjugation of DyLight®594 to CBP

To aid detection with a fluorescent microscope, a Dylight®594 dye was conjugated onto the CBP. A DyLight® dye was chosen as it has successfully been introduced to anti-rabbit IgG antibodies previously, and was shown to successfully function as a secondary antibody for the

detection and characterisation of CCL2 expression in rat brain sections (Das *et al*., 2011). Analysis of the CBP structure showed that 12 out of 13 primary amine-containing amino acids (lysines) on the protein's surface were peripheral to the previously reported binding site for the CC chemokine MCP-1 (CCL2) (Counago *et al*., 2015; Figure 3). NHS ester-activation was therefore used to conjugate the dye to the surface of the CBP.

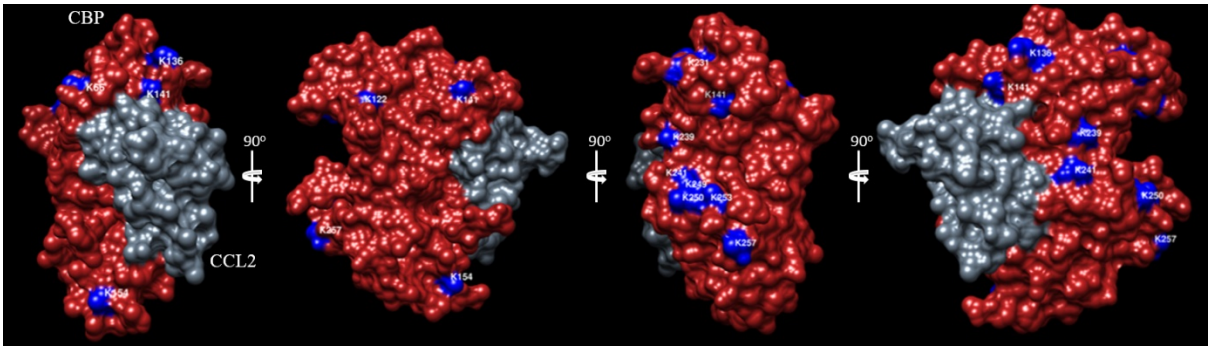

Figure 3. Visualisation of lysine residues of the CBP-CCL2 complex. Figure displays all primary amine/lysine (blue) residues on the surface of *orf virus* CBP (red) available for conjugation. CBP is complexed with CCL2 (grey), to determine potential impact of fluorescent dye conjugation. Figure is rotated 90° around the y-axis, completing a 360° view. Proteins modelled using UCSF Chimera, based on PDB file 4ZK9.

However, labelling of residue K141, or even potentially K241 adjacent to the chemokine binding domain could interfere with chemokine binding, so protocols were developed to achieve both saturating and sub-saturating levels of dye conjugation. Theoretically, conjugation of a saturated level of DyLight®594 to CBP would allow for easiest to detection of the protein in fluorescence assays. Whereas conjugation of a minimal level of dye, would be least likely to impede on chemokine-CBP interactions. The efficiency and reliability of the Dylight®594 conjugation protocols were then assessed.

Prior to dye conjugation with CBP, conjugation protocols were trialled using a test protein, BSA. Three protocols were developed in which varying amounts of Dylight®594 dye was added (see methods section 2.3). To determine the successfulness of the conjugation protocols, the labelled proteins were resolved by SDS-Page under reducing conditions with the abundance and fluorescence of the proteins were assessed (Figure 4). Ponceau S staining of the membrane revealed bands at the correct molecular weight for BSA (66kDa; Figure 4A). Also noting that

equivalent amounts of BSA from each labelling protocol were visualised in lanes loaded with equivalent amounts of protein (Figure 4A). The amount of fluorescence associated with the BSA also correlated with the amount added into the conjugation reaction, as the highest fluorescence was seen with protocol 1, intermediate fluorescence with protocol 2, and barely detectable fluorescence with protocol 3 (Figure 4B). There was no visible fluorescence observed for the unlabelled BSA (Figure 4B).

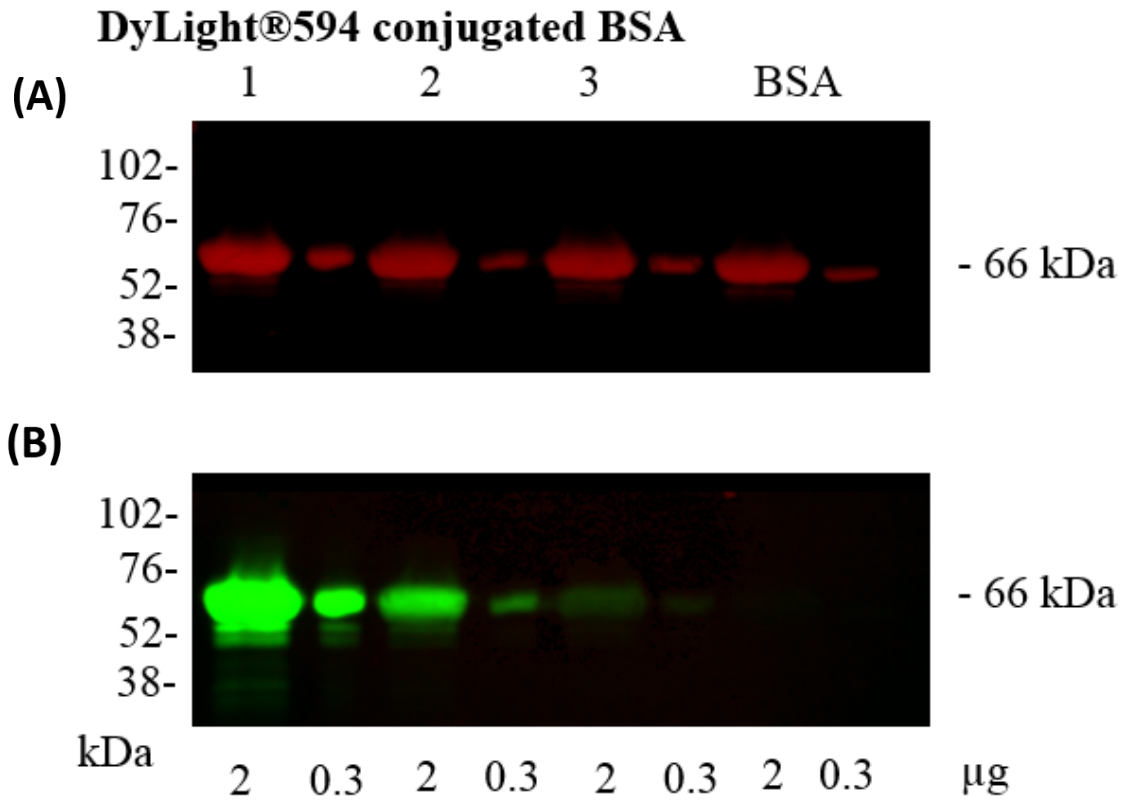

Figure 4. DyLight®594 conjugation to bovine serum albumin (BSA). BSA was conjugated with Dylight®594 dye using three different protocols, each using decreasing amounts of dye (1-3). Conjugated and non-conjugated proteins, at the amounts indicated, were resolved by SDS-Page then transferred to a membrane. **(A)** Proteins on the membrane were identified by Ponceau S staining. **(B)** Fluorescent dye on the protein was detected by fluorescent imaging using a 610BP filter, for fluorescence between 593 and 618 nm.

The three conjugation protocols were then used on CBP. The labelled proteins were resolved by SDS-Page under reducing conditions, with the abundance and fluorescence of the proteins assessed (Figure 5). Coomassie blue staining of the gel revealed bands at molecular weights consistent with the CBP monomer (48 kDa) and the CBP dimer (80kDa; Figure 5A). The expected molecular weight for the CBP is however 35 kDa, although glycosylation of the

protein has been reported to add up to 25 kDa (Counago *et al*., 2015). As the CBP protein was engineered with a C-terminal FLAG-tag, proteins were also detected by western blotting with an anti-FLAG antibody (Figure 5B); with the size of the bands detected being consistent with the monomeric form of the CBP. Equivalent amounts of CBP from each labelling protocol were observed with each method, and their sizes appeared equivalent (Figure 5A-B). The amount of fluorescence associated with the CBP again correlated with the amount added into the conjugation reaction, as the fluorescence was highest with protocol 1, and lowest with protocol 3 (Figure 5C). Both the monomer and dimer of the CBP were labelled with each protocol. There was no visible fluorescence observed for the unlabelled CBP (Figure 5C).

The number of DyLight®594 molecules conjugated to CBP following each protocol was then assessed using fluorescence spectrophotometry. The emission spectrum was adjusted to account for the extinction coefficient of CBP; and is presented across equivalent concentrations of conjugated and un-conjugated proteins (Figure 6). There was no indication of fluorescence in the range of DyLight®594 excitation/emission (593-618 nm) for the unlabelled CBP. This process was repeated for at least three batches of CBP, prepared using each of the three protocols, thereby obtaining the mean number of DyLight®594 molecules per CBP ± SEM (Table 6). Following protocol 1, 10 ± 1.69 DyLight®594 molecules were detected on each CBP, although the batch indicating an average of 13.68 was utilised for further testing. This indicates complete saturation of the lysine residues was achieved. Following protocol 2, 4.41 ± 1.26 DyLight®594 molecules were detected on the CBP, although the batch indicating an average of 6.42 was utilised for further testing, where approximately half of the lysine residues were labelled. Following protocol 3, there were 1.28 ± 0.46 DyLight®594 molecules detected per CBP, and a batch reaching 0.89 was utilised for further testing which meant that not every CBP was labelled.

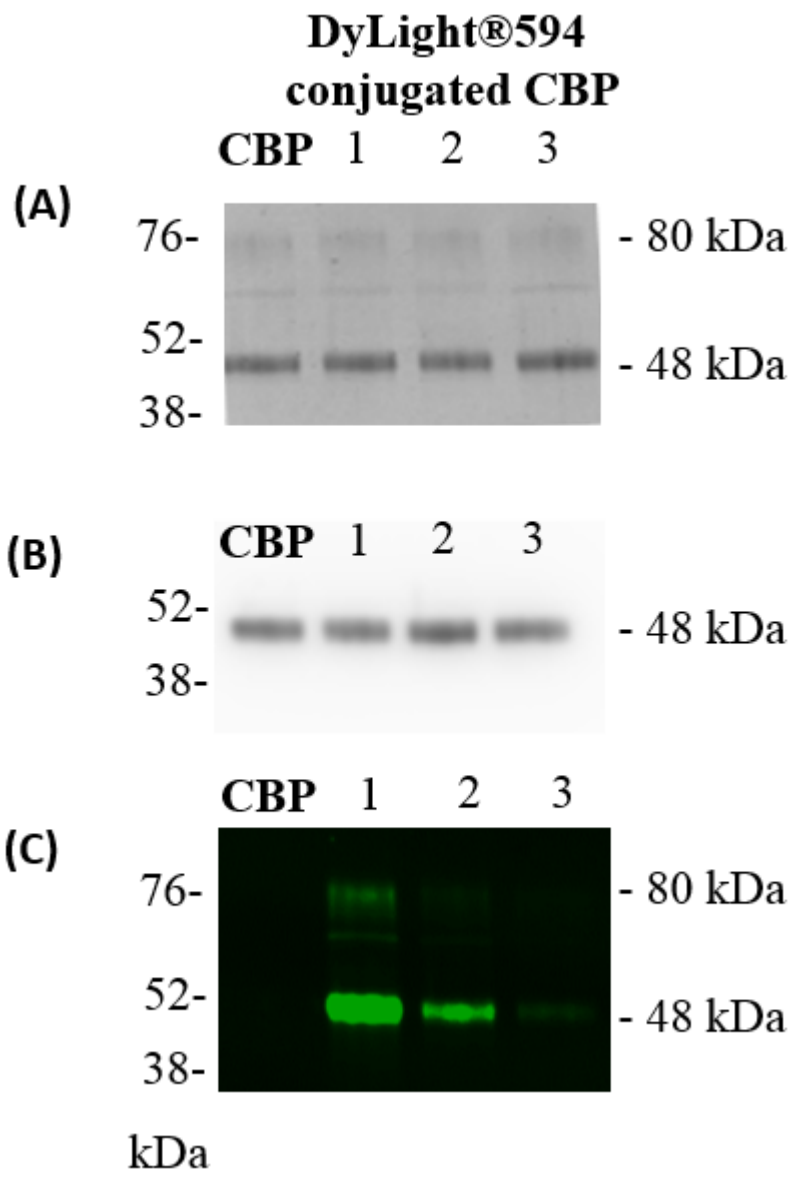

Figure 5. DyLight®594 conjugation CBP. CBP was conjugated with DyLight®594 dye using the three different protocols (1-3). Proteins (300ng per well) were resolved by SDS-Page then transferred to a membrane. Proteins were then identified by (A) Coomassie blue staining or by (B) Western blot analysis using an anti-FLAG (M2) antibody. (C) Fluorescent dye on the protein was detected by fluorescent imaging using a 610BP filter, for fluorescence between 593 and 618 nm.

Table 6. *Reproducablility of the conjugation protocols, for fluorescent conjugation at saturating, and subsaturating levels.*

	DyLight®594 molecules per CBP molecule			
Conjugation protocol	CBP batch 1	CBP batch 2	CBP batch 3	Mean ± SEM
1	13.68	8.34	8.87	10.30 ± 1.69
2	6.42	2.10	4.70	4.41 ± 1.26
3	0.89	0.76	2.20	1.28 ± 0.46

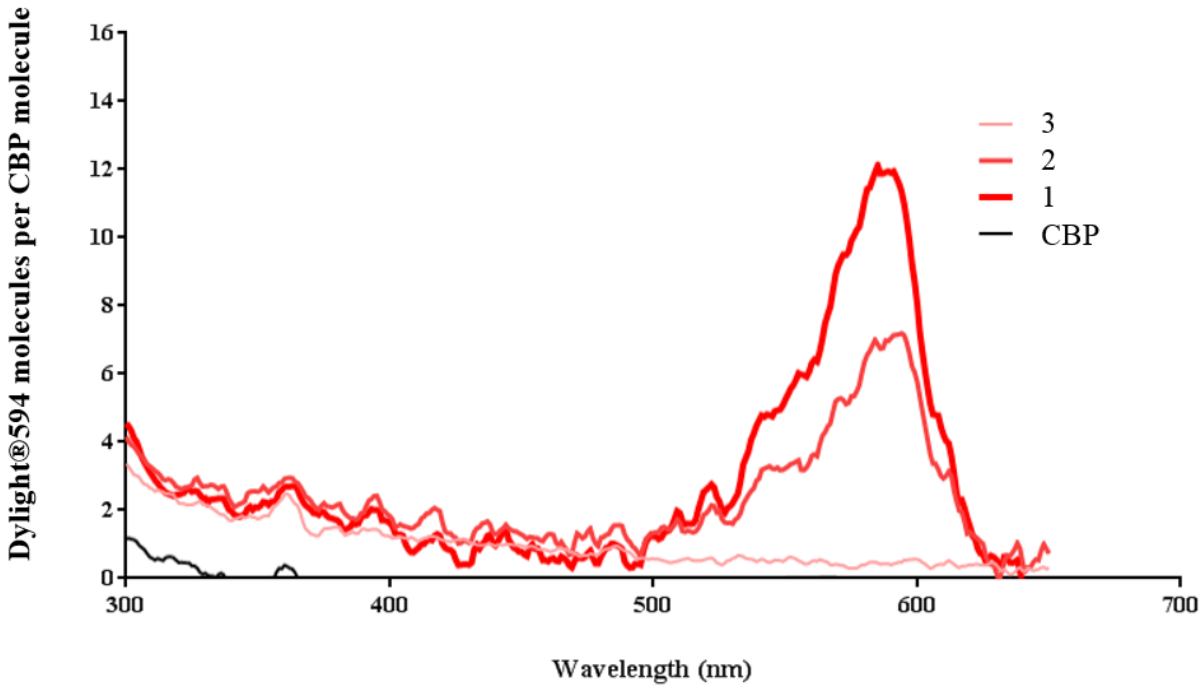

Figure 6. Quantitation of DyLight®594 molecules per CBP molecule. DyLight®594-conjugated CBP prepared using the three different protocols (1-3), and analysed using a fluorometer. The absorbance of each protein was taken at increments of 1nm in wavelength. The number of dye molecules per molecule of CBP was then calculated using the protein's extinction coefficient and emission spectra of DyLight®594.

3.1.ii Effect of DyLight®594 conjugation on CBP function

To examine the binding characteristics of DyLight®594-CBP, indirect chemokine binding ELISAs were utilised. This assay measures the loss of soluble chemokine through the competitive binding of CBP. It was shown that CBP inhibits, in a dose dependent fashion, the ability of the chemokine to be identified through antibody interactions, allowing for a means of detecting CBP efficacy (Figure 7).

This CBP has previously been shown to bind mCCL2 using surface plasmon resonance (SPR) (Lateef *et al*., 2009; Counago *et al*., 2015). Comparisons between unconjugated and conjugated CBP with saturating levels of DyLight®594, indicated there was no significant difference in mCCL2 binding, excluding at 2ng/mL (Figure 8A; $p > 0.05$). The CBPs with mid and low

levels of DyLight®594 conjugation showed no significant differences in mCCL2 binding compared to the unconjugated CBP (Figure 8B-C; $p > 0.05$). The only significant difference observed between labelled and unlabelled CBP was a suggested increase in efficacy of the labelled CBP. These findings suggest that the extent of dye conjugation does not substantially impact the binding characteristics of the CBP. In addition, the IC_{50} value for each labelled CBP was similar to native CBP, with exception to protocol 3 which indicated a higher affinity (1.2nM) (Table 7). Protocol 1 and 2 indicated IC_{50} values of 1.7 and 1.8 nM respectively, which was also similar to the observed affinity of native CBP (1.8nM).

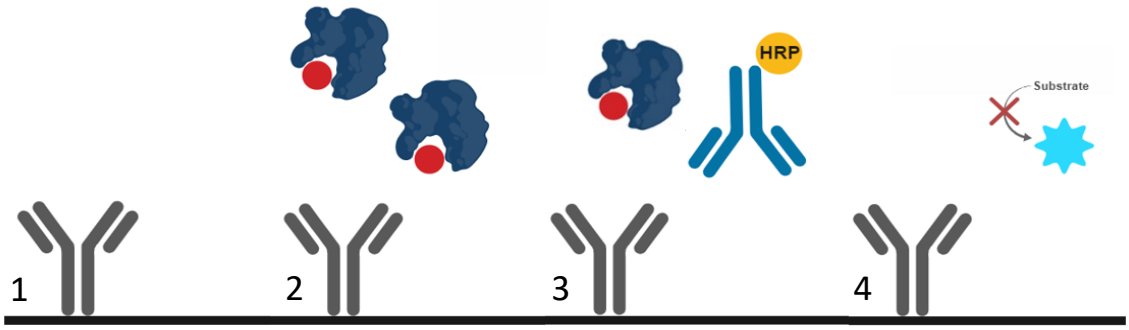

Figure 7. Competitive ELISA. Capture antibody (grey) was coated to the ELISA plate (1). Varying concentrations of CBP (Dark blue) was incubated with chemokine (red), before addition to capture antibody (2). Detection antibody (blue) conjugated with HRP (yellow) was then added (3). The presence of detection antibody was then detected by adding TMB (substrate), and the OD was taken at 450nm (4).

Table 7. *Summary of the determined IC_{50} values of CBP. Table displays the IC_{50} values (nM) of the CBP to chemokine ligands, adjusted to concentration of chemokine used, as determined via ELISA.*

	Degree of Conjugation			
Chemokine	CBP	1	2	3
mCCL2	1.8	1.7	1.6	1.2
hCCL2	0.8	1.0		
hCCL5	0.4	0.4		
mCXCL2	1.7	1.8		
hCXCL8	-	-		

CBP, 1, 2, and 3 represent conjugation protocol, as outlined in section 2.3.

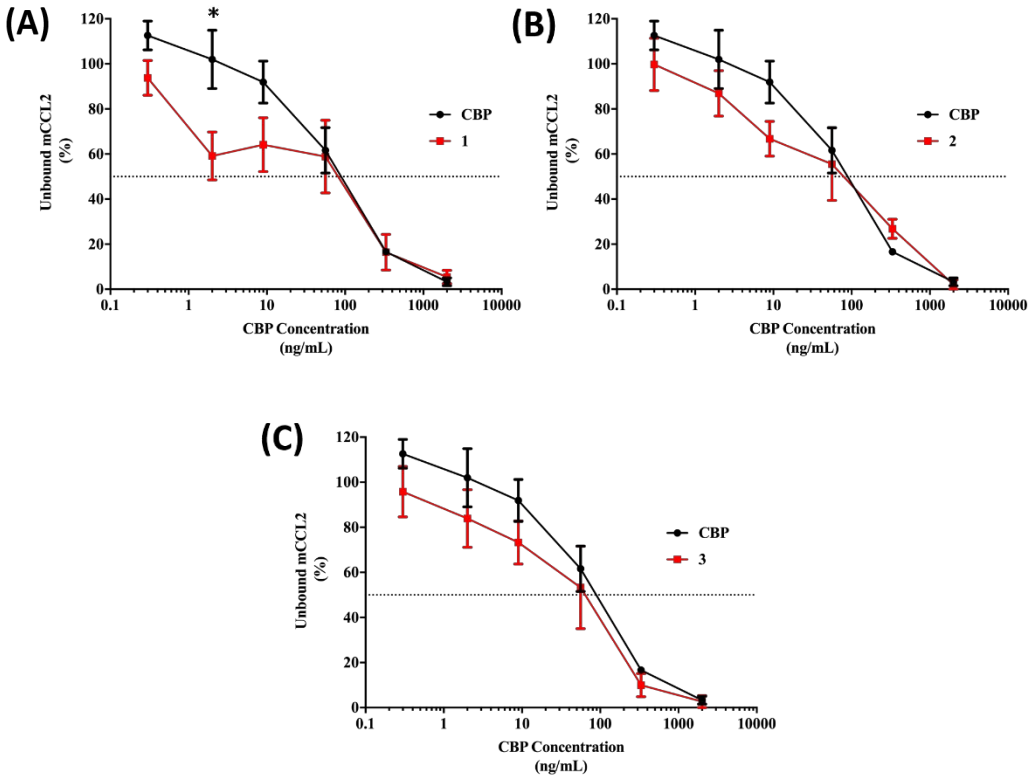

Figure 8. The extent of DyLight®594 conjugation does not alter CBP binding to mouse CCL2. Various concentrations of conjugated or native CBP were incubated with mouse CCL2. Unbound chemokine was then detected using a competition ELISA. **(A)** The conjugated CBP was prepared using protocol 1. **(B)** The conjugated CBP was prepared using protocol 2 **(C)** The conjugated CBP was prepared using protocol 3. Results are presented as the percentage of unbound chemokine, normalised to a CCL2 only control, without the presence of CBP. Values are expressed as mean ± SEM (n = 3). The data was analysed using two-way ANOVA, coupled with a Bonferonni post-hoc test for multiple comparisons. Significance between groups is denoted by an asterisk.

After establishing that there was no significant difference in CBP binding profile post dye saturation, indirect ELISAs were carried out on other chemokines, comparing non-conjugated CBP and saturated DyLight®594-CBP only. The chemokines investigated included hXCL1, hCCL2, hCCL5, hCXCL4, mCXCL2, and hCXCL8. All chemokines used for investigation have previously been shown to bind this CBP (Lateef *et al*., 2009; Counago *et al*., 2015; Sharif *et al*., 2016) with the exception of hCXCL8, which was included for use as a negative control.

Consistent with the binding profile for mCCL2, the DyLight®594-CBP did not substantially differ from the unconjugated CBP in its ability to bind hCCL2, the exception being at the lower concentrations tested (0.29ng/mL $p < 0.05$; Figure 9A). A similar profile of chemokine binding

was observed with hCCL5, where there were no differences in binding between the DyLight®594 conjugated and unconjugated forms of CBP, except for below 10 ng/mL ($p < 0.05$; Figure 9B). These findings suggest that the DyLight®594-CBP has a higher efficacy for chemokine binding. However, calculations of the IC_{50} for the CBP suggest the unconjugated and conjugated CBPs have equivalent binding affinities for both hCCL2 and hCCL5 (Table 7). There was no difference found between conjugated and unconjugated CBP in its ability to bind mCXCL2 across any concentrations ($p < 0.05$; Figure 9C). Consistent with previous CBP binding studies, dye conjugation did not potentiate any binding with hCXCL8 ($p < 0.05$; Figure 10). The binding for CXCL4 was also assessed, however findings failed to successfully indicate no binding (Supplementary Figure 1). The binding of XCL1 was also assessed, however no binding in the ELISA was shown indicating protocol/manufacture failure (data not included).

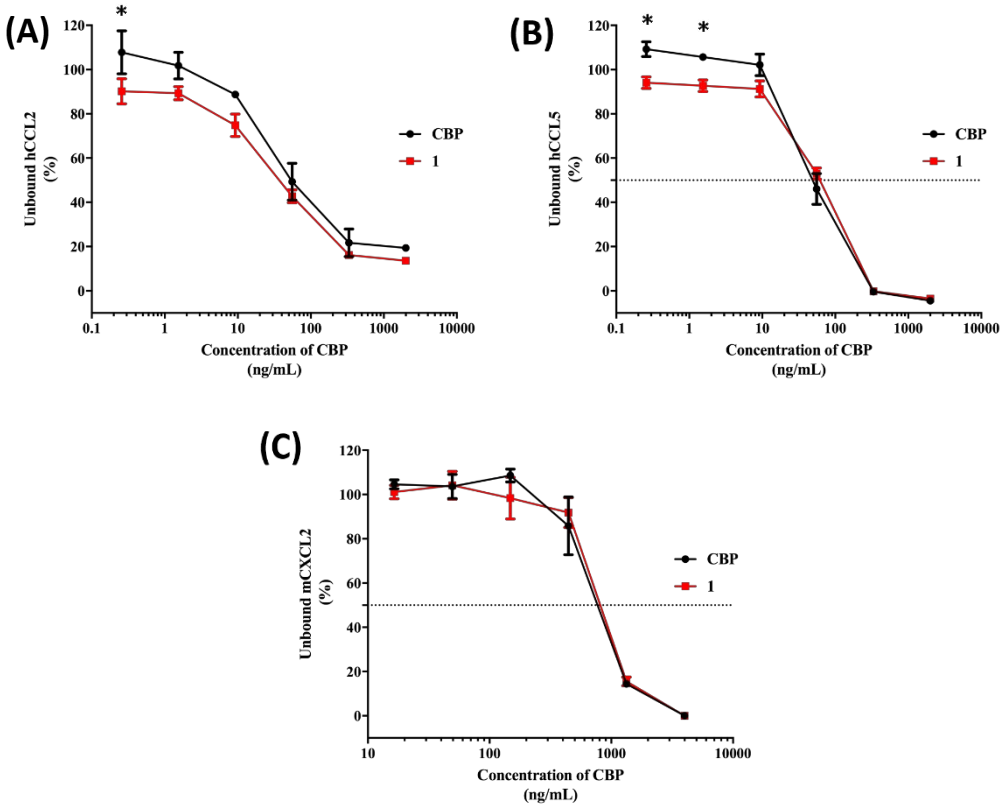

Figure 9. Saturation of CBP with DyLight®594 does not prevent binding to human chemokines CCL2 and CCL5. Various concentrations of conjugated or native CBP were incubated with (A) human CCL2 or (B) human CCL5. Unbound chemokine was then detected using a competition ELISA. The conjugated CBP was prepared using protocol 1. Results are presented as the percentage of unbound chemokine, normalised to a chemokine only control, without the presence of CBP. Values are expressed as mean ± SEM (n = 3). The data was analysed using two-way ANOVA coupled with Bonferroni post-hoc test for multiple comparisons. Significance between groups is denoted by an asterisk.

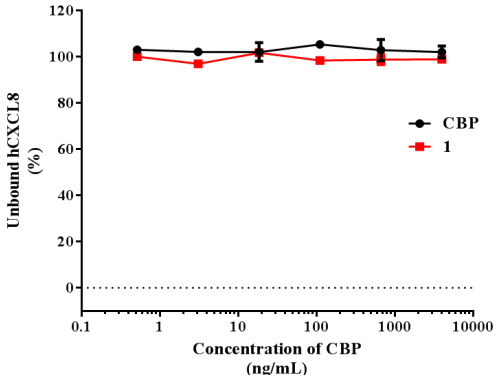

Figure 10. Saturation of CBP with DyLight®594 does not potentiate CXCL8 binding. Various concentrations of conjugated or native CBP were incubated with mouse CXCL8. Unbound chemokine was then detected using a competition ELISA. The conjugated CBP was prepared using protocol 1. Results are presented as the percentage of unbound chemokine, normalised to a CXCL8 only control, without the presence of CBP. Values are expressed as mean ± SEM (n = 3).

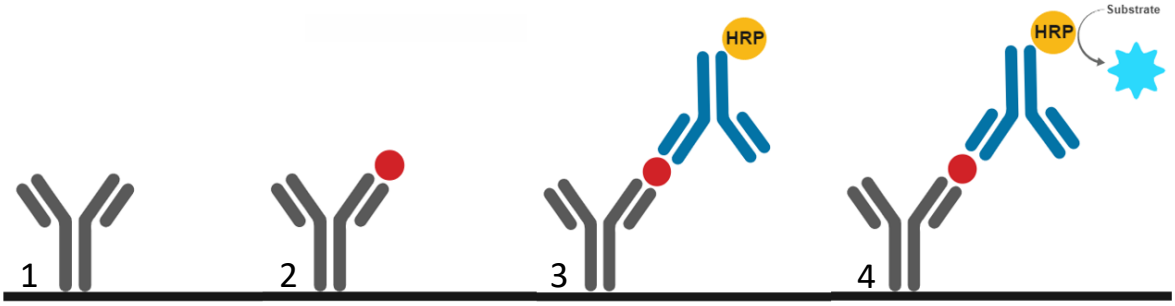

Figure 11. Chemokine detection ELISA. (1) Capture antibody (grey) was coated to the ELISA plate. (2) Supernatant samples (containing chemokine) were added to capture antibody. (3) Detection antibody (blue) conjugated with HRP (yellow) was added. (4) The presence of detection antibody was then detected by adding TMB (substrate), and the OD was taken at 450nm.

3.2 Development of an *in vitro* inflammation assay

Having developed a labelled Dylight®594-CBP, the aim was to use this tool to detect inflammatory chemokines in a cell-based inflammatory assay. The human monocytic cell line THP-1 was chosen for this assay, as these cells can express numerous chemokines, including CXCL2, CCL5, and CCL2 (Harrison *et al*., 2005; Higgins and Kovacevic, 2014).

The first step in setting up this assay was to determine which stimuli induces the greatest inflammatory response in these cells. The second step was to determine the time frame of that inflammatory response. THP-1 cells were left as monocytes or differentiated into macrophages

through exposure to PMA for 3 days (Park *et al*., 2007). The undifferentiated and differentiated cells were then treated with or without LPS to stimulate inflammatory cytokine and chemokine production. The cell supernatant was then collected across various time points, with cytokine and chemokine levels analysed using commercial ELISA kits (Figure 11).

Firstly, the level of TNFα was examined as to assess the level of inflammation/activation of the monocytes. Figure 12A indicates that treatment of THP-1 cells with LPS with or without PMA successfully produced an inflammatory response, indicated by the 300pg/mL increase in TNFα levels relative to control cells at both 3 and 6 hours post treatment ($p < 0.05$). The level of TNFα however, had substantially reduced for all LPS-treated groups by 24 hours post treatment, no longer reaching significance compared with control. PMA-treatment alone led to a 2-fold increase in TNFα production at 3 and 6 hours, but this difference was not found to be significantly different from the untreated cells ($p > 0.05$).

Having shown that the THP-1 cells were producing an inflammatory response to LPS stimulation, the timing and level of inflammatory CC chemokines produced by these cells was then assessed. The chemokines CCL2 and CCL5 were chosen, as CBP exhibits high affinity binding for them (Counago *et al*., 2015; Sharif *et al*., 2016). Figure 12B shows that treatment of THP-1 cells with LPS, with or without PMA, successfully induced production of CCL2, with a significant 8 to 10-fold increase relative to the control cells at 24 hours post treatment ($p < 0.05$). PMA-treatment alone did not increase CCL2 production ($p > 0.05$). Figure 12C shows that treatment of THP-1 cells with LPS, with or without PMA, also induced production of CCL5, with significant 1.4 and 1.8-fold increases relative to the control cells at 6 and 24 hours post treatment, respectively ($p < 0.05$). PMA-treatment did not increase CCL5 production ($p > 0.05$). TNFα, CCL2, and CCL5 expression levels correlate with previous findings utilising LPS stimulation of THP-1 cells (Haberstroh et al., 2002; Tai et al., 2013).

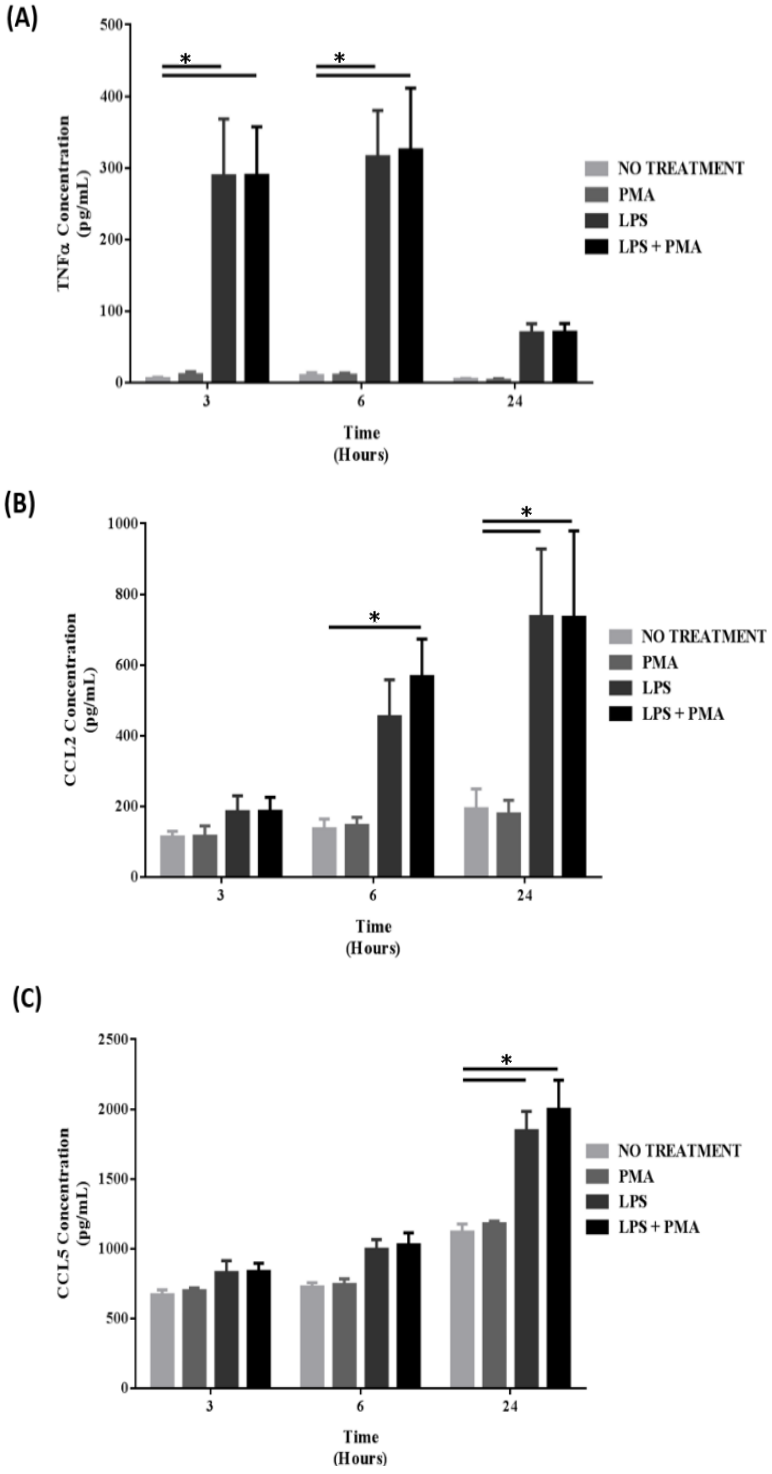

Figure 12. (A) Tumour necrosis factor (TNFα) production by human THP-1 monocytes increased 3-6 hours after treatment with lipopolysaccharide (LPS) with and without phorbol-12-myristate-13-acetate (PMA). (B) Human CCL2 concentration was increased response to LPS exposure. (C) Human CCL5 concentration was increased in response to LPS treatment. THP-1 cells were treated with or without PMA for 3 days (5 ng/mL), then treated with or without LPS (100 ng/mL) for the indicated time frame. TNFα, CCL2, and CCL5 proteins, secreted in cell supernatant was quantified by ELISA with values expressed as the mean ± SEM (n = 3). The data was analysed using two-way ANOVA coupled with Bonferroni post-hoc test for multiple comparisons. Significance denoted by an asterisk.

3.2.i Conjugation of DyLight®594 to an anti-CCL2 antibody

Before using the Dylight®594-CBP to detect chemokines expressed by THP-1 cells, a chemokine-specific antibody needed to be labelled with Dylight®594 to allow for appropriate comparisons between CBP and antibody sensitivity and specificity. As the THP-1 cells produced greater levels of CCL2 than CCL5 in response to LPS, compared to non-LPS treated cells, an anti-CCL2 antibody was chosen to provide comparison with the DyLight®-CBP. The antibody selected (monoclonal, mouse IgG1) had previously been shown to detect hCCL2 in immunofluorescent cytology and immunohistochemistry protocols using macrophages isolated from RA patients and healthy patients and hepatic tissue from Simian immunomodulatory virus (SIV) infected macaques (Rhys *et al*., 2018; Fisher *et al*., 2018).

Conjugation protocol 1 was utilised to label the anti-CCL2 antibody. The labelled antibody was resolved by SDS-Page under reducing conditions, with the abundance and fluorescence of the antibody assessed (Figure 13B). Coomassie blue staining of the gel revealed bands at molecular weights consistent with the IgG1 structure, consisting of two heavy-chains (52 kDa each) and two light-chains (26-29kDa each; Figure 13A). The presence of two distinct bands at 26 and 29 kDa indicates some variance in light chain size.

The number of DyLight®594 molecules conjugated to anti-CCL2 antibody was then assessed using fluorescence spectroscopy. The emission spectrum was adjusted to account for the antibody's extinction coefficient; and is presented for equivalent amounts of conjugated CBP and anti-CCL2 antibody (Figure 14). The mean number of DyLight®594 molecules per antibody was determined to be 15.3. A typical mouse IgG1 antibody consists of 16 lysine residues (Nagaoka and Akaike, 2003), indicating full saturation. As DyLight® dyes have been successfully conjugated to antibodies without loss of function previously (Cilliers *et al*., 2017) it was assumed that conjugated anti-CCL2 antibody would maintain functionality.

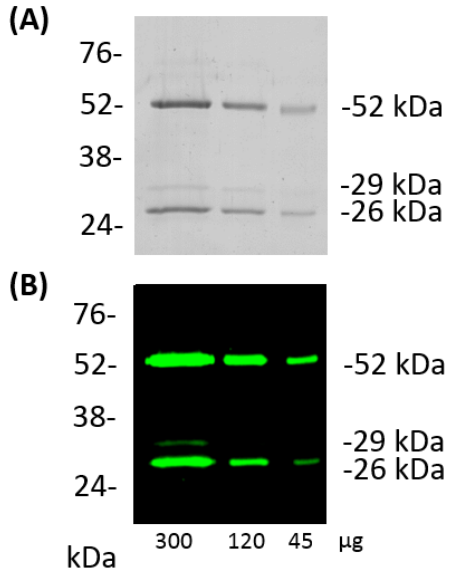

Figure 13. DyLight®594 conjugation to anti-CCL2 antibody. Anti-CCL2 antibody was conjugated with Dylight®594 dye using protocol 1. Varying amounts of anti-CCL2 antibody was resolved by SDS-Page then transferred to a membrane. Proteins were then identified by (A) Coomassie blue staining or by (B) Fluorescent dye on the protein was detected by fluorescent imaging using a 610BP filter, for fluorescence between 593 and 618 nm.

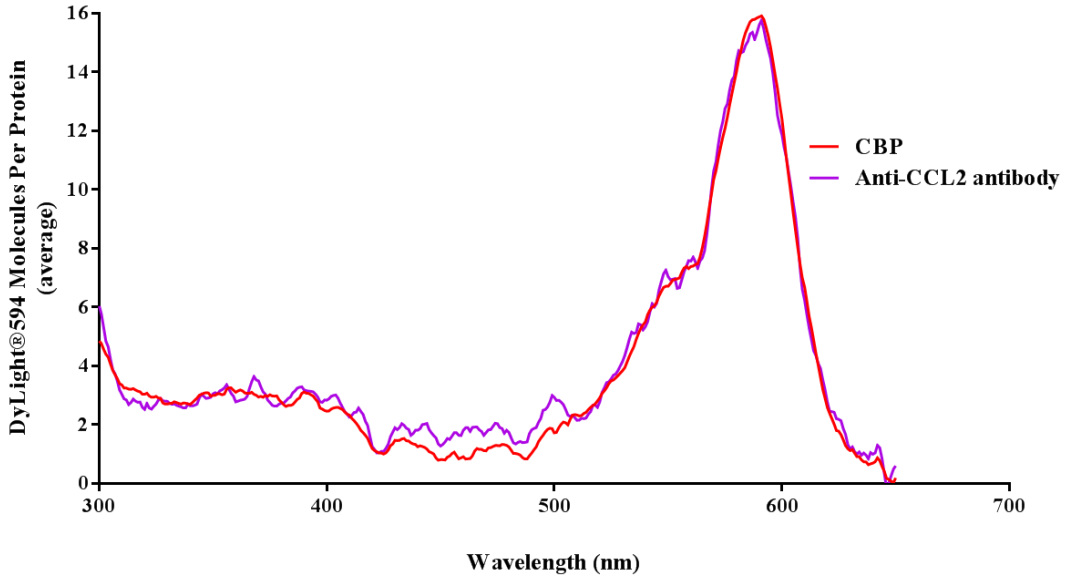

Figure 14. Quantitation of DyLight®594 molecules per molecule of anti-CCL2 antibody relative to that of CBP. Dylight®594-conjugated Anti-CCL2 antibody and CBP were prepared using protocol 1, and analysed using a fluorometer. The absorbance of each protein was taken at increments of 1nm in wavelength. The number of dye molecules per molecule of protein was then calculated using the proteins' respective extinction coefficient and emission spectra of DyLight®594.

3.2.ii Sensitivity of DyLight®594-CBP Binding to THP-1 Cells

Having prepared DyLight®594 conjugated CBP and anti-CCL2 antibody, it was now possible to directly compare their ability to detect chemokine(s) produced by activated THP-1 cells. As CCL2 was detected in the supernatant of LPS and PMA-treated cells, this stimulation protocol was chosen for the assay. As maximal levels of CCL2 in the supernatant was achieved by 24 hours, the time point of 6 hours was chosen as it was anticipated the level of intracellular chemokine would be at its highest prior to this peak in secretion.

THP-1 cells grown on coverslips with PMA for 3 days prior to treatment with LPS for 6 hours were fixed and permeabilised. The cells were then incubated with a dilution series of equimolar amounts of the DyLight®594 conjugated CBP and anti-CCL2 antibody. With the degree of fluorescent conjugation near equivalent, it was assumed that equal degrees of binding would produce equivalent levels of fluorescence. However, with CBP having a higher affinity and more ligands available, there would likely be a greater detection of fluorescence observed. Figure 15A illustrates that a dose dependent increase in the fluorescence intensity was observed with both the DyLight®594-CBP and the DyLight®594-anti-CCL2 antibody. However, the antibody exhibited increased assay sensitivity (increased fluorescence) compared to the CBP.

The localisation of Dylight®594 conjugated anti-CCL2 antibody and CBP was examined. Assuming both proteins are binding chemokines, the proteins should exhibit similar binding patterns. As the cells are permeabilised, binding should also be observed within the cells for both proteins. Observations on the localisation of protein binding of both CBP and anti-CCL2 antibody did not appear different (Figure 16). Binding was observed both within the cell, and externally. Both CBP and anti-CCL2 antibody indicate a high level of surface fluorescence, indicating binding of expressing protein.

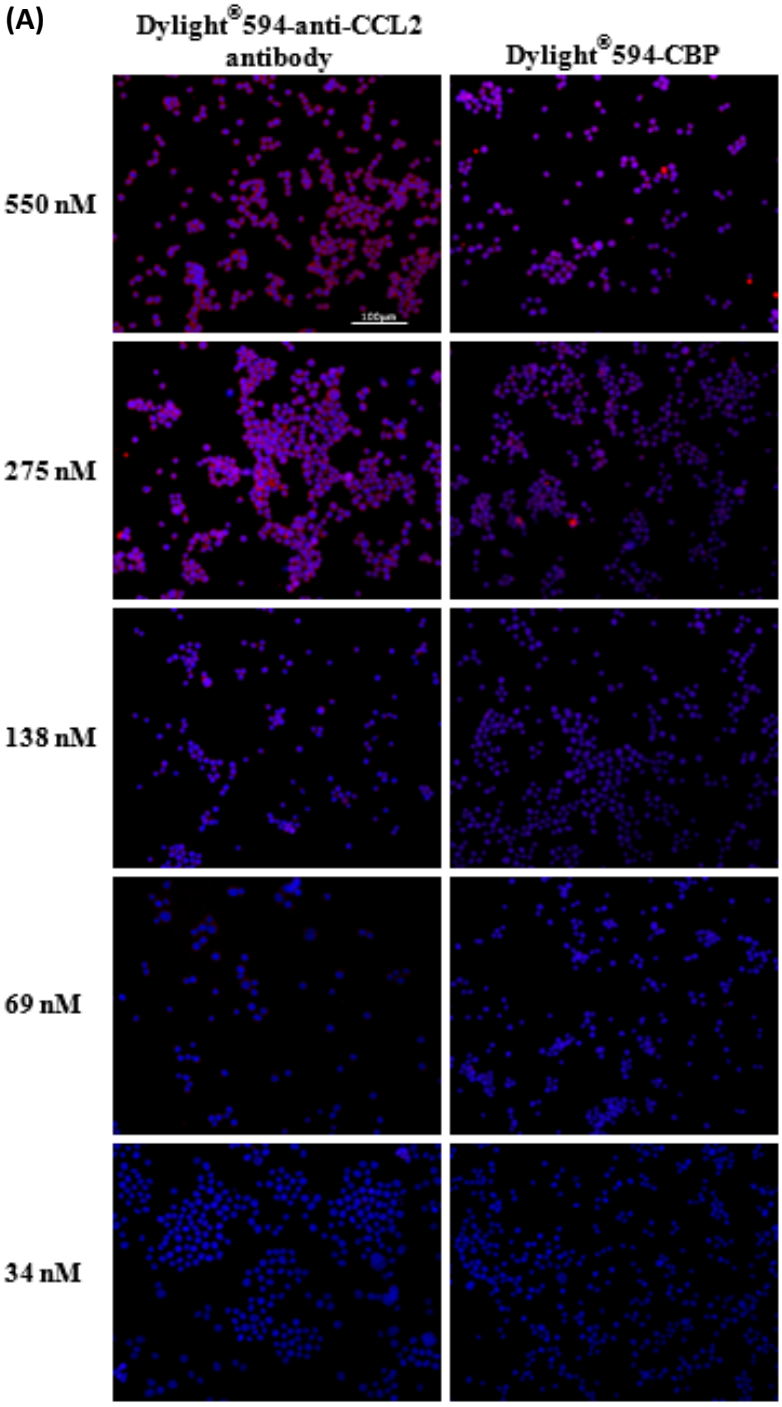
(A)
Dylight®594-anti-CCL2 antibody
Dylight®594-CBP
550 nM
275 nM
138 nM
69 nM
34 nM

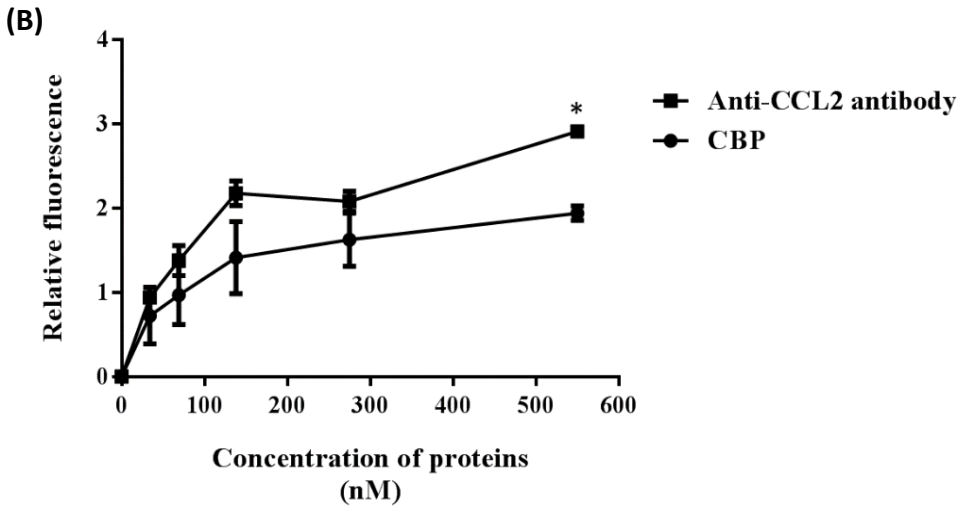

Figure 15. Dylight®594-anti-CCL2 antibody displayed a higher sensitivity for detection, compared to Dylight®594-CBP, across LPS + PMA activated cells. THP-1 cells were treated with PMA for 3 days (5 ng/mL), then stimulated with LPS (100 ng/mL) for 6 hours. Cell were fixed and permeabilised cells, followed by incubation with varying concentrations of DyLight®594-conjugated anti-CCL2 antibody or CBP (molar equivalent) (red) and counter-stained with DAPI (blue). (A) Representative fluorescent images are shown of cells treated for 6 hours. (B) Data expressed as Relative fluorescence, being a measure of fluorescence relative to DAPI staining. Values are expressed as the mean ± SEM (n = 3). The data was analysed using two-way ANOVA coupled with Bonferroni post-hoc test for multiple comparisons. Significance denoted by an asterisk.

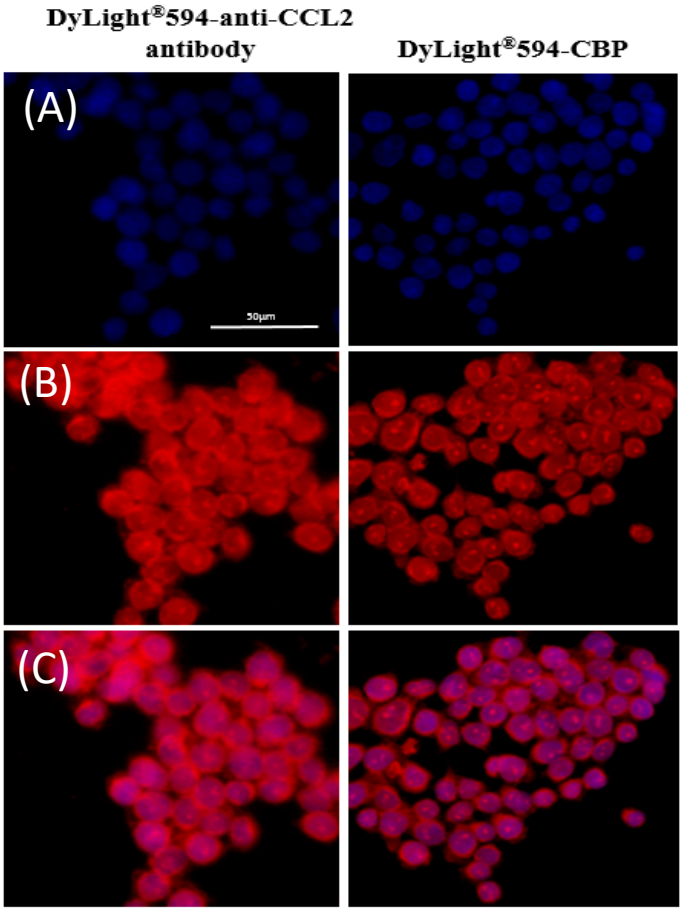

Figure 16. The localisation of Dylight®594 conjugated CBP and anti-CCL2 antibody does not appear different. THP-1 cells were treated with PMA for 3 days (5 ng/mL), then stimulated with LPS (100 ng/mL) for 6 hours. Cell were fixed and permeabilised cells, followed by incubation with DyLight®594-conjugated anti-CCL2 antibody or CBP (550nm) and counter-stained with DAPI. Scale bar is as indicated. (A) image representing DAPI stain, imaged at 400nm. (B) representing Dylight®594 fluorescence, imaged at 595nm. (C) represents a merged image of both (A) and (B).

3.2.iii Specificity of DyLight®594-CBP for Activated THP-1 Cells

Having shown DyLight®594 conjugated CBP and anti-CCL2 antibody could bind activated THP-1 cells, it was then important to show that the staining was specific to chemokines. As CCL2 production levels varied between untreated, PMA, LPS, and LPS and PMA-treated THP-1 cells, an assay was conducted to examine the relative level of DyLight®594 conjugated CBP and anti-CCL2 antibody following these different cell treatments.

THP-1 cells grown on coverslips, treated with PMA and/or LPS for 3 to 24 hours, were fixed and permeabilised. The cells were then incubated with DyLight®594 conjugated CBP or anti-CCL2 antibody. A molar equivalent concentration of 550nM was chosen based in the significant increase in staining detected in the previous assay (Figure 15).

The relative fluorescence of DyLight®594 anti-CCL2 antibody was significantly greater in cells treated with LPS, with or without PMA, at 6 and 24 hours ($p < 0.05$; Figure 17A, B). The maximal level of fluorescence was achieved with the DyLight®594-anti-CCL2 antibody was with cells treated with LPS at 24 hours (Figure 17B), reaching a relative fluorescence of 2, compared to 1.1 reached by no treatment.

The maximal level of fluorescence achieved with the DyLight®594-CBP, was observed with cells treated with LPS and PMA at 24 hours (Figure 17A, C), reaching a relative fluorescent level of 1.3 compared to 0.75 of untreated control, although not significant. The relative fluorescence of DyLight®594-CBP was however not significantly greater in any treated cells, compared with untreated cells ($p < 0.05$; Figure 17C). At 3 hours, there were no significant differences between groups, although no treatment did indicate the lowest level of fluorescence (Figure 17A). These findings indicate that while the fluorescently-labelled antibody can specifically detect activated THP-1 monocytes, the CBP failed to differentiate between cells that had or had not been treated with inflammatory stimuli.

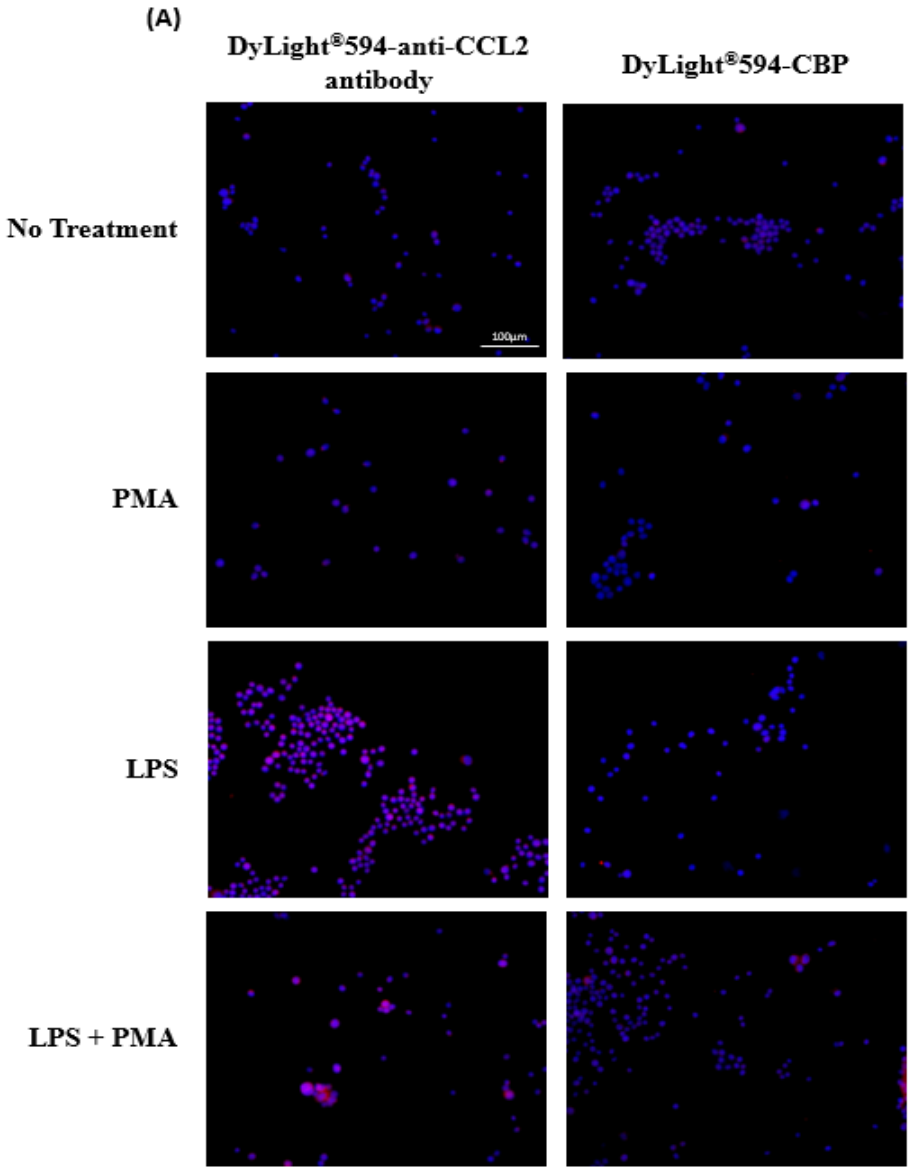
(A)
DyLight®594-anti-CCL2 antibody
DyLight®594-CBP
No Treatment
PMA
LPS
LPS + PMA
100μm

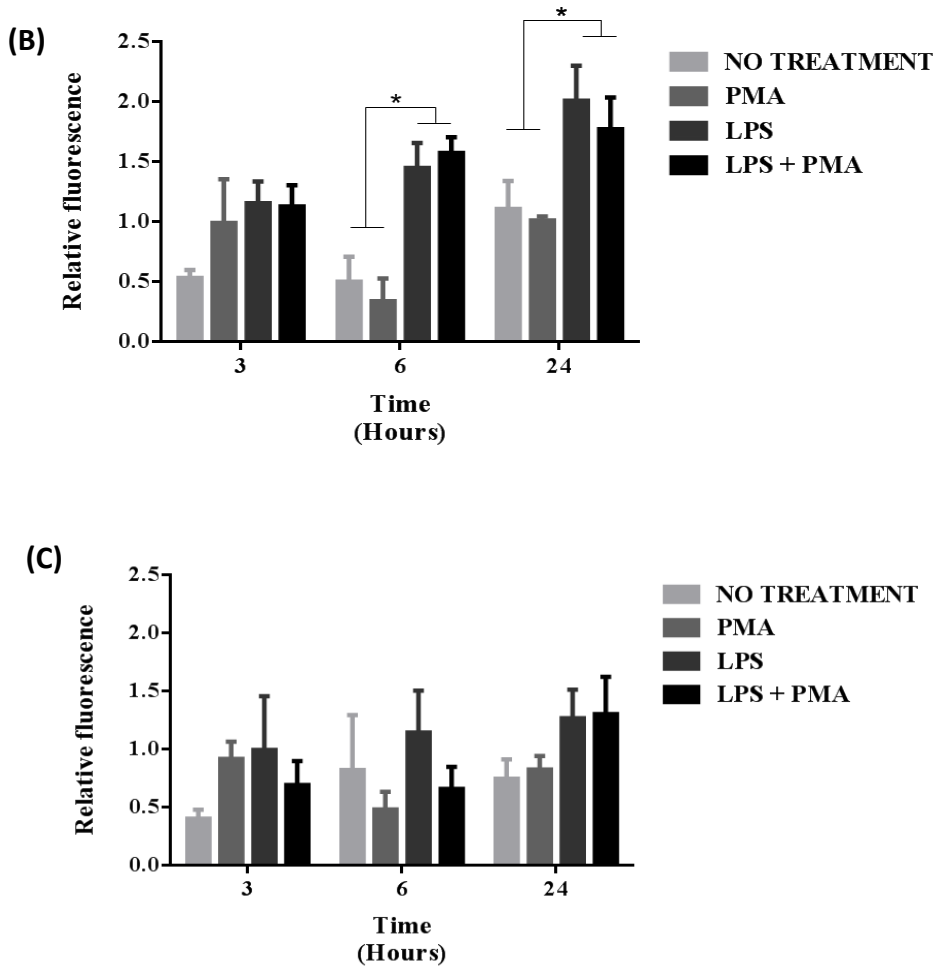

Figure 17. Selective staining of activated THP-1 monocytes with DyLight®594-anti-CCL2 antibody but not DyLight®594-CBP. THP-1 cells were treated with or without PMA for 3 days (5 ng/mL), then treated with or without LPS (100 ng/mL) for the indicated time frame. Cells were fixed and permeabilised, followed by incubation with 550nM of DyLight®594-conjugated anti-CCL2 antibody or CBP (red) (molar equivalent) and counter-stained with DAPI (blue). **(A).** Representative fluorescent images are shown of cells treated for 6 hours. Scale bar is as indicated. Mean relative fluorescence was calculated for each treatment, and displayed for **(B)** DyLight®594-conjugated anti-CCL2 antibody or **(C)** DyLight®594-conjugated CBP, being a measure of fluorescence relative to DAPI staining. Values are expressed as the mean ± SEM (n = 3). The data was analysed using two-way ANOVA coupled with Bonferroni post-hoc test for multiple comparisons. Significance between groups denoted by an asterisk.

3.2.iv Specificity of DyLight®594-CBP for Chemokines Produced by Activated THP-1 cells

Although DyLight®594 conjugated CBP could bind activated THP-1 cells, it was unable to differentiate between activated cells producing chemokines, and non-activated cells. This suggests that CBP binding to the cells may not be chemokine-specific. A series of competitive binding assays were conducted to look at the specificity of DyLight®594 conjugated CBP and anti-CCL2 antibody interactions with activated THP-1 monocytes.

LPS and PMA-activated THP-1 cells were incubated with a 4-fold molar excess of unlabelled anti-CCL2 antibody prior to incubation with the DyLight®594 conjugated CBP and anti-CCL2 antibody (1/100 dilution) (Figure 18). Pre-incubation with the unlabelled antibody is expected to block any specific interactions between the fluorescently-labelled antibody or CBP, and CCL2 within the cells. The unlabelled antibody clearly reduced the level of fluorescence relative to the DyLight®594-anti-CCL2 antibody alone (Figure 18B). However, pre-incubation with the antibody had no impact on fluorescence observed with the DyLight®594-CBP. The relative fluorescence of the DyLight®594-CBP staining did not differ with or without competition from the unlabelled antibody ($p > 0.05$; Figure 18C).

Next, activated THP-1 cells were incubated with a 4-fold molar excess of unlabelled CBP prior to incubation with the DyLight®594 conjugated CBP and anti-CCL2 antibody (550nM). Pre-incubation with the CBP is expected to block any specific interactions between the fluorescently-labelled antibody or CBP, and chemokines in general within the cells. The unlabelled CBP had no impact on fluorescence after binding with either the DyLight®594-conjugated anti-CCL2 antibody or CBP. Quantitative analysis confirmed that the relative fluorescence of DyLight®594-CBP and DyLight®594 anti-CCL2 antibody staining did not differ with or without competition from the unlabelled CBP ($p > 0.05$; Figure 18B-C).

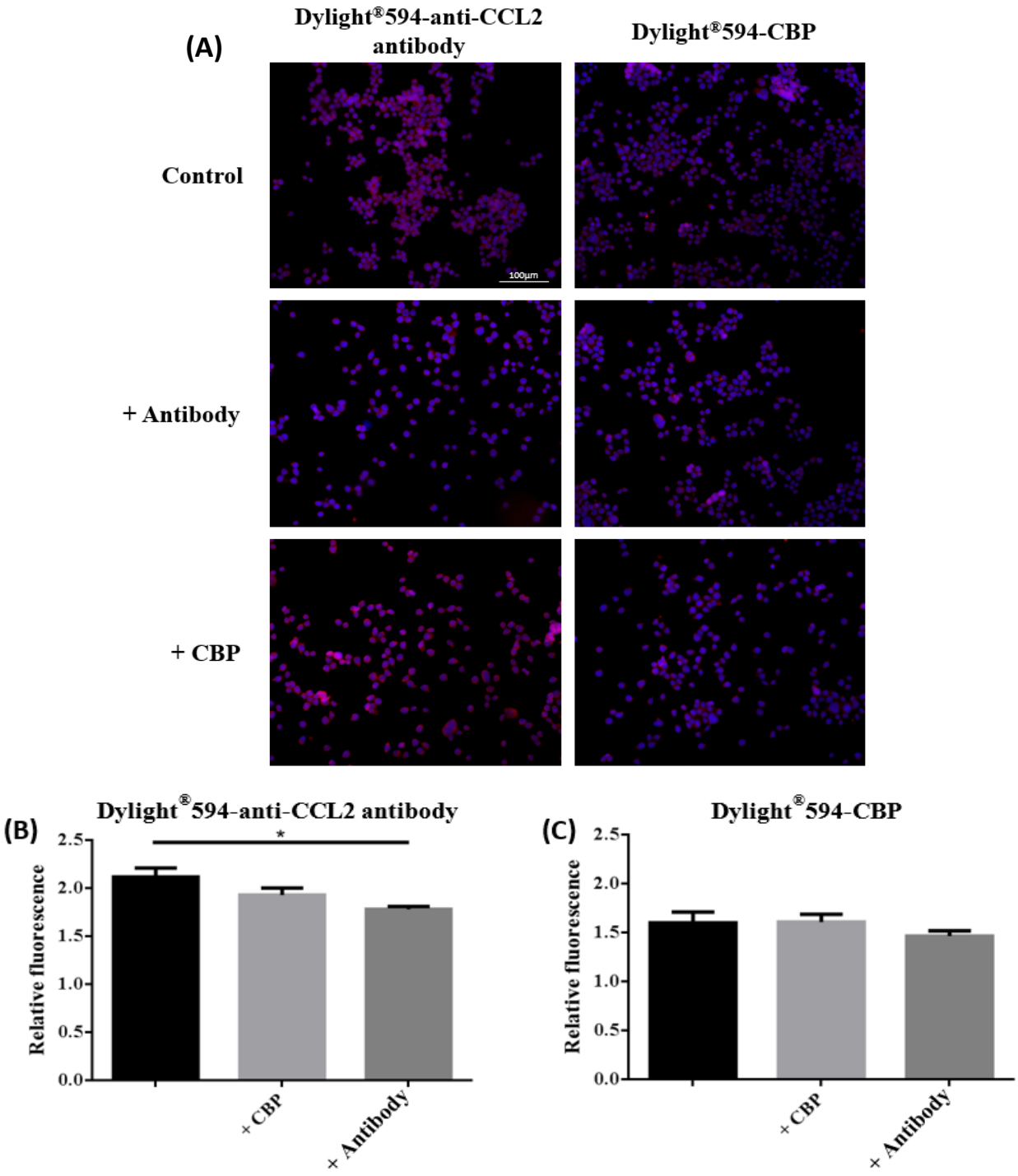

Figure 18. Dylight®594-anti-CCL2 antibody indicates specificity for CCL2, whereas DyLight®594-CBP does not. THP-1 cells were treated with PMA for 3 days (5 ng/mL), then stimulated with LPS (100 ng/mL) for 6 hours. Fixed and permeabilised cells were then incubated with 2.2µM of anti-CCL2 antibody or CBP overnight, followed by incubation with 550nM of DyLight®594-conjugated anti-CCL2 antibody or CBP (red), and counter-stained with DAPI (blue). **(A)** Representative fluorescent images are shown of cells treated for 6 hours. Scale bar is as indicated. Relative fluorescence was calculated for each treatment, and displayed for **(B)** DyLight®594-conjugated anti-CCL2 antibody or **(C)** DyLight®594-conjugated CBP, being a measure of fluorescence relative to DAPI staining. Values are expressed as the mean ± SEM (n = 3). The data was analysed using two-way ANOVA coupled with Bonferroni post-hoc test for multiple comparisons. Significance between groups denoted by an asterisk.

Next, DyLight®594-CBP and DyLight®594-anti-CCL2 antibody were incubated with a 4-fold molar excess of CCL2 prior to the incubation with activated THP-1 monocytes (Figure 19). Pre-incubation of the fluorescently-labelled antibody or CBP, with CCL2, is expected to block any specific interactions with CCL2 within the cells. The CCL2 clearly reduced the level of fluorescence relative to the DyLight®594 anti-CCL2 antibody alone (Figure 19A-B). However, pre-incubation with CCL2 did not alter fluorescence with the DyLight®594 CBP. The relative fluorescence of the DyLight®594-CBP staining did not differ with or without with hCCL2 pre-incubation ($p > 0.05$; Figure 19C). Alternately, a significant 18% reduction in relative fluorescence by the DyLight®594 anti-CCL2 antibody (1.7 to 1.4 respectively) was observed following competitive binding with the CCL2 ($p < 0.05$; Figure 19B).

Next, DyLight®594-CBP and DyLight®594-anti-CCL2 antibody were incubated with a 4-fold molar excess of heparin prior to the incubation with activated THP-1 monocytes (Figure 20). Pre-incubation of the fluorescently-labelled antibody or CBP, with heparin, should not impede on either the anti-CCL2 antibody, nor the CBP, of which neither have been indicated to successfully bind heparin. The addition of heparin clearly reduced the level of fluorescence relative to the DyLight®594-CBP alone, however did not alter fluorescence with the DyLight®594 anti-CCL2 antibody (Figure 20A). Quantitative analysis confirmed there was a significant 35% reduction in relative fluorescence with the DyLight®594 CBP staining when pre-incubated with the heparin (1.7 to 1.1 respectively) ($p < 0.05$; Figure 20C). DyLight®594 anti-CCL2 antibody was not altered with competitive heparin binding ($p < 0.05$; Figure 20B).

Together, the data indicates that the fluorescently-labelled CBP is unable to specifically detect chemokines in fixed and permeabilised cells, suggesting that the fluorescence detected may in fact indicate heparin binding.

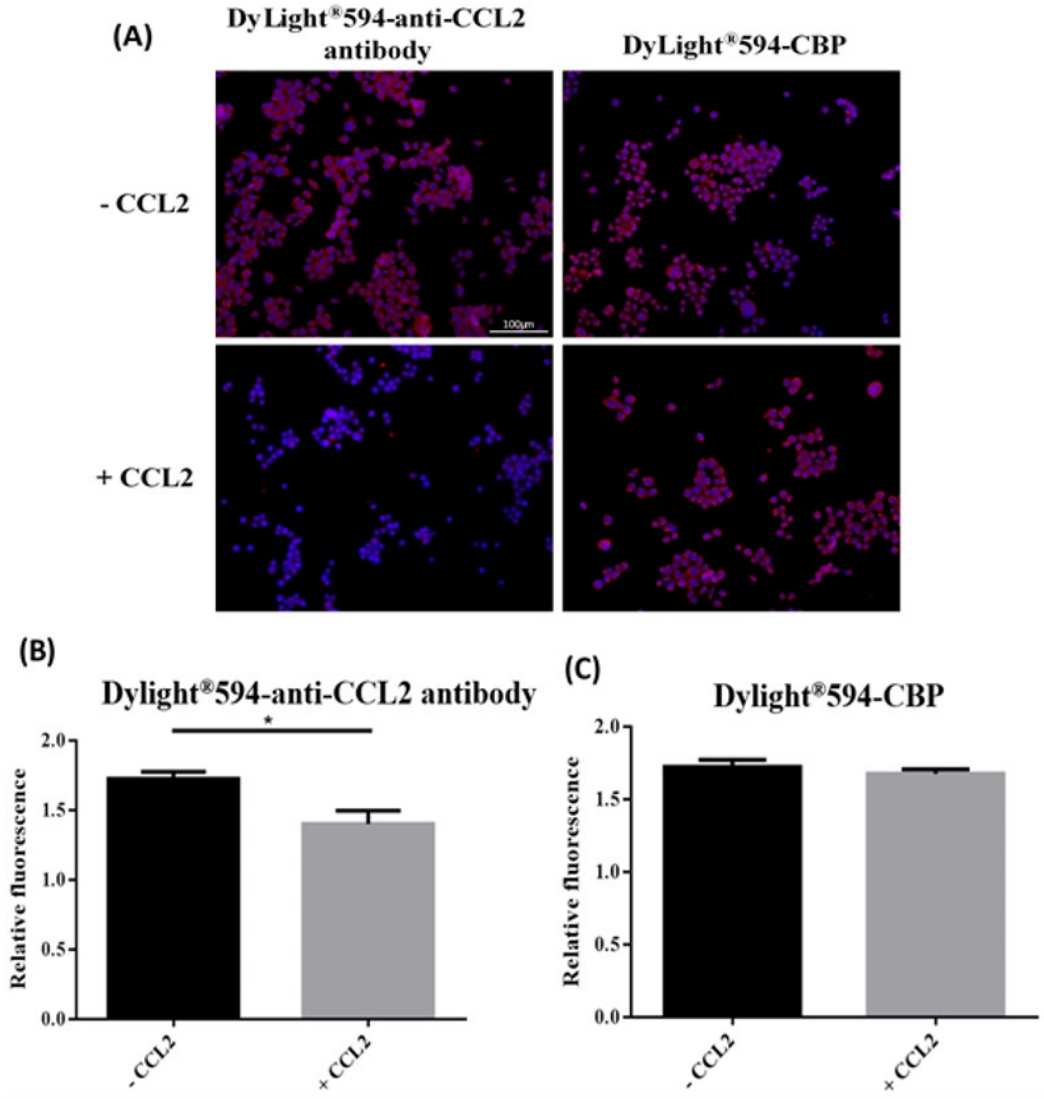

Figure 19. Dylight®594-anti-CCL2 antibody indicates specificity for CCL2, whereas Dylight®594-CBP does not. THP-1 cells were treated with PMA for 3 days (5 ng/mL), then stimulated with LPS (100 ng/mL) for 6 hours. DyLight®594-conjugated anti-CCL2 antibody and CBP were incubated with 2.2µM CCL2. Fixed and permeabilised cells were then incubated with a 550nM of DyLight®594-conjugated anti-CCL2 antibody or CBP (red) with or without CCL2 incubation, and counter-stained with DAPI (blue). **(A)** Representative fluorescent images are shown of cells treated for 6 hours. Scale bar is as indicated. Relative fluorescence was calculated for each treatment, and displayed for **(B)** DyLight®594-conjugated anti-CCL2 antibody or **(C)** DyLight®594-conjugated CBP, being a measure of fluorescence relative to DAPI staining. Values are expressed as the mean ± SEM (n = 3). The data was analysed using two-way ANOVA coupled with Bonferroni post-hoc test for multiple comparisons. Significance between groups denoted by an asterisk.

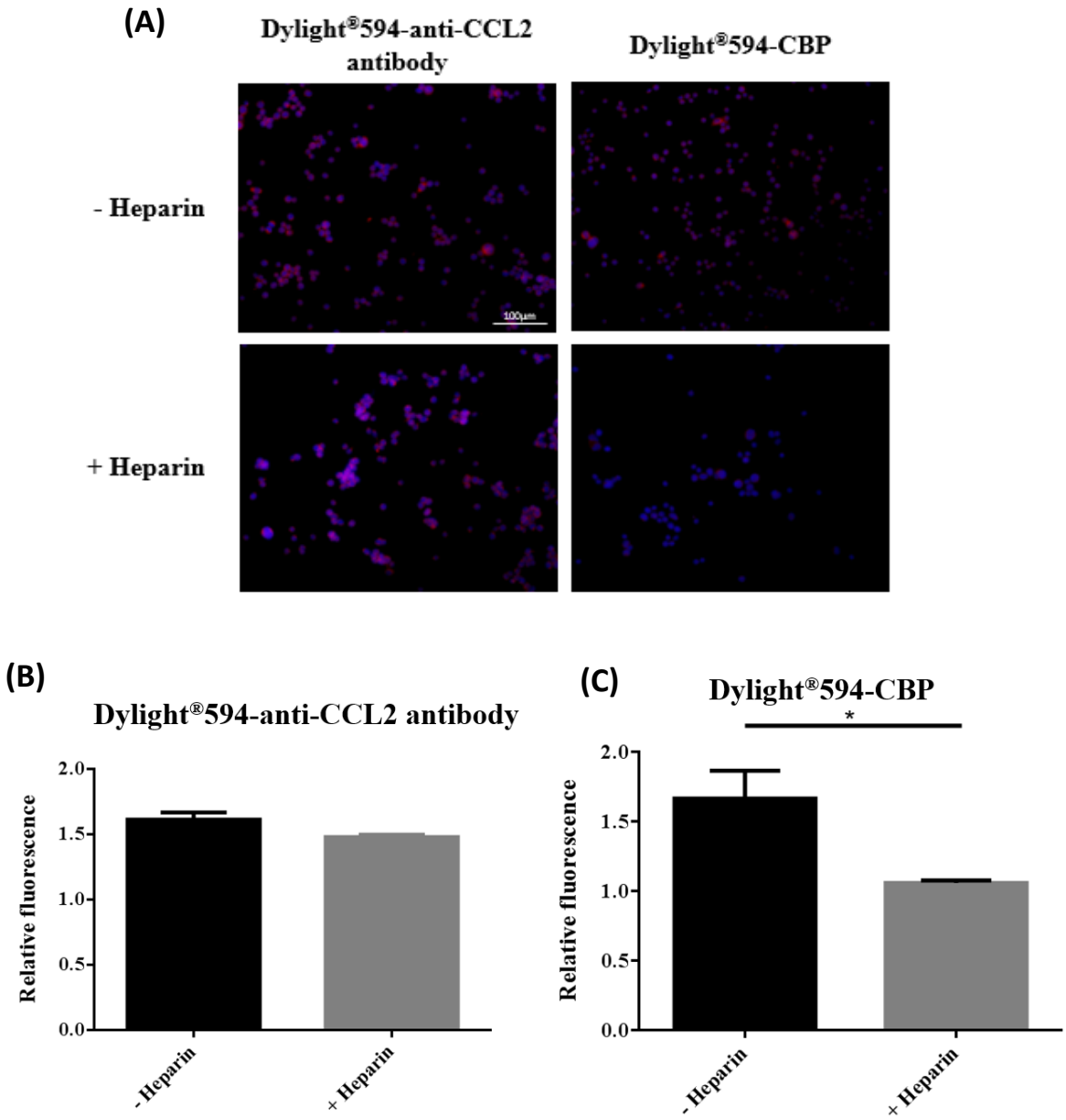

Figure 20. DyLight®594-CBP may indicate specificity for heparin, as opposed to CCL2. THP-1 cells were treated with PMA for 3 days (5 ng/mL), then stimulated with LPS (100 ng/mL) for 6 hours. DyLight®594-conjugated anti-CCL2 antibody and CBP were incubated with 2.2µM heparin. Fixed and permeabilised cells were then incubated with a 550nM of DyLight®594-conjugated anti-CCL2 antibody or CBP (red) with or without heparin incubation, and counter-stained with DAPI (blue). **(A)**. Representative fluorescent images are shown of cells treated for 6 hours. Scale bar is as indicated. Relative fluorescence was calculated for each treatment, and displayed for **(B)** DyLight®594-conjugated anti-CCL2 antibody or **(C)** DyLight®594-conjugated CBP, being a measure of fluorescence relative to DAPI staining. Values are expressed as the mean ± SEM (n = 3). The data was analysed using two-way ANOVA coupled with Bonferroni post-hoc test for multiple comparisons. Significance between groups denoted by an asterisk.

3.3 CBP in Western Blotting

The use of vCBPs was then considered for the use of chemokine detecting within a western blot. Typically, after running a protein on a gel and transferring the protein to a membrane, an antibody is utilised to detect the protein on the membrane. Visualisation is then achieved through either an enzymatic conjugation/substrate interaction, or the use of a fluorescent antibody. Utilising CBP as a substitute would likely fail, as extensive protein interactions are required to facilitate chemokine binding. The protocol involves the reduction of the chemokine, through the disruption of disulphide bonds, therefore the chemokine loses its tertiary structure, rendering CBP-chemokine binding unlikely (Homma *et al*., 2004; Counago *et al*., 2015).

The fluorescent labelled antibody was identified to exhibit CCL2 detection across multiple concentrations of anti-CCL2 antibody (Figure 21). However, in no instance was binding observed for the labelled CBP across any concentration assessed.

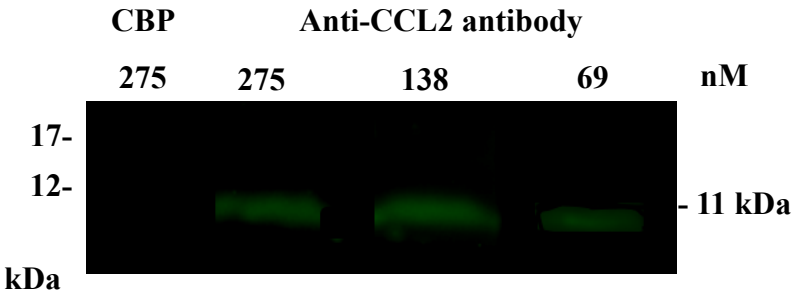

Figure 21. DyLight®594-CBP was not able to detect hCCL2 within a western blot protocol. Equal amounts of hCCL2 (300ng per well) were resolved by SDS-PAGE gel then transferred to a membrane. Membranes were then incubated with varying concentrations of either Dylight®594 conjugated CCP or anti-CCL2 antibody. Only the highest concentration (275nM) of Dylight®594-CBP was shown. Fluorescence was detected by imaging using a 610BP filter, for fluorescence between 593 and 618 nm.

3.4 CBP in ELISA

The use of vCBPs were then considered for integration into various ELISA techniques by supplanting the use of antibodies. The use of native CBP was assessed for use as the detection antibody. The vCBP was introduced into the system after the chemokine ligand had been captured by the antibody, as outlined in Figure 22. It was hypothesised that the utilisation of CBP as a detection antibody would not be successful, as the formation of a capture antibody-chemokine-CBP complex was unlikely to be facilitated. The formation of this complex would be unable to form, either as the CBP has likely occluded the antibody epitope, or CBP has competitively removed the chemokine from the capture antibody.

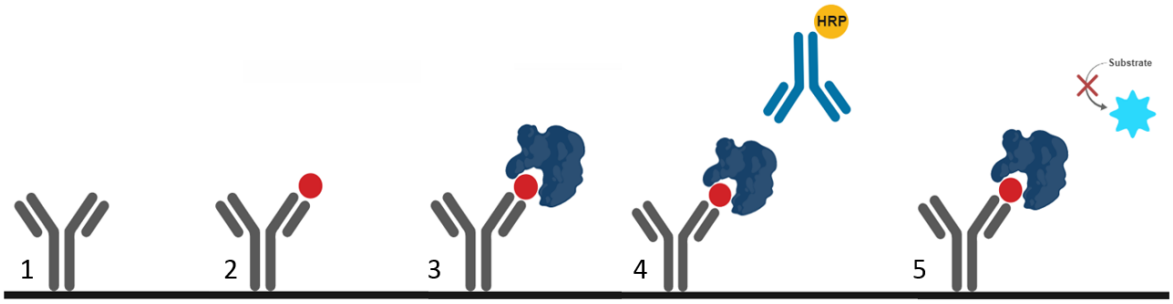

Figure 22. CBP as a replacement detection antibody for hCCL2. (1) Capture antibody (grey) was coated to the ELISA plate. (2) Chemokine was added to capture antibody. (3) CBP was incubated with pre-bound CCL2. (4) Detection antibody (blue) conjugated with HRP (yellow) was added. (5) The presence of detection antibody was then detected by adding TMB (substrate), and the OD was taken at 450nm.

The data indicates that there is a dose response trend occurring, where at the two highest concentrations of CBP there is reduced detection of unbound CCL2 (70% and 83%; Figure 23). There were no significant differences observed across the lower dose range. Complete inhibition of CCL2 detection was not observed which indicates that CBP cannot fully out-compete the detection antibody.

The use of CBP was also assessed as a potential capture antibody substitute, as outlined in Figure 24. It was hypothesised that, based upon previous indications of CBP maintaining functionality after charge-based adhesion in SPR, ELISA plates coated with CBP would be able to bind soluble chemokine (Counago *et al.*, 2015; Sharif *et al.*, 2016). Upon further

investigation, there were linear concentration/detection relationships observed (Figure 25). This indicated that CBP was successfully capturing the chemokine, also allowing for the access of the detection antibody to the ligand, thereby achieving detection in the ELISA. The R^2 values were calculated as a means for assessing the linearity of the relationship. The mean value was 0.942 ± 0.029, indicating the data expressed a linear dose/response relationship (Table 8).

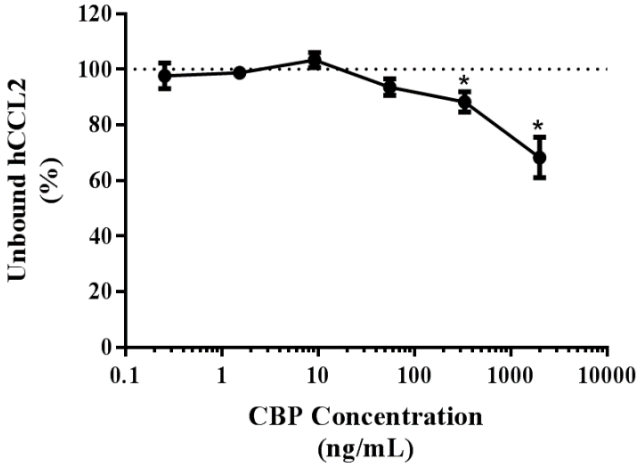

Figure 23. At high concentrations of CBP, the detection of chemokines via the detection antibody was reduced. Various concentrations of native CBP were incubated with human CCL2 pre-captured on the capture antibody. Unbound chemokine was then detected using a competition ELISA. Results are presented as the percentage of unbound chemokine, normalised to a CCL2 only control, without the presence of CBP. Values are expressed as mean ± SEM (n = 3). The data was analysed using one-way ANOVA coupled with Bonferroni post-hoc test for multiple comparisons. Differences between concentrations were compared to a CCL2 control, set at 100%. Significance between groups denoted by an asterisk.

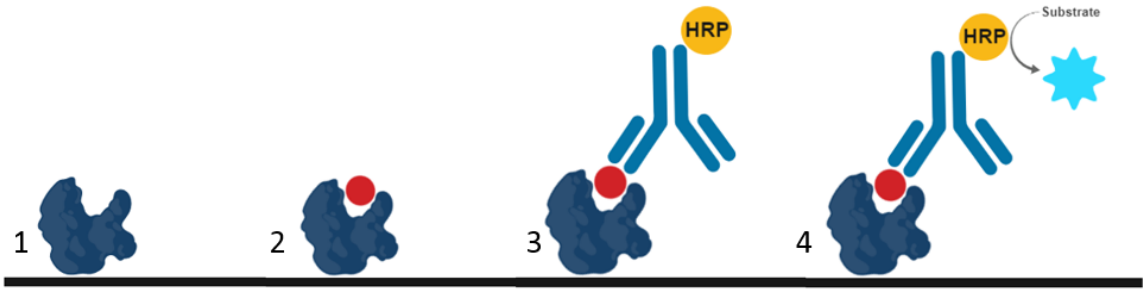

Figure 24. CBP as a capture antibody substitute for human CCL2. (1) CBP (dark blue) was coated to the ELISA plate. (2) A standard concentration of chemokine (red) was then added to the CBP. (3) Detection antibody (blue) conjugated with HRP (yellow) was added. (4) The presence of detection antibody was then detected by adding TMB (substrate), and the OD was taken at 450nm.X

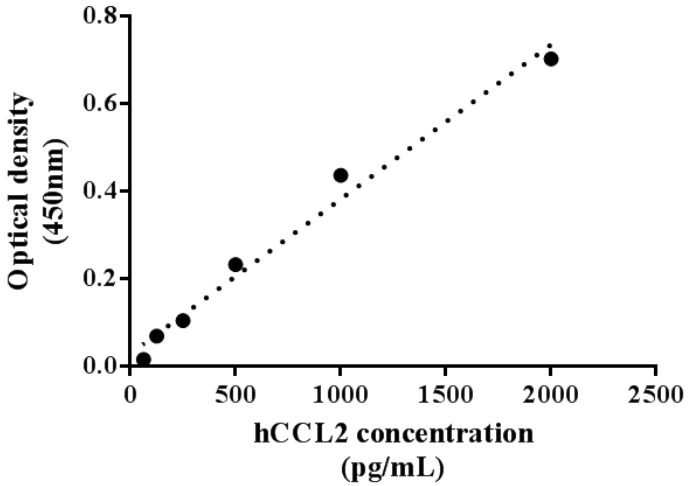

Figure 25. A linear relationship was observed utilising CBP as a capture antibody substitute. CBP was coated to the ELISA plate. A dilution series of human CCL2 was then added, and chemokine was then detected. Results are presented as the percentage of unbound chemokine, normalised to a CCL2 only control, without the presence of CBP. Values are expressed as mean ± SEM (n = 3).

Table 8. *The linear trends observed utilising CBP as a capture antibody.*

	CBP based standard curve			
	Replicate 1	Replicate 2	Replicate 3	Mean ± SEM
R^2 value	0.8852	0.9822	0.9586	0.942 ± 0.029

4 Discussion

Chemokines are increasingly being implicated in the pathogenesis of more and more diseases. With developing elucidation of chemokine involvement comes the potential for use of chemokines as diagnostic markers for these diseases. Viral CBPs provide novel qualities towards the detection of chemokines, exhibiting the unique ability to bind to multiple chemokine ligands across different classes. Using the vCBP derived from ORFV strain NZ2, CBP, this study aimed to investigate the potential application of vCBPs as broad-spectrum chemokine detectors. Specifically, CBP conjugated with a fluorescent dye was investigated for efficacy in immuno-fluorescent cytometry and western blotting, whilst the utility of the native protein was examined for utilisation in ELISA protocols.

4.1 CBP and its Utility in Immunofluorescent Cytology

As to trial the use of CBP in cytometry assays, a protocol was developed to enable different levels of conjugation of fluorescent dye onto CBP. The protocol established was rather consistent with the addition of a saturating level of the fluorescent dye, whereas the protocols for generating sub-saturating levels of dye conjugation were far more variable. Usefully, when the desired level of conjugation was not achieved utilising the outlined protocol, the proteins could undergo multiple rounds of conjugation to achieve the desired level of conjugation. By increasing the scale of the reaction, improvements towards the consistency of the conjugation protocols could be made. As the protocol developed relies on a subjective measurement of dye, with greater batches requiring more dye, it would be easier to control the dye to protein-concentration ratio (associated with lysine residues), allowing for accurate replicability.

The CBP-chemokine interaction is heavily dependent on charge-based interactions (Counago *et al*., 2015; Seet *et al*., 2003). There are largely negative and hydrophobic regions of CBP

essential for ligand engagement specifically localised on β-sheet II (Counago *et al*., 2015). There are extensive interactions with the chemokine ligands at this site, which result in a high affinity for most chemokines (Counago *et al*., 2015). It is understood that the CBP-chemokine interaction occludes the GPCR domain of the bound chemokine, thereby inhibiting receptor activation (Counago *et al*., 2015). This finding is supported by the dose dependent inhibition of CCL2 induced monocyte chemotaxis via CBP, as shown in a migration assay (Lateef *et al*., 2009). There are notable key residues for GAG binding of the chemokine which are engulfed by CBP when complexed (Counago *et al*., 2015). Theoretically, this may also lead to inhibition of the chemokine-GAG interaction, although currently only indicated as a putative interaction (Counago *et al*., 2015). Antibodies by contrast, engage a much smaller epitope of the chemokine, also with high affinity. For example, an anti-CCL2 antibody shown to interact with residues 18-24 and 45-51, binds human CCL2 with high affinity (0.022 nM, obtained via SPR) and inhibits CCL2 binding to its receptor (Obmolova *et al*., 2012).

Structural analysis of CBP specifically highlighting the lysine residues was critical, as to understand the potential impact of conjugation on chemokine binding. The conjugation protocol utilises free primary amine residues, which are exclusively present on lysine residues (Nanna *et al*., 2017). The amine residue is characteristically a positive charge, and it is understood that the conjugation of an ester onto the protein, including in the form of a dye, will reduce the net charge of the conjugated residue (Nanna *et al*., 2017). The alteration in charge is a commonly investigated feature of antibody conjugation as it can alter the stability, pharmacokinetics, and pharmacodynamics of a therapeutic (Nanna *et al*., 2017). The binding face of CBP required for interaction with the chemokine is largely negative, and there are no lysine residues located close to this site (Counago *et al*., 2015). However, there is still the potential for conjugation of the fluorophore to alter efficacy of the protein, as lysine residues are located within the CBP dimer interface (Counago *et al*., 2015). Based upon a net charge theory, the lower the extent of lysine neutralisation by fluorophore conjugation, the lesser likelihood of the binding characteristics of

CBP being impacted. Varying degrees of fluorescent conjugation were completed as a method to determine any impact upon chemokine binding activity. Based on the localisation of the lysine residues within the CBP, it was hypothesised that fluorescent conjugation would have minimal impact on the functionality of CBP. Supporting this hypothesis, it was shown that fluorescent conjugation, at any degree, did not substantially impact upon the ability of CBP to bind selected chemokines. No noticeable impact was observed following dye conjugation of CBP, at any degree, when binding several CC and CXC chemokine ligands (mCCL2, hCCL2, hCCL5, and mCXCL2). In addition, the presence of fluorophore conjugation did not facilitate the binding of CBP to CXCL8, for which binding is not typically exhibited (Counago *et al*., 2015; Seet *et al*., 2003). A protein labelled with the largest amount of dye possible with no detriment towards protein function, would provide an easily detectable and highly sensitive tool (Pretzer and Wiktorowicz, 2008). For this reason, this study proceeded with the CBP conjugated with saturating levels of the fluorophore.

The full impact of fluorescent conjugation on the activity of the CBP however, was not completely addressed within this study. The binding sites for CBP across chemokine class and species has been shown in crystal structures and homology models to vary to some extent (Counago *et al*., 2015). In addition, the interactions between CBP and many chemokines have yet to be characterised. Thereby, conjugation to the lysine residues may be more critical for the formation of charge-based interactions with specific chemokines. Attempts were made to compare the binding ability of the conjugated and unconjugated CBP towards CXCL4, and XCL1. However, here the indirect ELISA failed to detect inhibitory interactions between CBP and these chemokines, whereas these interactions had previously been observed (Seet *et al*., 2003; Counago *et al*., 2015; Sharif *et al*., 2016).

For XCL1, no indication of binding was observed with both conjugated, and unconjugated CBP, thereby implying a failing in the ELISA protocol occurred. Interestingly, the affinity of CBP

for this chemokine is weaker (0.6 nM, determined via ELISA) for C chemokines than for the CC and CXC chemokines, as observed by ELISA (Seet *et al*., 2003; Counago *et al*., 2015). The antibodies utilised in the original XCL1 ELISA were no longer available, and it may be that CBP is unable to out-compete the replacement antibodies in the adjusted protocol.

In the case of CXCL4, the effect was opposite to that expected, with increased levels of chemokine correlating with increasing levels of CBP. This result could potentially be due to the introduction of CXCL4 into the system. Counago *et al*. (2015) has shown that CBP, when expressed in HEK293s in the presence of serum, can be purified in complex with CXCL4. Although within the current study, CBP was produced under serum free conditions, these findings indicate that some of the purified protein was coupled to CXCL4, and that this could be detected in the ELISA.

As vCBPs bind with high affinity to a broad range of inflammatory chemokines, the fluorescently-conjugated version would be useful in the detection of inflammatory diseases. To test this, a monocyte (THP-1) cell line known to secrete several inflammatory chemokines upon activation and stimulation was utilised (Park *et al*., 2007). To model inflammation in these cells, this study utilised PMA, which activates P2X7R and AMPK/MAPK pathways that commence differentiation of monocytes to macrophages (Lin *et al*., 2018), and LPS, which stimulates TLR4 and Myd88 activation of NFkB and the subsequent pro-inflammatory gene expression (Lu *et al*., 2008). Under these conditions, THP-1 cells were shown to secrete numerous inflammatory mediators including CCL2, CCL5, and TNFα, all of which all can be indicative of an inflammatory response (Wolf *et al*., 2017; Benamar *et al*., 2008; Popa *et al*., 2007). The degree of protein expression by THP-1 cells noted in this study largely mimicked that observed in previous literature, in which LPS stimulated THP-1 cells were utilised (Haberstroh *et al*., 2002; Tai *et al*., 2013).

Through the utilisation of an antibody selective for CCL2, it can be assumed that any binding observed is exclusively through interactions of this protein. Using immunofluorescent cytometry, the labelled antibody was able to bind to THP-1 cells immobilised on coverslips to an extent which was proportional to the level of secreted CCL2 produced under different activating conditions. Labelled CBP was also able to bind THP-1 cells, but the levels did not correlate with the secreted CCL2. This finding indicates that although the labelled CBP can be utilised to detect monocytes, it may lack the specificity needed to detect chemokines under inflammatory conditions, as observed with the anti-CCL2 antibody.

As the amount of labelled CBP detected on the cells did not correlate with the levels of secreted CCL2 or anti-CCL2 antibody detected, attempts were made to examine if CBP was in fact capable of binding CCL2 expressed by the cells, via blocking the CBP-chemokine interaction. Blocking this interaction was undertaken in two ways. The first utilised unlabelled antibody or CBP to pre-bind chemokine on/in cells prior to the incubation of the labelled proteins with cells. The second used pre-binding of CCL2 to the labelled antibody or CBP prior to incubation with cells. It was hypothesised that blocking of the CCL2 binding site, either with proteins which also bind CCL2, or pre-binding proteins with CCL2, would be indicative of CCL2 specific interaction. Whilst the unlabelled anti-CCL2 antibody was able to block binding to the cells by the labelled version of itself, the unlabelled CBP failed to block this interaction. In addition, the binding of the labelled CBP to cells was not inhibited by either the antibody or CBP. Similarly, whilst pre-binding CCL2 with the labelled antibody reduced the level of fluorescence in samples, no such reduction was observed with the labelled CBP. These findings illustrated that the fluorescence detected following incubation with the labelled antibody was specific for CCL2, as expected. By contrast, the evidence suggests the CCL2 is not (at least) the primary target of CBP in this setting. It should be noted that in each case, the blocking action of the unlabelled antibody or chemokine did not completely inhibit the detection of THP-1-expressed CCL2 by the labelled antibody. This could be further examined by utilising increased amount

of blocking protein to saturate all expressed chemokine, thereby giving more comprehensive results.

Although fluorescence was observed in the cells with labelled CBP, there is a possibility that the binding is non-specific in nature. These samples were fixed as to immobilise cells and proteins for later analysis. Methanol fixation was use, which may alter the tertiary structure of a protein as it impacts charges within the protein, resulting in the solubilisation of fixed samples (Rolls, 2012). As an antibody is generally able to access the small epitope, it can often maintain binding to a denatured or partially denatured protein (Bass *et al*., 2016). CBP-chemokine interactions require extensive interactions, engaging approximately 25% of the chemokine surface (Counago *et al*., 2015). As methanol fixation may alter the chemokine tertiary structure, it is possible the CBP-chemokine interaction is no longer facilitated. Investigation utilising non-fixed cells was not undertaken, primarily due to initial difficulties regarding cell adherence and a lack of cells remaining after the various incubation steps. There are other techniques for fixation which may facilitate charge-based binding better such as formalin fixation, of which presents a less altered protein (Matsuda *et al*., 2011). CBP detection of chemokines may also be more likely in native human samples such as unfixed cytology samples (synovial fluid, cervical smears) or frozen tissues (cancer biopsies) (Villanueva and Schumacher, 1987; Arbyn *et al*., 2008; Brender *et al*., 2005; Bas *et al*., 2002). Further study is therefore needed to assess whether CBP would show potential utility in these scenarios.

With the observed CBP binding not presently supported to be chemokine-based, there is another potential interaction which could explain the findings. During the inflammatory response, the involvement of GAGs is understood to be a supportive role. GAGs bind to and present inflammatory mediators including chemokines to cells, thereby facilitating chemokine receptor/ligand interactions and promoting the formation of a chemotactic gradient (Thompson *et al*., 2017). HS is an important GAG, of which assists with the formation of the chemokine

gradient, thereby promoting leukocyte extravasation (Farrugia *et al*., 2018). Alongside the ability of several vCBPs to bind chemokines, some also possess the ability bind GAGs (Lucas and McFadden, 2004). It has been proposed that the vCBP-GAG interaction could either prevent the formation of the chemotactic gradient, occurring when chemokines bind to GAGs on endothelial cells, or, to create their own gradient on endothelial cells enhancing their own ability to capture chemokines (Proudfoot *et al*., 2003). The vCBP used in this study has a proposed GAG binding site, being a dense, positively charged groove located on β-sheet I which shares distinct homology with the characterised GAG binding site of M-T1 (Counago *et al*., 2015; Seet *et al*., 2001). However, experimental attempts to assess CBP binding with heparin (a polysaccharide closely related in structure to HS) have so far failed to indicate any interaction. It was hypothesised that by pre-binding labelled CBP with heparin, any GAG binding site would be occupied, thereby blocking the ability of CBP to interact with GAGs on the monocytes. Interestingly, upon heparin pre-binding there was a reduction in the amount of labelled CBP detected on THP-1 cells; an effect not observed by the anti-CCL2 antibody. This assay is therefore the first experimental evidence to potentially demonstrate an interaction between CBP and heparin.

Although interesting experimentally, the ability for vCBPs to interact with GAGs arises a potentially detrimental feature for diagnostic utilisation. For diagnostics specificity is key, however with GAGs lining almost all cell types there may be a risk of non-specific binding, therefore an inability to accurately identify disease-related chemokine activity. Considering the potential application of these proteins in imaging protocols, this would most certainly lead to a loss of specificity, being comparable to failures of image-based chemokine receptor targeting (Nishizawa *et al*., 2010). However, vCBPs such as M-T7 and M3 are not indicated to bind directly with GAGs (Lalani *et al*., 1997; Alexander-Brett and Fremont, 2007) and their use may overcome the limitations of GAG-binding vCBPs.

Alternately, some research suggests that upregulated heparinase, of which breaks down heparins for cleavage from the cell surface, is observed in inflammatory diseases such as IBD (Waterman *et al*., 2007; Day and Forbes, 1999). Heparinase cleavage of HS is also known to promote the dissemination of the inflammatory cells through the body, facilitating the metastasis of numerous cancers including pancreatic, breast, colon, and lung (Vlodavsky *et al*., 2001; Vlodavsky *et al*., 2012). Thereby, a potentially beneficial role of targeting GAGs for prognosis/diagnosis of cancer metastasis may exist. However, further characterisation of GAG interactions with vCBPs would be required to investigate their potential use in this setting.

As CBP exhibits binding across several chemokines, the expression of other chemokines within the assay may impact upon its sensitivity. For example, CCL5 was observed to exhibit constitutive expression by the THP-1 monocytes, regardless of treatment and at earlier time points compared with CCL2. Previous SPR findings indicate that CBP has a higher affinity for CCL5 compared to CCL2 (Lateef *et al*. 2009) when utilising mouse chemokines. Similarly, in the current study, the IC_{50} of CBP for CCL5 was greater than that observed for CCL2 when using human chemokines (0.4nM to 0.8nM, as observed by ELISA). This finding suggests, that if labelled CBP is predominantly binding CCL5, it may not be possible to detect substantial differences across the time points as the labelled protein may not have reached saturating levels for the amount of available chemokine. This could be further investigated by utilising CCL5-specific antibodies, or the CCL5 protein itself, to block CBP binding to the cells in this system. Monocytes have also been shown to express a multitude of other chemokines under constitutive and inflammatory conditions (Harrison *et al*., 2005), with CBP likely binding to numerous of these chemokines (Counago *et al*., 2015; Sharif *et al*., 2016). A similar approach could be utilised to block these chemokine-specific interactions to better assess their involvement in the CBP binding observed in this study. Alternately, utilising differing cell lines for which chemokine expression is more limited and specific could provide these insights.

For more extensive characterisation of potential applications for CBP in diagnostics, varying tissues and tissue states should be investigated. This study utilised a monocytic cell line of which is known to be a potent expresser of chemokines (Park *et al*., 2007). Comparatively, experimental and clinical testing for inflammation involves numerous sample types of which all possess drastically differing characteristics, including cancer cells, blood or synovial samples, and frozen biopsies. Other sample types may indicate more successful application of vCBPs for the detection of chemokines. However, further consideration would be required as the expression of GAGs may be biasing the presence of a true chemokine-vCBP interaction.

4.2 Other Uses for CBP

This study also examined the potential utilisation of labelled CBP within western blotting protocols. Whilst the labelled anti-CCL2 antibody could detect reduced protein as hypothesised, CBP was unable to detect chemokine in this state, likely due to reduction of the protein disrupting its tertiary structure. Utilising chemokines which have not been reduced by 2-ME, thereby retaining their tertiary structure, would be the next step in examining the potential application of vCBPs in western blotting protocols (Homma *et al*., 2004). Similarly, assessing chemokines run on native gels without SDS would allow for the retention of chemokine charge, therefore potentially allowing vCBP binding (Gudiksen *et al*., 2006).

ELISA protocols utilise multiple antibody interactions to provide a common methodology for protein detection across both scientific research and clinical diagnostics. The replacement of capture or detection antibodies in the ELISA protocol with a vCBP could increase the sensitivity and usability of the assay. This study first investigated the use of native CBP as a substitute for the capture antibody. The use of a broad-spectrum binding protein would eliminate the need for chemokine-specific capture antibodies, potentially allowing it to be used across arrange of chemokine-specific ELISAs. As CBP exhibited high affinity chemokine binding when coupled to SPR chips (Lateef *et* al., 2009; Counago *et al*., 2015; Sharif *et al*., 2016), this suggests the

capture of chemokines via CBP coated to an ELISA plate may be possible. A linear relationship in the amount of human CCL2 chemokine standard was observed similarly to that of the capture antibody, suggesting the chemokine also successfully bound to CBP-coated wells. This was consistent with SPR findings in which charge-based interactions between the CBP and chip were shown not occlude the chemokine binding site. Interestingly, this finding also suggests CBP-bound chemokine can form a complex with the detection antibody simultaneously. As the detection antibody used was a monoclonal antibody, it binds with a singular epitope on the chemokine. The immunogenic epitope for the detection antibody was unknown, however based on the theoretical CBP-chemokine-antibody complex formed, the epitope likely lies outside the chemokine receptor-binding face occluded with CBP interaction. An important next step would be a direct comparison utilising equimolar amounts of the commercial capture antibody and CBP to ascertain their relative sensitivity for human CCL2 in this assay. As the antibody utilised was part of a kit, the concentration of the antibody was not provided, so this was unable to be completed without purchasing the antibody clone at a known concentration.

This ELISA experiment was only undertaken with human CCL2, thereby to assess the true utility of CBP further examination is required with additional chemokines. As observed with the CCL2 ELISA, CBP will need to be paired with a detection antibody that recognises the binding epitope outside of the chemokine domain bound by CBP. Predominantly, CBP binds chemokines at their receptor-binding face, therefore ideal detection antibodies would be those that bind chemokines without neutralising function. The epitope an antibody recognises, and the potential neutralising capabilities of the antibody are not always known, therefore screening would be required to identify those compatible with the vCBP in an ELISA scenario.

If this protocol were to be investigated further, the broad-spectrum binding characteristic of CBP would need to be tested in samples with a mixed pool of chemokines (such as synovial or serum samples). It is possible that in this scenario, the specific chemokine to be detected may

only represent a minor fraction of that captured by CBP, thus reducing the sensitivity of the assay. Similarly, if GAGs are in the system there may be a potential interaction with CBP. As such, the use of CBP as a broad-spectrum detection antibody substitute may be more appropriate.

Utilising a vCBP which could bind chemokines already captured by the specific capture antibody would both maintain the specificity for detection, and also eliminate the need for specific detection antibodies across numerous ELISA protocols (Clark *et al*., 1986). However, as mentioned above, investigation could be required to identify capture antibodies that bind chemokines whilst leaving the domain needed for CBP interactions free. To assess whether this was possible, the ability of CBP to directly compete with the detection antibody in a human CCL2 ELISA was examined. The assumption being that if it could, it was able to bind the chemokine in complex with the capture antibody. Interestingly, at high concentrations of the vCBP there was blocking of the detection antibody observed. Although suggesting the formation of a capture antibody-chemokine-CBP complex, there is also a distinct possibility that CBP is outcompeting the antibody for the chemokine. To further investigate this theory, complex assembly could be analysed using immunoprecipitation, SDS-page, or western blotting. If the formation of a CBP-chemokine-antibody complex is shown, the next step would be repeat the ELISA with CBP to determine whether the FLAG-tag could be detected with the anti-FLAG M2-HRP-conjugated antibody. Alternatively, CBP could be conjugated directly with biotin or HRP and then assessed.

4.3 Summary

The aim of this study was to develop and investigate the use of CBP as potential diagnostic tool for inflammation. If successful, this study would suggest there is potential application for all vCBPs as diagnostic tools, providing a vast range of potential binding profiles to utilise for detection of chemokines for diagnostics (Lucas and McFadden, 2004).

From this study, there is not a clear indication of efficacy for labelled CBP in immuno-fluorescent cytology. Although there were indications of positive findings with this protocol, without further characterisation an assumption cannot be made as to whether the vCBP would make a useful diagnostic. This study was unable to confirm that CBP could bind chemokines fixed on/in monocytes, and there was only an indication of a heparin-based interaction. Irrespective of the nature of binding, the labelled antibody showed a higher sensitivity for the chemokine, therefore being a more sensitive potential diagnostic tool than CBP. Although there was a suggestion of heparin binding observed with CBP, there may be little use for a heparin-based diagnostic tool. As GAGs are expressed on almost all cell types, the introduction of the labelled CBP may not be beneficial in detecting inflammation (Couchman and Pataki, 2012).

From this study, the most promising application of vCBPs within biological testing comes in the form of adapted ELISA protocols. With the development of vCBPs as a dynamic detection antibody substitute, the ability to utilise a singular detection protein across multiple ELISAs could provide both an increase in efficiency, and a decrease in cost. Similarly, the use of a specific capture antibody could have utility for the detection of several chemokines. Although matching between capture antibodies and vCBP would be required to ensure non-overlapping epitopes, the present study does indicate some potential.

As indicated within the current study, the physical state of the chemokine is likely a huge factor in which determines the applicability of vCBPs for detection. In ELISA techniques and native human samples, the chemokines tested are neither fixed nor altered. As several tests for chemokines in biological samples use serum and synovial testing (as with RA), or utilise frozen tissues (as with cancer), the application of vCBPs to detect native chemokines warrants further investigation (Villanueva and Schumacher, 1987; Arbyn *et al*., 2008; Brender *et al*., 2005; Bas *et al*., 2002). While the use of vCBPs as broad-spectrum chemokine detectors in diagnostic procedures is an interesting concept, any potential benefits of this approach are yet to be proven.

Supplementary Figures

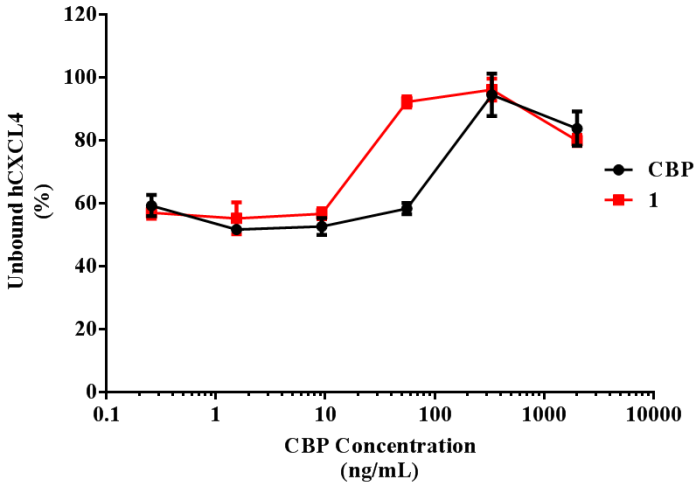

Supplementary Figure 1. CBP appears to be introducing CXCL4 into the ELISA, resulting in opposing binding curve. Various concentrations of conjugated or native CBP were incubated with human CXCL4. Unbound chemokine was then detected using a competition ELISA. The conjugated CBP was prepared using protocol 1. Results are presented as the percentage of unbound chemokine, normalised to a CXCL4 only control, without the presence of CBP. Values are expressed as mean ± SEM (n = 3).

References

Alcami A (2003). Viral mimicry of cytokines, chemokines and their receptors. Nat Rev Immunol 3: 36-50.

Aldinucci D, Colombatti A (2014). The inflammatory chemokine CCL5 and cancer progression. Mediators Inflamm 2014: 292376.

Alexander-Brett JM, Fremont DH (2007). Dual GPCR and GAG mimicry by the M3 chemokine decoy receptor. J Exp Med 204: 3157-3172.

Allam SI, Sallam RA, Elghannam DM, El-Ghaweet AI (2018). Clinical significance of serum B cell chemokine (CXCL13) in early rheumatoid arthritis patients. Egypt Rheumatol epub ahead of print.

Arbyn M, Bergeron C, Kilnkhamer P, Martin-Hirsch P, Siebers AG, Bulten J (2008). Liquid compared with conventional cervical cytology: a systematic review and meta-analysis. Obstet Gynecol 111: 167-177.

Bahar MW, Kenyon JC, Putz MM, Abrescia NGA, Pease JE, Wise EL *et al*. (2008). Structure and function of A41, a vaccinia virus chemokine binding protein. PLoS Pathog 4: 5.

Baker MP, Reynolds HM, Lumicisi B, Bryson CJ (2010). Immunogenicity of protein therapeutics. Self Nonself 1: 314-322.

Barnes DA, Tse J, Kaufhold M, Owen M, Hesselgesser J, Strieter R *et al*. (1998). Polyclonal antibody directed against human RANTES ameliorates disease in the Lewis rat adjuvant-induced arthritis model. J Clin Invest 101: 2910-2919.

Barnes PJ (2006). How corticosteroids control inflammation: quintiles prize lecture 2005. Br J Pharmacol 148: 245-254.

Barthel SR, Gavino JD, Descheny L, Dimitroff CJ (2007). Targeting selectins and selectin ligands in inflammation and cancer. Expert Opin Ther Targets 11: 1473-1491.

Bas S, Perneger TV, Seitz M, Tiercy JM, Roux-Lombard P, Guerne PA (2002). Rheumatology 41: 809-814.

Bass JJ, Wilkinson DJ, Rankin D, Phillips BE, Szewczyk NJ, Smith K *et al*. (2017). An overview of technical considerations for western blotting applications to physiological research. Scand J Med Sci Sports 27: 4-25.

Bazan JF, Bacon KV, Hardiman G, Wang W, Soo K, Rossi D (1996). A new class of membrane-bound chemokine with a CX3C motif. Nature 385: 640-644.

BD Biosciences (2019). Cytokine ELISA Protocol.

Behman AB, Lisok A, Chatterjee S, Poirier JT, Pullambhatla M, Luker GD *et al*. (2016). Targeted imaging of the atypical chemokine receptor 3 (ACKR3/CXCR7) in human cancer xenografts. J Nucl Med 57: 981-988.

Bekker P, Ebsworth K, Walters MJ, Berahovich RD, Ertl LS, Charvat TT (2015). CCR9 antagonists in the treatment of ulcerative colitis. Mediators Inflamm 2015: 628340.

Belperio JA, Ardehali A (2008). Chemokines and transplant vasculopathy. Circ Res 103: 454-466.

Benamar K, Geller EB, Alder MW (2008). Elevated level of the proinflammatory chemokine, RANTES/CCL5, in the periaqueductal grey causes hyperalgesia in rats. Eur J Pharmacol 592: 93-95.

Bhatia R, Kavanagh K, Stewart J, Moncur S, Serrano I, Cong D *et al*. (2018). Host chemokine signature as a biomarker for the detection of pre-cancerous cervical lesions. Oncotarget, 9: 18548-18558.

Boni MF (2009). Vaccination and antigenic drift in influenza. Vaccine 26: 8-14.

Bosshart H, Heinzelmann M (2016). THP-1 cells as a model for human monocytes. Ann Transl Med 4: 438.

Brender E, Burke A, Glass RM (2005). Frozen section biopsy. JAMA 294: 24.

Cilliers C, Nessler I, Chrostodolu N, Thurber GM (2017). Tracking antibody distribution with near-infrared fluorescent dyes: impact of dye structure and degree of labeling on plasma clearance. Mol Pharm 14: 1623-1633.

Clark MF, Lister RM, Bar-Joseph (1986). ELISA techniques. Methods Enzymol 118: 742-766.

Couchman JR, Pataki CA (2012). An introduction to proteoglycans and their localization. J Histochem Cytochem 60: 885-897.

Counago RM, Knapp KM, Nakatani Y, Fleming SB, Corbett M, Wise LM *et al*. (2015). Structures of orf virus chemokine binding protein in complex with host chemokines reveal clues to broad binding specificity. Structure 23: 1199-1213.

Culley FJ, Pennycook AMJ, Tregoning JS, Dodd JS, Walzl G, Wells TN (2006). Role of CCL5 (RANTES) in viral lung disease. J Virol 80: 8151-8157.

Dabbagh K, Xiao Y, Smith C, Stepick-Biek, Kim SG, Lamm WJE *et al*. (2000). Local blockade of allergic airway hyperreactivity and inflammation by the poxvirus-derived pan-CC-chemokine inhibitor vCCI. J Immunol 165: 3418-3422.

Das M, Leonardo CC, Rangooni S, Pennypacker KR, Subhra M, Mohapatra S (2011). Lateral fluid percussion injury of the brain induces CCL20 inflammatory chemokine expression in rats. J Neuroinflammation 8: 148.

Day R, Forbes A (1999). Heparin, cell adhesion, and pathogenesis of inflammatory bowel disease. Lancet 354: 62-65.

Deshmane SL, Kremlev S, Amini S, Sawaya BE (2009). Monocyte chemoattractant protein-1 (MCP-1): an overview. J interferon Cytokine Res 29: 313-326.

Dominguez-Villar M, Hafler DA (2018). Regulatory T cells in autoimmune disease. Nature Immunol 19: 665-673.

Dorgham K, Dejou C, Piesse C, Gorochov G, Pene J, Yssel H (2016). Identification of the single immunodominant region of the native human CC chemokine receptor 6 recognized by mouse monoclonal antibodies. PLoS one 11: e0157740.

Engel P, Angulo A (2012). Viral immunomodulatory proteins: usurping host genes as a survival strategy. Adv Exp Med Biol 738: 256-276.

Farrugia BL, Lord MS, Melrose J, Whitelock JM (2018). The role of heparan sulfate in inflammation, and the development of biomimetics as anti-inflammatory strategies. J Histochem Cytochem 66: 321-336.

Felix J, Savvides SN (2017). Mechanisms of immunomodulation by mammalian and viral decoy receptors: insights from structures. Nat Rev Immunol 17: 112-129.

Fisher BS, Green RR, Brown RR, Wood MP, Hensley-McBain T, Fisher C *et al.* (2018). Liver macrophage-associated inflammation correlates with SIV burden and is substantially reduced following cART. PLoS Pathog 14: e1006871.

Fleming SB, Wise LM, Mercer AA (2015). Molecular genetic analysis of orf virus: a poxvirus that has adapted to skin. Viruses 23: 1505-1539.

García B, Merayo-Lloves J, Rodríguez D, Alcalde I, García-Suárez O, Alfonso J *et al*. (2016). Different use of cell surface glycosaminoglycans as adherence receptors to corneal cells by gram positive and gram negative pathogens. Front Cell Infect Microbiol 6: 173.

Gong JH, Ratkay LG, Waterfield JD, Clark-Lewis I (1997). An antagonist of monocyte chemoattractant protein 1 (MCP-1) inhibits arthritis in the MRL-lpr mouse model. J Exp Med 186: 131-137.

Gonzalez-Motos V, Kropp KA, Viejo-Borbolla A (2016). Chemokine binding proteins: an immunomodulatory strategy going viral. Cytokine Growth Factor Rev 30: 71-80.

Griffith JW, Sokol CL, Luster AD (2014). Chemokines and chemokine receptors: positioning cells for host defence and immunity. Ann Rev Immunol 32: 659-702.

Gudiksen KL, Gitlin I, Whitesides GM (2006). Differentiation of proteins based on characteristic patterns of association and denaturation in solutions of SDS. Proc Natl Acad Sci U S A 103: 7968-7972.

Haberstroh U, Pocock J, Gomez-Guerrero C, Helmchen U, Hamann A, Gutierrez-Ramos J *et al*. (2002). Expression of the chemokines MCP-1/CCL2 and RANTES/CCL5 is differentially regulated by infiltrating inflammatory cells. Kidney Int 62: 1264-1276.

Haringman JJ, gerlag DM, Smeets TJM, Baeten D, van den Bosch F, Bresnihan B *et al*. (2006). A randomized controlled trial with an anti-CCL2 (anti–monocyte chemotactic protein 1) monoclonal antibody in patients with rheumatoid arthritis. Arthritis Rheum 54: 2387-2392.

Haringman JJ, Kraan MC, Smeets TJM, Zwinderman KH, Tak PP (2003). Chemokine blockade and chronic inflammatory disease: proof of concept in patients with rheumatoid arthritis. Ann Rheum Dis 62: 715-721.

Harrison LM, van den Hoogen C, van Haaften WCE, Tesh VL (2005). Chemokine expression in the monocytic cell line THP-1 in response to purified shiga toxin 1 and/or lipopolysaccharides. Infect Immun 73: 403-412.

Heidarieh H, Hernaez, Alcami A (2015). Immune modulation by virus-encoded secreted chemokine binding proteins. Virus Res 209: 67-75.

Higgins KR, Kovacevic W (2014). Nucleotides regulate secretion of the inflammatory chemokine CCL2 from human macrophages and monocytes. Mediators Inflamm 7: 293925.

Homma M, Shiomi D, Homma M, Kawagishi I (2004). Attractant binding alters arrangement of chemoreceptor dimers within its cluster at a cell pole. PNAS 101: 3462-3467.

Hsu DC, Katelaris CH (2009). Long-term management of patients taking immunosuppressive drugs. Aust Prescr 32: 68-71.

Iida N, Grotendorst GR (1990). Cloning and sequencing of a new GRO transcript from activated human monocytes: expression in leukocytes and wound tissue.

Itatani Y, Kawada K, Inamoto S, Yamamoto T, Ogawa R, Taketo MM *et al*. (2016). The role of chemokines in promoting colorectal cancer invasion/metastasis. Int J Mol Sci 17: 643.

Jensen KK, Chen SC, Hipkin RW, Wiekowski MT, Schwarz MA, Chou CC *et al*. (2003). Disruption of CCL21-induced chemotaxis in vitro and in vivo by M3, a chemokine-binding protein encoded by murine gammaherpesvirus 68. J Virol 77: 624-630.

Jin J (2015). Nonsteroidal anti-inflammatory drugs. JAMA 314: 1084.

Kara EE, Comerford I, Fenix KA, Bastow CR, Gregor CE, McKenzie DR *et al*. (2014). Tailored immune responses: novel effector helper T cell subsets in protective immunity. PLoS Pathog 10: e1003905.

Keeley EC, Mehrad B, Strieter RM (2010). CXC chemokines in cancer angiogenesis and metastasis. Adv Cancer Res 106: 91-111.

Keshavarzian A, Fusunyan RD, Jacyno M, Winship D, MacDermott RP, Sanderson IR (1999). Increased interleukin-8 (IL-8) in rectal dialysate from patients with ulcerative colitis: evidence for a biological role for IL-8 in inflammation of the colon. Am J Gastroenterol 94: 704-712.

Kohidai L, Csaba G (1998). Chemotaxis and chemotactic selection induced with cytokines (IL-8, RANTES and TNF- α) in the unicellular tetrahymena pyriformis. Cytokine 10: 481-486.

Kohn TJ, DiPietro LA (2013). Inflammation and wound healing: the role of the macrophage. Expert Rev Mol Med 13: e23.

Kufareva I, Salanga CL, Handel TM (2015). Chemokine and chemokine receptor structure and interactions: implications for therapeutic strategies. Immunol Cell Biol 93: 372-383.

Lalani AS, Graham K, Mossman K, Rajarathnam K, Clark-Lewis I, Kelvin D *et al*. (1997). The purified myxoma virus gamma interferon receptor homolog M-T7 interacts with the heparin-binding domains of chemokines. J Virol 71: 4356-4363.

Lalani AS, Ness TL, Singh R, Harrison JK, Seet BT, Kelvin DJ *et al*. (1998). Functional comparisons among members of the poxvirus T1/35kDa family of soluble CC-chemokine inhibitor glycoproteins. Virology 250: 173-184.

Lasagni L, Francalanci M, Annunziato F, Lazzeri E, Giannini S, Cosmi L *et al*. (2003). An alternatively spliced variant of CXCR3 mediates the inhibition of endothelial cell growth

induced by IP-10, Mig, and I-TAC, and acts as functional receptor for platelet factor 4. J Exp Med 197: 1537-49.

Lateef Z, Baird MA, Wise LM, Mercer AA, Fleming SB (2009). Orf virus-encoded chemokine-binding protein is a potent inhibitor of inflammatory monocyte recruitment in a mouse skin model. J Gen Virol 90: 1477-1482.

Lateef Z, Baird MA, Wise LM, Young S, Mercer AA, Fleming SB (2010). The chemokine-binding protein encoded by the poxvirus orf virus inhibits recruitment of dendritic cells to sites of skin inflammation and migration to peripheral lymph nodes. Cell Microbiol 12: 665-676.

Lee J, Park C, Kim HJ, Lee YD, Lee ZH, Song YW *et al*. (2017). Stimulation of osteoclast migration and bone resorption by C–C chemokine ligands 19 and 21. Exp Mol Med 49: e358.

Lei Y, Takahama Y (2012). XCL1 and XCR1 in the immune system. Microbes Infect 14: 262-267.

Lin L, Huang S, Zhu Z, Han J, Wang Z, Weijian H *et al*. (2018). P2X7 receptor regulates EMMPRIN and MMP‑9 expression through AMPK/MAPK signaling in PMA‑induced macrophages. Mol med Rep 18: 3027-3033.

Liu L, Dai E, Miller L, Seet B, Lalani A, Macauley C *et al*. (2004). Viral chemokine-binding proteins inhibit inflammatory responses and aortic allograft transplant vasculopathy in rat models. Transplantation 15: 1652-1660.

Loberg RD, Ying C, Craig M, Yan L, Snyder LA, Pienta KJ (2007). CCL2 as an important mediator of prostate cancer growth *in vivo* through the regulation of macrophage infiltration. Neoplasia 9: 556-562.

Lodowski DT, Palczewski K (2009). Chemokine receptors and other GPCRs. Curr Opin HIV AIDS 4: 88-95.

Lu YC, Yeh WC, Ohashi PS (2008). LPS/TLR4 signal transduction pathway. Cytokine 42: 145-151.

Lucas A, McFadden G (2004). Secreted immunomodulatory viral proteins as novel biotherapeutics. J Immunol 173: 4765-4774.

Luster AD (1998). Chemokines – chemotactic cytokines that mediate inflammation. N Engl J Med 338: 436-445.

Macoska JA, Begley LA, Dunn RL, Siddiqui J, Wei JT, Sarma AV (2008). Pilot and feasibility study of serum chemokines as markers to distinguish prostatic disease in men with low total serum PSA. Prostate 68: 442-452.

Matsuda Y, Fujii T, Suzuki T, Yamahatsu K, Kawahara K, Teduka K *et* al. (2011). Comparison of fixation methods for preservation of morphology, RNAs, and proteins from paraffin-embedded human cancer cell-implanted mouse models. J Histochem Cytochem 59: 68-75.

Mbonye U, Karn J (2017). The molecular basis for human immunodeficiency virus latency. Annu Rev virol 4: 261-285.

Meincke M, Tiwari S, Hattermann K, Kalthoff H, Mentlein R (2011). Near-infrared molecular imaging of tumors via chemokine receptors CXCR4 and CXCR7. Clin Exp Metastasis 28: 713-720.

Miller LW, Dai E, Nash P, Liu L, Icton C, Klironomos D *et al*. (2000). Inhibition of transplant vasculopathy in a rat aortic allograft model after infusion of anti-inflammatory viral serpin. Circulation 4: 1598-1605.

Nagaoka M, Akaike T (2003). Single amino acid substitution in the mouse IgG1 Fc region induces drastic enhancement of the affinity to protein A. Protein Eng 16: 243-245.

Nanna AR, Li X, Walseng E, Pedzisa L, Goydel RS, Hymel D *et al*. (2017). Harnessing a catalytic lysine residue for the one-step preparation of homogeneous antibody-drug conjugates. Nat Commun 8: 1112.

Neel NF, Schutyser E, Sai J, Fan G, Richmond A (2005). Chemokine receptor internalization and intracellular trafficking. Cytokine Growth Factor Rev 16: 637-658.

Nicoll MP, Proenca JT, Efstathiou S (2012). The molecular basis of herpes simplex virus latency. FEMS Microbiol Rev 36: 684-705.

Nishizawa K, Nishiyama H, Oishi S, Tanahara N, Kotani H, Mikami Y *et al*. (2010). Fluorescent imaging of high-grade bladder cancer using a specific antagonist for chemokine receptor CXCR4. Int J Cancer 127: 1180-1187.

Ogata H, Takeya M, Yoshimura T, Takagi K, Takahashi K (1997). The role of monocyte chemoattractant protein-1 (MCP-1) in the pathogenesis of collagen-induced arthritis in rats. J Pathol 182: 106-114.

Oskeritzian CA (2012). Mast cells and wound healing. Adv Wound Care 1: 23-28.

Pallone F, Monteleone G (2001). Mechanisms of tissue damage in inflammatory bowel disease. Curr Opin Gastroenterol 17: 307-312.

Park EK, Jung HS, Yang HI, Yoo MC, Kim C, Kim KS (2007). Optimized THP-1 differentiation is required for the detection of responses to weak stimuli. Inflamm Res 56: 45-50.

Pease JE, Horuk R (2010). Small molecule antagonists of chemokine receptors – is promiscuity a virtue?. Curr Top Med Chem 10: 1351-1358.

Perdiger A (2009). Infliximab in the treatment of rheumatoid arthritis. Biologics 3: 183-191.

Pienta KJ, Machiels JP, Schrijvers D, Alekseev B, Shkolnik M, Crabb SJ *et al*. (2013). Phase 2 study of carlumab (CNTO 888), a human monoclonal antibody against CC-chemokine ligand 2 (CCL2), in metastatic castration-resistant prostate cancer. Invest New Drugs 31: 760-768.

Popa C, Netea MG, Riel PLCM, van der Meer JWM, Stalenhoef (2007). The role of TNF-α in chronic inflammatory conditions, intermediary metabolism, and cardiovascular risk. J Lipid Res 48: 751-762.

Pretzer E, Wiktorowicz JE (2008). Saturation fluorescence labeling of proteins for proteomic analyses. Anal Biochem 374: 250-262.

Punchard NA, Whelan CJ, Adcock I (2004). The journal of inflammation. J Inflamm 1: 1.

Pyo R, Jensen KK, Wiekowski MT, Manfra D, Alcami A, Taubman MB *et al*. (2004). Inhibition of intimal hyperplasia in transgenic mice conditionally expressing the chemokine-binding protein M3. Am J Pathol 164: 2289-2297.

R&D Systems (2019). How to Run an R&D Systems Quantikine ELISA.

Raman D, Sobolik-Delmaire T, Richmond A (2011). Chemokines in health and disease. Exp Cell Res 317: 575-589.

Reading PC, Symons JA, Smith GL (2003). A soluble chemokine-binding protein from vaccinia virus reduces virus virulence and the inflammatory response to infection. J Immunol 170: 1435-1442.

Ridiandries A, Bursill C, Tan J (2017). Broad-spectrum inhibition of the CC-chemokine class improves wound healing and wound angiogenesis. Int J Mol Sci 18: 155.

Rolls, G (2012). Fixation and fixatives (3)–fixing agents other than the common aldehydes. Wetzlar: Leica Biosystems

Sanchez-Martin L, Estecha A, Samaneigo, Sanchez-Ramon S, Vega MA, Sanchez-Mateos (2011). The chemokine CXCL12 regulates monocyte-macrophage differentiation and RUNX3 expression. Blood 117: 88-97.

Sarvaiya PJ, Guo D, Ulasov I, Gabikian P, Lesniak MS (2013). Chemokines in tumour progression and metastasis. Oncotarget 4: 2171-2185.

Seet BT, Barrett J, Robichaud J, Shilton B, Singh R, McFadden G (2001). Glycosaminoglycan binding properties of the myxoma virus CC-chemokine inhibitor M-T1. J Biol Chem 276: 30504-30513.

Seet BT, Johnston JB, Brunetti CR, Barrett JW, Everett H, Cameron C *et al*. (2003). Poxviruses and immune evasion. Annu Rev Immunol 21: 377-423

Sela-Culang IS, Kunik V, Ofran Y (2013). The structural basis of antibody-antigen recognition. Front Immunol 4: 302.

Sharif S, Nakatani Y, Wise L, Corbett M, Real NC, Stuart GS *et al*. (2016). A broad-spectrum chemokine-binding protein of bovine papular stomatitis virus inhibits neutrophil and monocyte infiltration in inflammatory and wound models of mouse skin. PLoS one 11: e0168007.

Sharp PM, Simmonds P (2011). Evaluating the evidence for virus/host co-evolution. Curr Opin Virol 1: 436-441.

Spaks A (2017). Role of CXC group chemokines in lung cancer development and progression. J Thorac Dis 9: 164-171.

Stamatovic SM, Keep RF, Mostarica-Stojkovic M, Andjelkovic A (2006). CCL2 regulates angiogenesis via activation of Ets-1 transcription factor. J Immunol 177: 2651–2661.

Sun JK, Uehara H, Karashima T, Mccarty M, Shih N, Fidler IJ (2001). Expression of lnterleukin-8 correlates with angiogenesis, tumorigenicity, and metastasis of human prostate cancer cells implanted orthotopically in nude mice. Neoplasia 3: 33-42.

Suzuki M, Kato C, Kato A (2015). Therapeutic antibodies: their mechanisms of action and the pathological findings they induce in toxicity studies. J Toxicol Pathol 28: 133-139.

Szekanecz Z, Koch AE (2015). Successes and failures of chemokine-pathway targeting in rheumatoid arthritis. Nat Rev Rheumatol 12: 5-13.

Szekanecz Z, Vegvari A, Szabo Z, Koch AE (2010). Chemokines and chemokine receptors in arthritis. Front Biosci 2: 153-167.

Tai K, Hiromichi I, Ikegaya S, Ueda T (2013). Minocycline modulates cytokine and chemokine production in lipopolysaccharide-stimulated THP-1 monocytic cells by inhibiting IκB kinase α/β phosphorylation. Trans Res 161: 99-109.

Thompson S, Martinez-Burgo B, Sepuru KM, Rajarathnam K, Kirby JA, Sheerin NS *et al*. (2017). Regulation of Chemokine Function: The Roles of GAG-Binding and Post-Translational Nitration. Int J Mol Sci 18: 1692.

Tsaur I, Noack A, Makarevic J, Oppermann E, Waaga-Gasser AM, Gasser M *et al*. (2014). CCL2 chemokine as a potential biomarker for prostate cancer: a pilot study. Cancer Res Treat 47: 306-312.

van de Sande MGH, de Hair MJH, van der Leij C, Klarenbeen PL, Bos WH, Smoth MD *et al*. (2011). Ann Rheum Dis 70: 772-777.

Vela M, Aris M, Llorente M, Garcia-Sanz JA, Kremer L (2015). chemokine receptor-specific antibodies in cancer immunotherapy: achievements and challenges. Front Immunol 6: 1-15.

Villanueva TG, Schumacher HR (1987). Cytological examination of synovial fluid. Diagn Cytopathol 3: 141-147.

Vlodavsky I, Beckhove P, Lerner I, Pisano C, Meirovitz A, Ilan N *et al*. (2012). Significance of heparinase in cancer and inflammation. Cancer Microenviron 5: 115-132.

Vlodavsky I, Friedmann Y (2001). Molecular properties and involvement of heparinase in cancer metastasis and angiogenesis. J Clin Invest 108: 341-347.

Walsh D, Mathews MB, Mohr I (2013). Tinkering with translation: protein sysntehesis in virus-infected cells. Cold Spring Hard Perspect Biol 5: 12351.

Waterman M, Ben-Izhak O, Eliakim R, Groisman G, Vlodavsky I, Ilan N (2007). Heparanase upregulation by colonic epithelium in inflammatory bowel disease. Mod Pathol 20: 8-14.

Wente MN, Keane MP, Burdick MD, Friess H, Büchler MW, Ceyhan GO *et al*. (2006). Blockade of the chemokine receptor CXCR2 inhibits pancreatic cancer cell-induced angiogenesis. Cancer Lett 241: 221-227.

Wolf S, Johnson S, Perwitasari O, Mahalingam S, Tripp RA (2017). Targeting the pro-inflammatory factor CCL2 (MCP-1) with bindarit for influenza A (H7N9) treatment. Clin Transl Immunology 6: e135.

Yates CC, Whaley D, Hooda S, Hebda PA, Bodnar RJ, Wells A (2009). Delayed reepithelialization and basement membrane regeneration after wounding in mice lacking CXCR3. Wound Repair Regen 17: 34-41.

Zhang X, Bloch S, Akers W, Achilefu S (2012). Near-infrared molecular probes for *in vivo* imaging. Curr Protoc Cytom 12: 1-28.